Tecnologie Avanzate e nano SCienza

INFM-National Laboratory

advanced Technology And nano SCience

2002
ACTIVITY REPORT

Submitted to the Scientific Council of TASC in July 2003

Director's Introduction to the Report

This document contains a report of the main activities of TASC in 2002, organised following the format of the previous reports available in the WWW.TASC.INFM.IT web site. The main objective of this report is to provide an overview of activities for evaluation by the Scientific Council of TASC. The material prepared for this report will be also available, shortly, on-line in the TASC web site for general consultation. Much internal collaboration has been at work in 2002 so that several projects actually involve two or several of the "research areas" identified by INFM. Also much external collaboration have had an important role, in part due to the rules of the public competitive funding programs for research which do imply participation by several institutions and groups. This positive facts do result is some double accounting of the research activity under the relevant "research areas". For the internal collaborations at TASC this is quite transparent in the report. For the external collaborations, or work done by TASC people in other INFM laboratories, I made a note by the title of those particular reports.

The TASC National Laboratory of INFM has been financed in 2002 for carrying on the relevant part of the Three-Year-Plan as approved by the Scientific Council. The central budget for operation was 516 K€, the salaries paid by INFM amounted to 529 K€ and the overall resources actually employed in 2002 were 4.060 K€ out of which 192 K€ were from commercial contracts and the balance from competitive public programs of the Italian Government and from the UE FP-V.

The strengthening of the scientific and technical staff was pursued according to the approved plans: five researchers were hired in 2002 via public competition, reaching a total of 26 at the end of 2002; five technicians were hired also via public competition reaching a total of 15. The new human resources staffed the facilities (beamlines, lithography, microscopy) and opened new research perspectives. In Particular the hiring of F. Martelli, a senior researcher with expertise in semiconductor materials and systems for telecommunication, has given start to a new research activity on the near-field optical investigation investigation of waveguides and photonic crystals, and the hiring of B. Davidson, expert in the growth of metal oxides and high Tc superconductors has opened the perspective of growing such materials at TASC.

The TASC facilities were fully operational in 2002. The **growth laboratories** (MBE, PECVD) have operated regularly with delivery of samples for in-house research, for collaborations and as supply to other INFM and international laboratories or industrial partners; the **5 INFM spectroscopy beamlines** on ELETTRA operated users shifts as well as in-house research, the **Centre for Electron Microscopy** (CEM) was successfully commissioned and started to run experiments both for in house research, and for external projects.
The lithography activity at TASC was upgraded to the role of general facility with the name **LIF@TASC** (Lithography facility at TASC) that includes the X-ray beam line LILIT, the e-beam lithography, the in-print lithography, the chemical laboratory, Reactive Ion Etching, Deep-RIE, Metallization, AFM and optical Lithographies. The choice was made to optimise the layout of LIF@TASC by including some new instruments in an expansion of the class 1000 clean room at TASC, as well by creating a new clean room in the TASC building to provide a technically and logistically improved environment to the nano-fabrication activity. The Technical Group was fully staffed in 2002: its action included design and fabrication of instrumentation as well as assistance for the operation and maintenance of the laboratories.
In 2002 TASC scientists were rewarded by the good success of the projects submitted, along with other INFM and CNR units, to the national program on Nanotechnology (FIRB, Integration Fund for Basic research), and on New Engineering Methods for Health. TASC has been financed under three main “strategic” projects in nanotechnology, with the role of national coordinator for one of these on C- Nanotubes, as well as in the case of a project in Medical Engineering (Nanotechnologies for drug delivery). These three year projects have brought in substantial financing so that the overall 2002 financial balance of TASC appeared, at the end of the year, quite good. It should nevertheless be kept in evidence that the ratio between core-financing and externally acquired funds is still sub critical, implying that planned “central” activities like the seed-projects could not be started.
In 2002 a new initiative was started that includes the creation of a joint group, under the leadership of F. Tommasini, involving TASC, the University and three medical research centres (Burlo Garofolo of Trieste, San Matteo of Pavia and S. Raffaele of Milano) about several developments and applications of nanotechnology to health (feasibility of wireless intraskull pressure probe, immunoinsulation of pancreatic islands, microtechnology for drug delivery in surgery). A kick-off meeting was organized and some funding was raised from a Bank foundation. The FIRB project has allowed purchasing a FIB (focussed ion beam lithography machine) that will be delivered and installed in 2003. The FIB will be installed in September 2003 in the extension of the TASC class 1000 clean room (decided in 2002 and completed in May 2003). A second laboratory, previously dedicated to He-surface scattering (now moved as side station on the ALOISA beamline) has been transformed into a new clean-room (to be completed in July 2003) for hosting imprint nanolithography, chemical and biological manipulation laboratories to support the biomedical group and collaborations. This new facility will play the role of an advanced outreach initiative to support interdisciplinary research projects in nanoscience and nanotechnology.
The laboratory was also quite active in 2002 in the presentation phase of the VI FP with a total of 16 Expressions of Interest for the FP-VI of UE (3 as coordinators DYNAMAG, MEDICUS, HM-MBE).

Reports from Research Projects 2002

Advanced semiconductor materials and devices (Research Area E2)

Coordinator:	Prof. Lucia Sorba
Staff:	Giorgio Biasiol Flavio Capotondi Daniele Ercolani Mukesh Kumar Marco Lazzarino Giorgio Mori Barbara Ressel Matteo Tonezzer

Growth of high mobility two-dimensional electron gases

The main research activity of the group is the fabrication of two dimensional electron gases (2DEGs) in epitaxially grown high-mobility GaAs/AlGaAs heterostructures. AlGaAs/GaAs heterostructures are grown by molecular beam epitaxy (MBE) in a facility dedicated to the growth of III-V high purity materials.

Currently, the MBE system routinely provides 2DEGs in a single AlGaAs/GaAs heterostructures with mobilities exceeding 10^6cm^2/Vs in a broad range of carrier densities. The progressive cleaning and the optimization of the structures have improved the electronic properties of the 2DEGs as shown in the Fig. 1. The best sample includes a 2DEG with mobility of $4.9\text{x}10^6$cm^2/Vs and carrier density of $3.8\text{x}10^{11}$cm^{-2} .

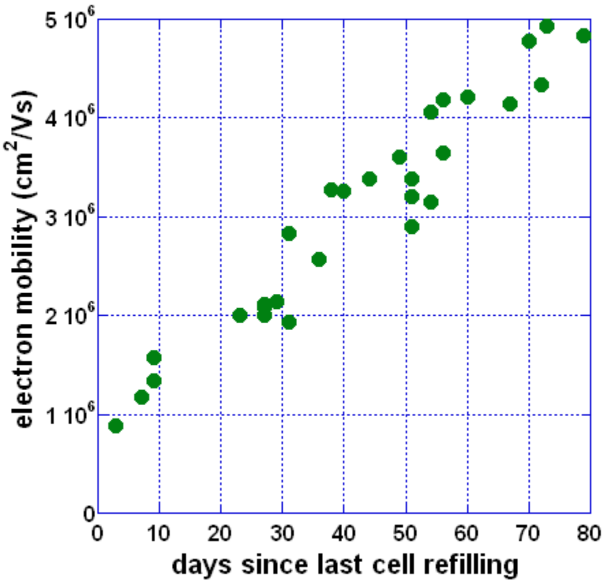

Fig. 1 Low-temperature electron mobility in different samples containing a 2DEG in a single GaAs/AlGaAs heterostructure, showing the progressive cleaning of the MBE system.

Furthermore, the research activity is focused on the fabrication of 2DEG in a single and coupled QW AlGaAs/GaAs structures. In the case of single QW structures carrier densities lower than 10^{11}cm^{-2} and mobility of the order of 10^6cm^2/Vs have been realized. In particular, we have fabricated 30nm-thick single QW structure with carrier density of $9.2\text{x}10^{10}$cm^{-2} and mobility of $2.04\text{x}10^6$cm^2/Vs while with carrier density $4.5\text{x}10^{10}$cm^{-2} we obtain mobility of $1.17\text{x}10^6$cm^2/Vs. For the coupled QW structure we have realized preliminary structures with 18mm-thick QW separated by 6.2nm-thick barrier with carrier density of $1.02\text{x}10^{11}$cm^{-2} and corresponding mobility $1.40\text{x}10^6$cm^2/Vs.

The amphoteric properties of Si as a dopant for (Al,Ga)As allow the formation of p-doped layers, by growing on (311)A-oriented substrates in appropriate conditions. In GaAs/AlGaAs Si-modulation doped heterostructures grown on such substrates we were able to obtain two-dimensional hole gases with mobilities up to $8.0\text{x}10^5$cm^2/Vs, for charge density of about $2.2\text{x}10^{11}$cm^{-2}.

The quality of the resulting 2DEGs is assessed by means of magneto-transport analysis performed at low temperature (1.5K) and under application of magnetic fields up to 7 Tesla. Van der Pauw and Hall-bar structures are fabricated by photolithographic techniques and by wet-etching. The carrier density and mobility are measured by the Hall and Shubnikov-de-Haas techniques.

Transport properties of $In_{0.75}Ga_{0.25}As$/ $In_{0.75}$ $Al_{0.25}As$ 2DEGs

Another activity of the group is focused on the realization of high quality two dimensional electron gases (2DEGs) in InGaAs/InAlAs quantum wells (QW). $In_xGa_{1-x}As/In_xAl_{1-x}As$ QWs with high In content offer potential advantages over GaAs/AlGaAs systems both for fundamental studies and for device applications, due to some peculiar material properties. First, the $In_xGa_{1-x}As$ effective mass is lower than in GaAs, thus making it an attractive material for the production devices, since the energy separation between electron levels is inversely proportional to the effective electron mass. Moreover, by increasing the In concentration it is possible to obtain a high transmissive interfaces that facilitate the so-called proximity effects in superconductor/semiconductor hybrid systems or spin-related effects in ferromagnet/semiconductor devices.

We have grown unintentionally doped 2DEGs in completely undoped $In_{0.75}Al_{0.25}As/In_{0.75}Ga_{0.25}As$ metamorphic quantum wells. Using those structures we are able to reduce the carrier density to values of $2\text{-}3\times 10^{11} cm^{-2}$ (that is more than three times less than the previously reported values in similar, modulation – doped structures) with electron mobilities up to $2.15\times10^5 cm^2/Vs$. In order to judge the quality of the 2DEGs we have measured at T = 1.5 K the longitudinal and transverse resistance of an $In_{0.75}Al_{0.25}As/In_{0.75}Ga_{0.25}As$ 2DEG as a function of the perpendicular magnetic field (see Fig. 1). Well defined plateaus are present in the transverse resistance, and in correspondence dissipationless regions in the longitudinal resistance are visible for filling factors smaller than four.

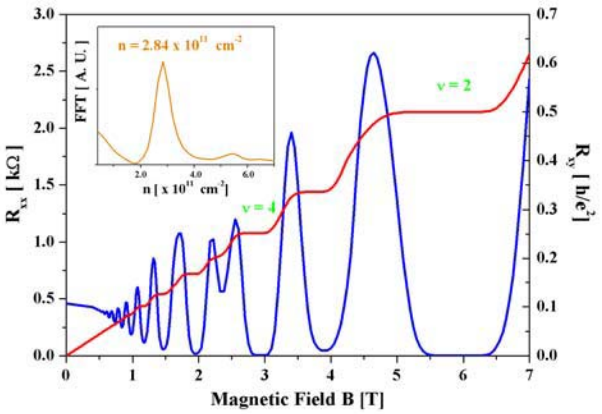

Fig. 1 Longitudinal and transverse resistance of an $In_{0.75}Al_{0.25}As/In_{0.75}Ga_{0.25}As$ 2DEG measured at T = 1.5 K as a function of the perpendicular magnetic field. Insert: Fourier analysis in the magnetic field region B < 2T.

Moreover, in order to understand the 2DEG formation in our completely undoped $In_{0.75}Al_{0.25}As/In_{0.75}Ga_{0.25}As$ junctions, we have investigated the presence of deep donor states whose energy lies in the the conduction band offset of the junction (ΔE_c=0.24eV). Measurements by means of photoinduced capacitance transient spectroscopy (PICTS) show that several deep levels are present in the gap of a metamorphic 500nm-thick $In_{0.75}Ga_{0.25}As$ layer grown on GaAs and, in particular, the activation energy of two of such levels is less ΔE_c. Poisson-Schrödinger simulations of the carrier density as a function of the depth of the 2DEGs from the surface confirm our hypothesis.

Collaboration: NEST-INFM (Pisa), University of Bologna, APE Beamline.

AFM defined quantum point contact

Since the last decade, the increasing need for fast and low power consumption electronics is driving toward mesoscopic and low dimensional devices. Nevertheless, the electronic behavior of low dimensional devices has not been completely understood and fabrication techniques are still at an incubation level.

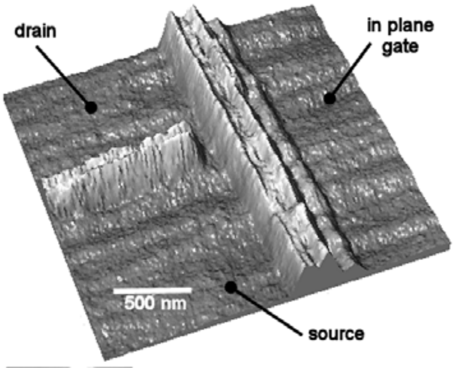

We used a recently developed lithographic technique, atomic force microscope local anodic oxidation, to fabricate quantum point contacts (QPC), that are the simplest one-dimensional device, and we characterized their transport properties both as function of temperature and magnetic field.

V-shaped QPCs, with a symmetric geometry, and T-shaped QPCs, with a strongly asymmetric geometry have been fabricated on a $GaAs/Al_{0.3}Ga_{0.7}As$ heterostructure where a high mobility two dimensional electron gas lies at 30 nm from the surface. A 3-D image of the latter device is reported in Fig. 1.

We studied the QPC conductance as a function of the voltage of the in-plane gates (IP). In-plane gates are used to shrink the lateral size of the QPC, reducing the number of states available to the conduction. Because of a compensation between the density of states and the velocity of electrons, the conductance does not vary linearly with IP voltage, but increases step by step. This behavior is known as conductance quantization.

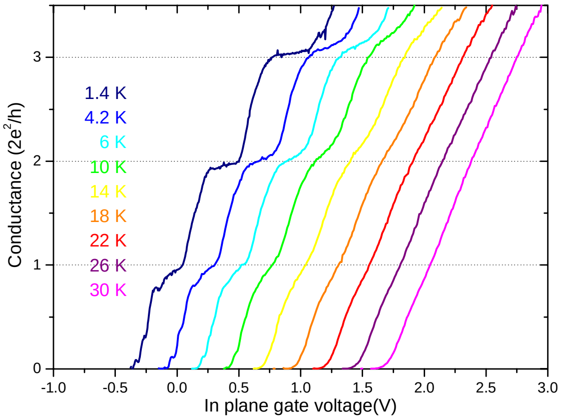

We studied the evolution of conductance quantization as a function of temperature and magnetic field. The temperature dependent behavior is illustrated in Fig. 2. Traces of quantization are observable up to 30K, that is one of the highest temperatures reported in literature for similar systems. When inserted into a strong magnetic field, the quantization features are enhanced, as expected because of the increase in the 1-D density of states, and, at field greater than 3.8 T a spin splitting is observed.

Chemical properties of GaAs oxides grown by AFM anodization

A newly developed lithographic technique, based on local anodic oxidation performed by means of an atomic force microscope tip, has collected an increasing interest, in recent years. Recently, low dimensional devices have been demonstrated using this technique. Several papers have been published on the growth mechanisms and on the electrical properties of such oxides, but very few addressed the issue of the chemical composition and, even more important, how to control it. Moreover, the chemical composition is a critical parameter on materials as titanium, niobium or gallium arsenide that produce more than one stable oxide form.We addressed in particular the GaAs issue for its importance in the mesoscopic physics field.

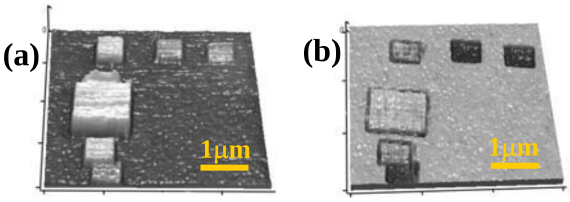

GaAs oxides structures of different thickness were produced by varying the writing voltages, writing speed, humidity and atmospheric composition. The chemical properties were studied by means of spatial resolved photoemission studies performed at the Nanospectroscopy Beamline at Elettra (Trieste).

We found that the chemical composition of the grown oxides depends strongly on the writing conditions. The oxide grown consists essentially of gallium oxide, while we did not observe presence of arsenic oxide. Thermal desorption studies confirmed this hypothesis because the grown structures are thermally stable up to 400^{o}C while arsenic oxides are expected to desorb at lower temperature. We suppose that arsenic reacts with hydrogen to form volatile gases during the oxidation process The oxidation process at low bias produces a thin layer of oxygen-rich gallium oxide (Ga_2O_3) while, increasing the bias the oxidation process produces a thick layer of low-oxygen-content oxide (Ga_2O) covered by a thin surface layer of Ga_2O_3. Finally we observed a strong oxide desorption after exposing the samples to a strong photon flux (10^{17} ph/sec/cm^2) with photon energy of 130eV. We found that the desorption process takes place in the first 30” after which a steady state is reached. A layer of 3nm to 5nm of oxide is removed, independently from the AFM oxidation process. We suppose that only the Ga_2O_3 is desorbed during this process. In the figure we show a structure created by AFM oxidation before (a) and after (b) photon exposure.

Collaboration: Nanospectroscopy beamline @ Elettra

Observation of strong coupling effects in intersubband resonators (Collaboration: NEST-INFM, Pisa)

Intersubband transitions are attracting increasing interest both for the implementation of new photonic devices (infrared cameras, quantum cascade lasers) and for fundamental physics studies, such as collective phenomena and many-body interactions in the excitations of the two-dimensional electron gas (2DEG). For such investigations and applications, it is crucial to understand and control the interactions of such transitions with the electromagnetic radiation in photon confinement structures. However, the development of microcavity structures is by far less developed than in the case of interband transitions, despite the interest related to this new spectral range, and to the peculiar potential advantages of this system (such as ultrafast relaxation times, tailorable oscillator strength, 2D coupling, etc.).

We have developed a modulation-doped GaAs/AlGaAs multiple quantum well (MQW) structure embedded in a microcavity resonator tuned to the intersubband electronic transition of the QW, with the aim of investigating modifications of the intersubband resonance due to the coupling with the cavity mode. Since the effective oscillator strength of the MQW structure must be high enough to observe substantial coupling effects, we had to incorporate a large number of QWs in the structure (17 in our case), and we had to take in account a relatively high carrier density in the individual wells (around $4X10^{11}cm^{-2}$). For photon confinement, a monolithic wavelength-size high-Q resonator was designed in the form of an oblique prism-shaped microcavity exploiting total internal reflection at the semiconductor-air interface on one side (surface), and at an $Al_{0.33}Ga_{0.67}As$/AlAs interface on the other. The cavity resonance was tuned on the intersubband transition energy (chosen to about 140 meV) for an incidence angle of about 60º, through accurate many-body calculations of the intersubband excitations.

To maximize the reflectivity, we optimized the growth protocol to reach an atomically smooth interface between the 3900nm-thick AlAs mirror and the cavity. Besides, were able to reach a doping uniformity better that 10% among the different modulation-doped QWs, as verified by low-temperature Shubnikov-de Haas oscillations.

Reflectivity spectra at a temperature of 10 K are reported in the figure for different angles of incidence within the GaAs waveguide, around a value of 60º. The dispersion of the reflectivity dips shows clearly an anti-crossing behavior, due to the strong coupling of the photonic cavity mode with the intersubband plasmon, thanks to the perfect tuning of the intersubband resonator. At resonance (about 60.05º) the reflectance shows two anti-crossed modes of mixed photon-plasmon character with comparable linewidths. The modes are separated by a Rabi splitting of 15 meV that, to our knowledge, was never observed before for intersubband transitions, although theoretically predicted. This strong coupling regime is observable also at room temperature where the splitting drops to ~10 meV. The result might open the way to the development of intersubband cavity electrodynamics. Further developments in the near future include the possibility of controlling externally the splitting of the transition by varying the 2DEG density in the wells, e.g., by applying a gate voltage to the MQWs.

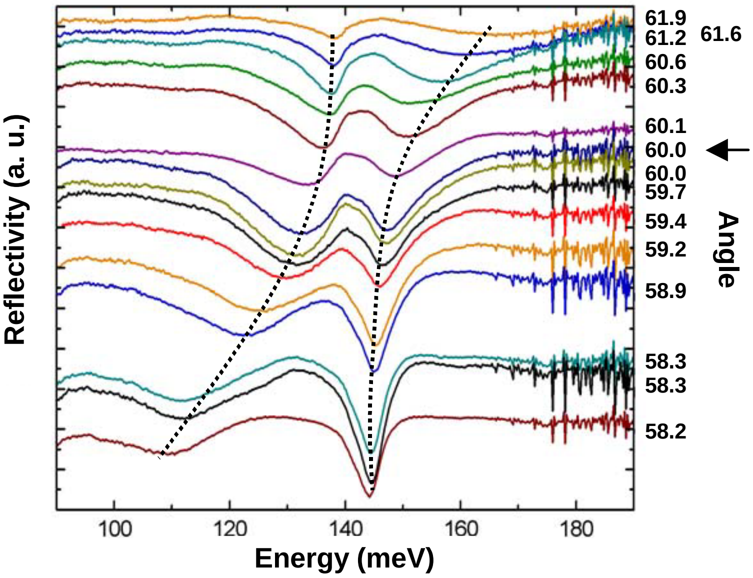

Fig. 1 Reflectance spectra at 10 K of the microcavity- intersubband resonance for various angles of incidence. The anti-crossing of the strongly coupled intersubband polaritons is clearly apparent. Dotted lines are added as a guide to eye.

Quasi-particle Tunneling between Fractional Quantum Hall Edges (Collaboration: NEST-INFM, Pisa)

Two dimensional electron gases (2DEGs) in the Fractional Quantum Hall (FQH) regime can give rise to “exotic” phenomena driven by electron-electron interactions. The fundamental charged excitations of FQH liquids are predicted to display a fractional charge and to obey fractional statistics. In addition, the one-dimensional edge states flowing at the border of incompressible FQH phases can form chiral Luttinger liquids.

Recent advances in nanofabrication and experimental techniques have opened the way to a higher level of understanding of FQH effect and to new research directions in condensed matter physics. In fact, mesoscopic systems are emerging as probes of the properties of correlated FQH states. Quantum point contact (QPC) constrictions, for instance, can be adopted to induce a controllable inter-edge scattering between two FQH edges. In the so-called *strong backscattering* regime one observes the tunneling of *electrons* between two quantum Hall fluids separated by the QPC. In the opposite limit of *weak backscattering* the quantum Hall fluid is weakly perturbed by the QPC constriction. In this case the inter-edge tunneling current for simple fractional states ($=1/q$, with q an odd integer) consists of Laughlin quasiparticles of charge $e^{*}=\ e$ that scatter between the edges through the quantum Hall fluid.

In this work we report the observation of nonlinear inter-edge tunneling in the *weak backscattering* regime. The devices here studied were realized starting from a high-mobility $\mathrm{GaAs/Al_{0.3}Ga_{0\,.7}As}$ 2DEG with low-temperature mobility $\sim 1\mathrm{X}10^{6}$ cm^{2}/Vs and density $n\sim 5\mathrm{X}10^{10}$ cm^{-2}. The 2DEG was located 140 nm from the surface. The measurements were performed in a dilution refrigerator. The QPC constriction was nanofabricated on Hall-bar mesas using e-beam lithography and Al metallization. The width and length of the QPC constriction were 300 nm and 600 nm, respectively. We present the inter-edge differential tunneling conductance dI_T/dV_T as a function of V_T in a wide range of T and . In the FQH regime our data cannot be described by electron tunneling but display the features of Wen's theory of quasiparticle tunneling. We demonstrate that while the differential tunneling characteristic shows the tendency towards a diverging behavior as the temperature is lowered at $=1/3$, it develops a peak at $V_T=0$ as T is increased (see Fig. 1). Width and shape of this zero-bias peak are determined by the fractional charge of the quasiparticle. We also discuss the results obtained for filling factors between $=2/3$and $=1/3$ that display an evolution not explained by current theories (see Fig. 2). We believe that these results combine to provide the first evidence of nonlinear quasiparticle tunneling in FQH systems.

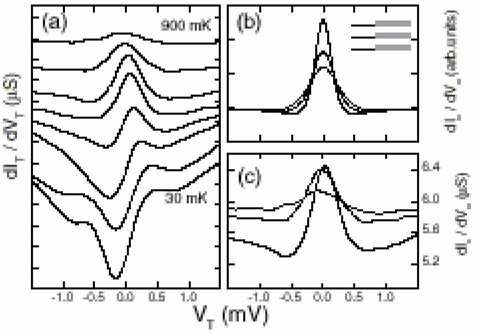

Fig.1. (a) Differential tunneling conductance (dI_T/dV_T) for filling factor $\nu=1/3$ at different temperatures (30, 100, 200, 300, 400, 500, 700, 900 mK from bottom to top). (b) Calculated dI_T/dV_T in the framework of the *weak-backscattering* theory at T = 500 ,700, and 900 mK. (c) Selected differential tunneling conductance curves at the same temperatures as in (b).

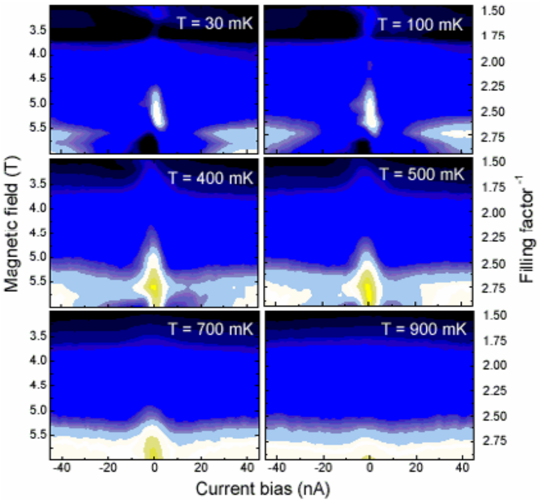

Fig. 2. Color plots of dI_T/dV_T as a function of the driving current I_{dc} and magnetic field at different temperatures. $\nu=1/3$ occurs at $B\sim 6$T. Bright yellow regions correspond to a high value of the tunneling conductance.

Collaboration: NEST-INFM, Pisa, Unversity of Roma Tre and University of Missouri

CRYOSNOM on patterned semiconductor structures

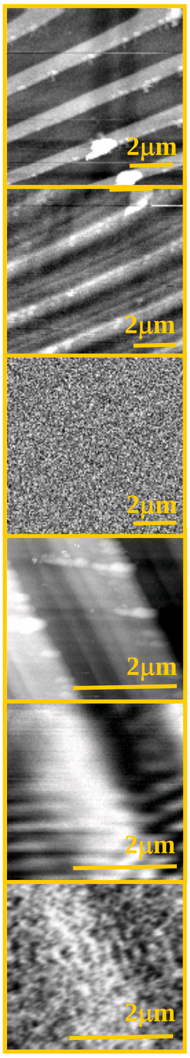

Low temperature optical spectroscopy with spatial resolution beyond the diffraction limit, is a fundamental tool to study the optical properties of nanostructured materials. Essential parameters to be controlled in an optical spectroscopy experiment are temperature and magnetic field, with huge number of exciting phenomena appearing only at very low temperatures. To this purpose, we developed a Scanning Near Field Optical Microscope (SNOM) able to operate at very low temperature (1.5K) and at high magnetic field (7T).

We choose two ideal benchmarks for set up characterization in the last year of activity.

Magnetic features were investigated on ferromagnetic nanopatterns made of permalloy. Topography and optical signals did not show any significant changes or distortion in magnetic field.

Spectroscopy potentialities were studied on a pre-patterned heterostructure. The sample consists of a GaAs/AlGaAs structure grown by molecular beam epitaxy, in which three separated quantum wells are formed. The quantum well thickness are, from surface to substrate, 2.5nm, 5.0nm and 10.0nm respectively. A titanium structure, consisting of a grating of period 2 μm, has been evaporated on top of the sample to shadow locally the optical emission.

SNOM images are reported in figure. The first three images from the top to the bottom are recorded at room temperature and correspond to topography, unfiltered optical signal and filtered optical signal, respectively. The filter used is tuned on the emission wavelength of the narrowest quantum well vat 10K. As the emission wavelength shifts with temperature, in the last picture we do not observe any contrast.

The last three bottom images are recorded at 5K: topography and unfiltered optical signal are unchanged but now the filtered signal shows a contrast given by light emitted from the sample. Finally, intensities of the quantum well spectra showed a completely different dependence on the distance from surface in near and far field. Normalized intensity in near field decays exponentially with the distance from surface, as expected for a pure near field luminescence.

Collaboration: Ape Research

Progetto PONTE –μpompe

The natural trend toward miniaturization, that first involved electronics, since several years is changing deeply the world of mechanics, and soon it will extend also to the fluidic environment. Mechanical devices miniaturized down to a micron scale are usually called MEMS (Micro Electro Mechanical Systems): typical examples are accelerometers in car airbags. The natural extension to the micro fluidics, with large impact applications such as local drug delivery systems, is the challenging task of this decade.

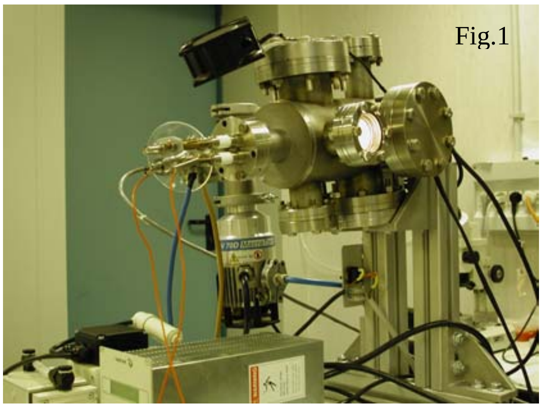

Fig.1

We started a project aimed at the developing of active and passive devices for the control of fluids at high pressure, based on anodic bonding and piezoelectric actuation.

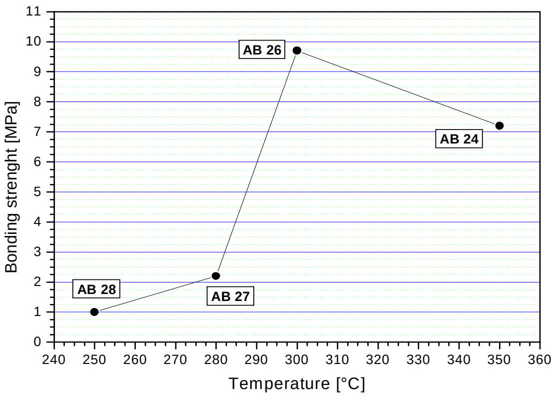

We built an home made anodic bonding machine, illustrated in Fig. 1, which operates with a base pressure of 1x 10^{-7}mbar, with a maximum temperature of 700°C and a maximum bias of 5kV. The pressure between the two bonding parts is controlled manually by a set of screws and an alignment stage is under development. We optimized the anodic bonding machine in order to achieve satisfactory bonding between silicon wafers (clean or covered by thin layers of silicon nitride) with standard microscope glasses. We developed a procedure that allows bonding on glasses without crakings due to thermal stress, that was never reported in literature. In Fig. 2 we show the maximum bond strength obtained as a function of bonding temperature. We also demonstrated bondability of silicon on silicon by eutectic bonding.

Future Developments

In the current year a new instrument will be acquired which will allow to perform magneto-transport measurements down to 300mK and with magnetic fields up to 14 T at lambda point

Pubblications 2002-2003

1. P. Machetta, M. Lazzarino, V. Kapeliouchko, T. Poggio, G. Canil, A. Sanguineti and V. Arcella, “PTFE nanoemulsions as ultralow-k dielectric materials” Macromol Symp. **179**, 347 (2002).
2. M. Lazzarino, S. Heun, B. Ressel, K. C. Prince, P. Pingue and C. Ascoli, “Atomic force microscope anodic oxidation studied by spectroscopic microscopy”, Appl. Phys. Lett **81**, 2842 (2002).
3. S. Heun, M. Rudolf, M. Lazzarino, B. Bonanni, L. Gregoratti, A. Barinov, B. Kaulich, G. Biasiol, and L. Sorba, “Morphology and chemistry of S-treated GaAs(001) surfaces”, Surf. Rev. Lett. **9**, 413 (2002).
4. E. Prati, S. Faralli, M. Martinelli, G. Annino, G. Biasiol, and L. Sorba, “Improved microwave Hall effect measurements method”, Rev. Sci. Instr. **74**, 154 (2003).
5. M. Cecchini, V. Piazza, F. Beltram, M. Lazzarino, M. B. Ward and A. J. Shields, H. E. Beere and D. A. Ritchie, “High-performance planar light-emitting diodes”, Appl. Phys. Lett. **82**, 636 (2003).
6. S. Roddaro, V. Pellegrini, F. Beltram, G. Biasiol, L. Sorba, R. Raimondi, and G. Vignale, “Nonlinear quasiparticle tunneling between fractional quantum Hall edges”, Phys. Rev. Lett. **90**, 046805 (2003).
7. D. Dini, R. Köhler, A. Tredicucci, G. Biasiol, L. Sorba, and F. Beltram, “Rabi splitting of intersubband cavity polaritons”, Phys. Rev. Lett. **90**, 116401 (2003).
8. G. Biasiol, L. Sorba, D. Dini, R. Köhler, A. Tredicucci, and F. Beltram, “Electron-Photon Strong Coupling in Intersubband Resonators”, Inst. Phys. Conf. Ser. (accepted).

Outgoing projects

2002-2003 PA-INFM INTERCON "Intersubband Confined Electrodynamics" in collaboration with NEST-INFM.

2002-2003 MIUR-COFIN "Stati collettivi di coppie elettroniche in sistemi duedimensionali" in collaboration with The Scuola Normale Superiore (Pisa).

2003-2005 MIUR-FIRB "Quantum phases of ultra-low electron density semiconductor heterostructures"in collaboration with the University of Modena, MDM-INFM, NEST-INFM.

2002-2003 INFM-PONTE "Hippy (Micromachined **Hi**gh **P**ressure **P**umps for H**y**drodinamics)".

2003-2004 INFM-PONTE "HASU (Sviluppo di sensori Hall a semiconduttore per misure locali di campo magnetico in ultra alto vuoto)".

MATERIALS DIVISION (Research Areas E1, E3)

E1

One of the main emphasis of the research activity has been on delta-doping and self-compensation during molecular beam epitaxy (MBE) of semiconductors. Even for the most widely utilized dopants in current technology, such as Si in GaAs(001) epilayers, there is little understanding of the microscopic mechanisms leading to self-compensation with increasing dopant density and its relation with the growth parameters. Fig. 1 shows a compilation of data from different authors (solid lines) showing the free electron density as determined from Hall measurements at room temperature as a function of the nominal Si coverage within the delta-doped layers in GaAs(001). Dramatic variations in the onset and extent of self-compensation are observed as a function of the Si deposition temperature and rate. We proposed to study self-compensation in Si delta-doped GaAs with a combination of experimental techniques, starting with the growth protocol most frequetly used in technology, involving Si deposition under As flux at the ordinary GaAs growth temperature of 600°C. Hall data for our delta-doped layers are denoted by blue squares in Fig. 1.

Samples were fabricated by MBE as single delta-doped layers (Fig. 1) but also as ten-period delta-doping superlattices for microscopy studies, with Si coverages within the delta layers ranging from 0.006 to 2 monolayers (ML; 1 ML=6.26×10^{14} cm^{-2}).

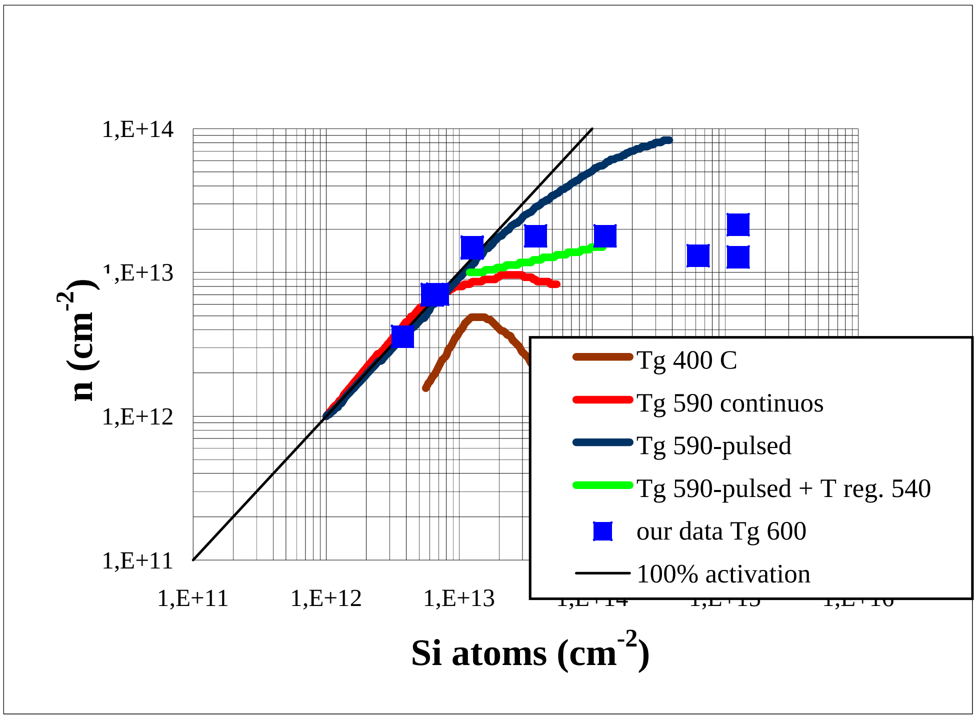

Fig. 1 Compilation of Hall data at room temperature for the free electron density in Si delta-doped GaAs(001) epilayers (1 monolayer, ML=6.26×10^{14} atoms/cm^2 (solid lines). The blue squares denote the corresponding results for the samples produced in Trieste at 600°C and used for the self-compensation studies.

The sheet carrier density was determined in the van der Paw geometry for as-grown samples (Fig. 1), and for single delta-doped layers subjected to post-growth annealing at 600°C (Fig. 2). The annealing time corresponded to the time required to fabricate the corresponding ten-period superlattice, so that the as-grown (annealed) Hall sample was representative of the last-deposited (first-deposited) delta-doped layer within the superlattice. Full electrical activation of the Si donors was observed for Si coverages up to 0.02 ML (Figs. 1-2). At higher Si coverages self-compensation yielded a coverage-independent carrier density of 1.5-2.0×10^{13} cm^{-2}. Upon annealing, the carrier density *decreased* by a factor of 2.5 to 3.0 in the self-compensated samples (Fig. 2), while it remained unchanged in the samples below the onset of self-compensation. This was the strongest indication to date that self-compensation involved sequential nucleation and growth processes, and a metastable equilibrium between two Si-phases.

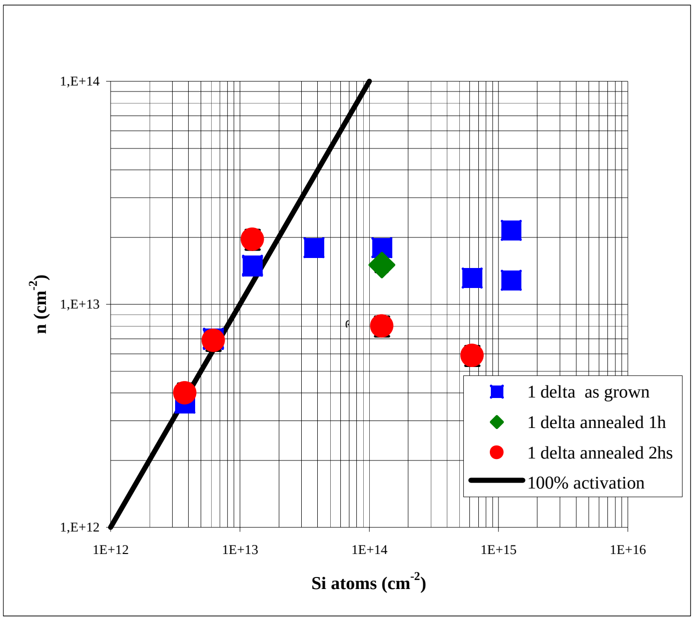

Fig. 2 Hall data at room temperature for the free electron density in single Si delta-doped layers fabricated by MBE at 600°C in GaAs(001). We show results for as-grown epilayers (blue squares) and following post-growth annealing for 1 and 2 hours at the growth temperature.

Cross-sectional scanning tunneling microscopy (XSTM) measurements were performed by Modesti et al. (F1) in ultra-high-vacuum on the superlattice samples, by cleaving the 0.1 mm-thick wafers *in situ* to yield atomically flat, electronically unpinned {110} surfaces normal to the [001] growth direction. Such studies showed only the presence of an asymmetric distribution of Si donor impurities on substitutional Ga sites in all samples below the onset of self-compensation. In the self-compensated samples XSTM revealed, instead, Si precipitates in the form of 1-2 nm-wide clusters at the nominal position of the delta-doped layers, superimposed to the broader distribution of isolated Si donors. Studies of the different periods within the superlattice showed a growth of the Si precipitates at the expenses of the free-donor Si phase with increasing time at the growth temperature, in qualitative agreement with the results of Fig. 2, together with the gradual diffusion toward the surface of the donor distribution. Si clustering was also observed by EXAFS techniques (see publication #226).

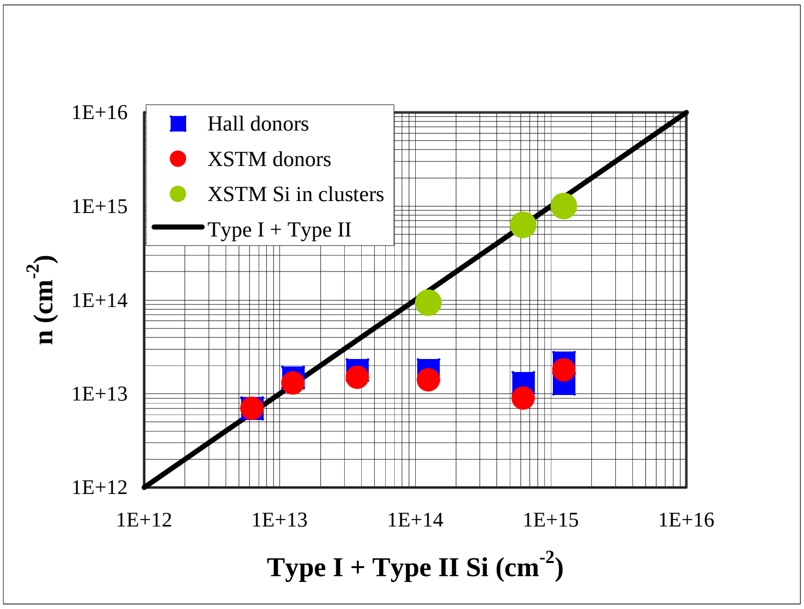

Fig. 3 Average concentrations of individual Si donors (red symbols) and of the Si atoms within the precipitates (green symbols) as derived from the XSTM studies of the superlattice samples. The concentration of free electrons derived from Hall measurements (blue symbols) and the overall Si coverage as derived from flux calibrations (solid line) are also shown for comparison.

The average concentrations of individual Si donors and of the Si atoms within the precipitates as derived from the XSTM studies of the superlattice samples are compared in Fig. 3 with the concentration of free electrons derived from Hall measurements and the overall Si coverage as derived from flux calibrations. The remarkable agreement between the two sets of data confirms the absence of individual Si acceptors and the neutral average character of the Si atoms within the clusters.

We conclude that, at least at 600°C, self-compensation in Si delta-doped GaAs involves nucleation and growth of Si precipitates, while the individual Si acceptors reported by other authors are notably absent. Tunneling spectroscopy and theoretical calculations (not shown) suggest that the precipitates locally pin the Fermi level near mid-gap. The Si-rich clusters are in metastable equilibrium with a second Si-phase, comprised of highly mobile isolated Si donor impurities on substitutional Ga sites, that accounts for the reported surface riding of the Si impurity distribution during MBE growth.

Another delta-doping system which is currently attracting much attention involves Mn impurities in GaAs for spintronic applications. Bulk doping of GaAs with Mn can be used to fabricate ferromagnetic Ga(1-x)Mn(x)As alloys, but the solubility of Mn in III-V semiconductors is comparatively low and its incorporation is possible in a very limited range of growth temperatures. Mn concentrations x achieved in Ga(1-x)Mn(x)As are between 0.02 and 0.08, and the substrate temperature needs to be comparatively low, typically ~ 250°C. However, for such a temperature the growth of many III-V semiconductors leads to the incorporation of excess anions in the epilayer, and arsenic-related point defects in Ga(1-x)Mn(x)As may alter deeply the properties of the magnetic layers. Large concentrations of As antisites have been observed by XSTM to give rise to donor states in Ga(1-x)Mn(x)As. Since the ferromagnetic properties of Ga(1-x)Mn(x)As are considered to be induced by hole-mediated indirect exchange, As antisites may pin the Fermi level away from the Mn-induced acceptor states and thus hinder ferromagnetism.

In addition to the issue of materials quality, a second related and important issue concerns the achievable Curie temperature. The low-temperature growth of GaMnAs limits the Mn content in the compound, thus also limiting the hole concentration and the Curie temperature that can be reached. The highest reported Curie temperature in bulk Ga(1-x)Mn(x)As is 110K, for epitaxial alloys with x=0.05 grown by low-temperature MBE.

Two methods have recently been proposed to overcome these problems, i.e., the growth of digital GaAs/MnAs alloys and delta-doping of GaAs with Mn. In both cases the basic idea is to achieve locally higher Mn concentrations where high hole densities can be trapped. We have begun studies of Mn delta-doping in GaAs, depositing Mn at room temperature onto GaAs(001)c(4x4) surfaces - in a deposition chamber interconnected with the main MBE chambers - and studying the onset of self-compensation as a function of Mn concentration and GaAs regrowth temperature.

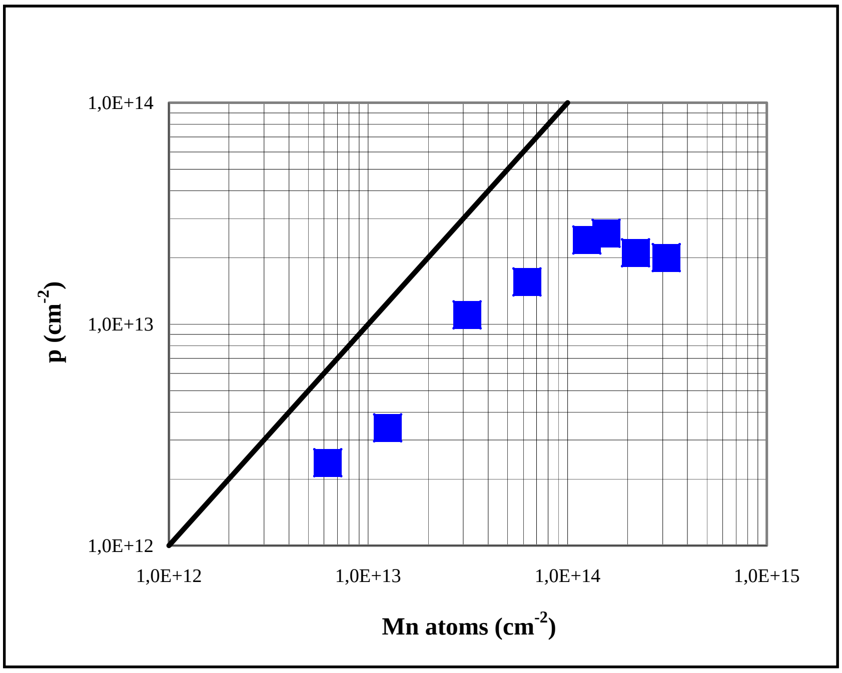

Fig. 4 Hall data at room temperature for the free hole density in single Mn delta-doped layers fabricated by MBE in GaAs(001). The GaAs regrowth temperature was 450°C. We show results for as-grown epilayers (blue squares). Post-growth annealing at 600°C did not change the measured hole density.

Representative results for a GaAs regrowth temperature of 450°C are shown in Fig. 4. The hole carrier density was obtained through Hall measurements. The overall Mn concentration was estimated from Mn flux calibrations using in-situ x-ray photoemission spectroscopy data (XPS) and confirmed *a posteriori* using secondary ion mass spectrometry (SIMS).

The data in Fig. 4 indicate that self-compensation in Mn delta-doped GaAs exhibits a behavior remarkably different from the case of Si. The maximum electrical activation rate of Mn is of the order of 50%, at a Mn coverage below 0.01 ML. Although such a value is over two orders of magnitude higher than that observed in bulk Ga(1-x)Mn(x)As alloys, where x values of a few percents correspond to maximum doping densities in the 10^{20} cm^{-3} range, it indicates that even in most favorable cases about half of the deposited Mn atoms do not behave as divalent impurities on substitutional Ga sites. Another remarkable observation is that although the GaAs regrowth temperature has an important affect on the Mn electrical activation, with maximum hole concentrations observed for temperatures in the 400 to 600°C, post-growth annealing has no effect on the measured hole concentration. Finally, the spatial distribution of Mn atoms was found to be very sensitive to the growth temperature. In Fig. 5 we show transmission electron microscopy results obtained by Carlino et al. (E5) on a five-period Mn delta-doped structure fabricated with a regrowth temperature of 315°C. Each Mn layer in the image correspond to a nominal coverage of 0.5 ML.

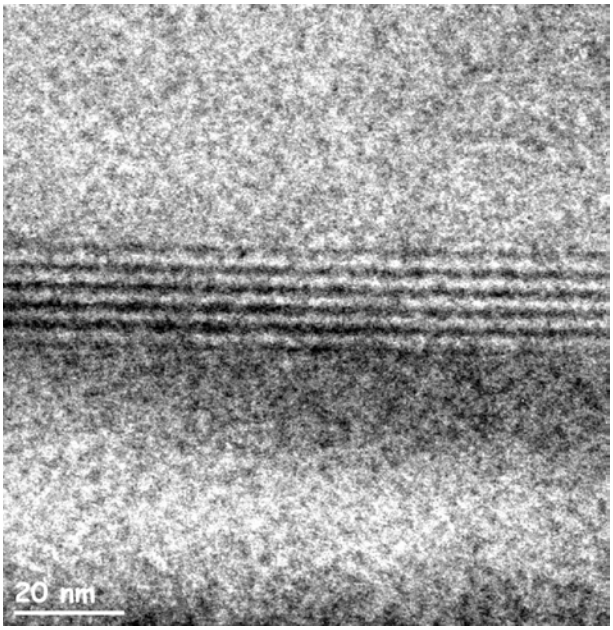

Fig. 5 Transmission electron micrograph of a five-period Mn delta-doped structure fabricated with a regrowth temperature of 315°C in GaAs(001). The Mn equivalent coverage in each layer was $3.1x10^{14}$ cm^{-2} (0.5 ML).

The apparent Mn delta-doped layer width is of the order of 1-2 nanometers in Fig. 5, but was found to increase to about 20 nm in the samples where GaAs regrowth occurred at 450°C. Clearly, to maximize exchange interactions and the resulting Curie temperature will be of paramount importance to find a trade-off between electrical activation and the spatial localization of the Mn atoms. The current record to beat for theCurie temperature is about 50 K for digital alloys where the native Mn-induced hole concentration was found to be sufficient to achieve ferromagnetism, and about 172 K in delta-doped GaAs where the hole concentration was boosted using a modulation-doped structure containing AlGaAs:Be layers.

Other work in progress targeting the development of new materials is focussed on Ga(1–x)In(x)As(1–y)N(y) and Ga(1-x)In(x)As alloys. The former material system is being addressed by a large number of investigators for the development of 1.3 and 1.55 µm emitters on GaAs. The COFIN project "New materials for long-wavelength emitters on GaAs" (A. Franciosi national coordinator), funds the development of these materials at TASC. The INFM PRA project "Cross-sectional scanning tunneling microscopy and spectroscopy of semiconductor nanostructures" (A. Franciosi co-principal investigator) funds their characterization by means of XSTM and TEM. An initial practical problem was that the rf nitrogen plasma source successfully used to grow GaN did not allow elemental nitrogen flux rates low enough for the growth of high quality Ga(1–x)In(x)As(1–y)N(y) alloys. We therefore implemented a new gas mixing chamber with a ultra-high-vacuum compatible gas manifold and run the rf plasma sources using Ar/nitrogen mixtures.

Pseudomorphic GaAs(1-y)N(y), alloys were initially grown on GaAs(001) buffer layers to calibrate the rf plasma source. Reciprocal space maps recorded with a double crystal x-ray diffractometer were used to gauge strain and nitrogen incorporation. The measured experimental data are shown in Fig. 6 (red symbols) together with results from the literature. Nitrogen concentrations up to 3-4% were easily obtained, with good overall structural quality of the epilayers, as derived from reciprocal space maps.

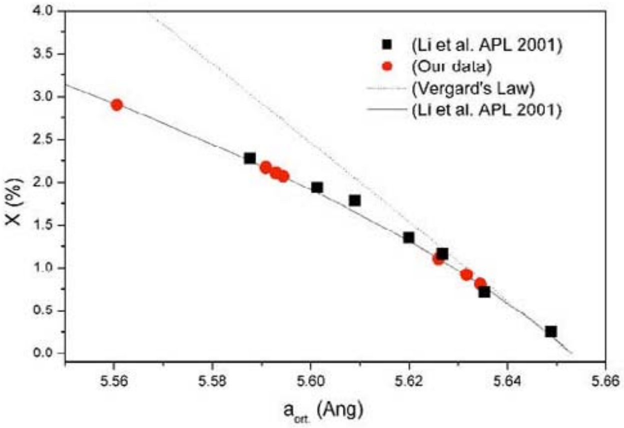

Fig. 6 Composition of pseudomorphich GaAs(1-y)N(y) epilayers grown in Trieste on GaAs(001) using rf plasma-enhanced MBE (red symbols). Recent results from the literature are also shown for comparison (black symbols). The dashed line shows the behavior expected from Vegard's law.

Photoluminescence (PL) studies of the same samples showed, however, that only samples grown with minimum rf power yielded competitive optical properties. We therefore followed a double approach: First, we kept the rf power to a minimum and used to Ar/N ratio and the growth rate to control the composition. Second, we developed post-growth annealing protocols to minimize non-radiative recombination channels. The two strategies proved successful, as demonstrated by the representative PL data in Figs. 7-8.

In Fig. 7 we show the PL emission obtained from a 0.1 µm-thick GaAs(0.93)N(0.07) epilayer pseudomorphically grown on a GaAs(001) buffer layer, before (blue line) and after (red line) a post-growth annealing cycle of one hour at 640°C. The effect of the annealing cycle is a drastic reduction of the emission at 0.8-1.0 eV, deriving mainly from pont defects, and a large enhancement and sharpening of the near-band-edge (NBE) emission at 1.1 eV.

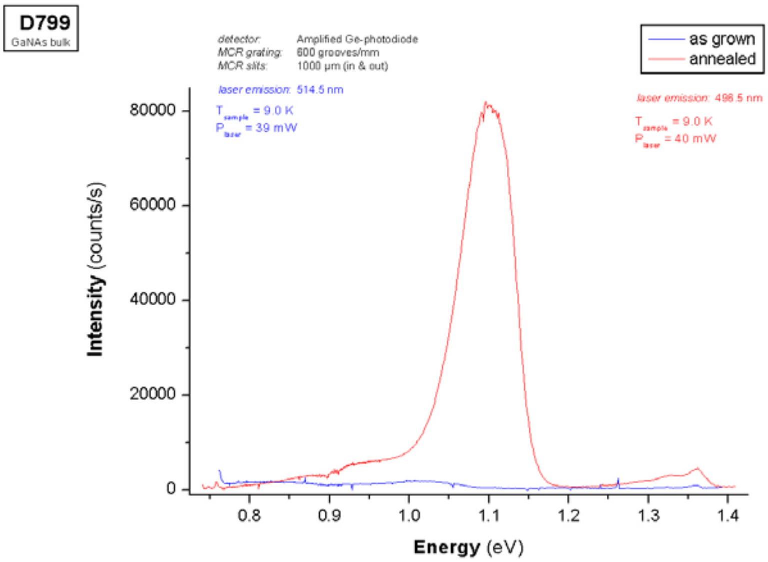

Fig. 7 PL measurements at 9.4 K for a 0.1 µm thick pseudomorphic epilayer of GaAs(0.97)N(0.03) grown by rf plasma-enhanced MBE at TASC. Optical excitation was performed using the 496.5 nm line of an Ar ion laser and 40 mW of cw power. We show results from the as-grown sample (blue line) and from the same sample following a one-hour annealing cycle at 640°C (red line).

Finally, in Fig. 8 we show PL results from a sample that included a first quaternary Ga(1-x)In(x)As(1-y)N(y) quantum well (QW) and a second ternary Ga(1-x)In(x)As QW grown with identical nominal values of the In concentration x (0.15) and well width W (6.0 nm). We show results from the as-grown sample (blue line), and from the same sample following an post-growth annealing cycle of one hour at 670°C (red line). The data for the ternary QW are consistent with x=0.165 and W=5.6 nm, in good agreement with the nominal values. The quaternary well gives rise to a main optical transition at 0.95 eV, with intensity about two orders of magnitude lower than that of the ternary well (blue line). Following the annealing cycle, the quaternary QW emission sharpens and shift to about 1.05 eV, and its intensity reaches about 20% of that of the ternary QW.

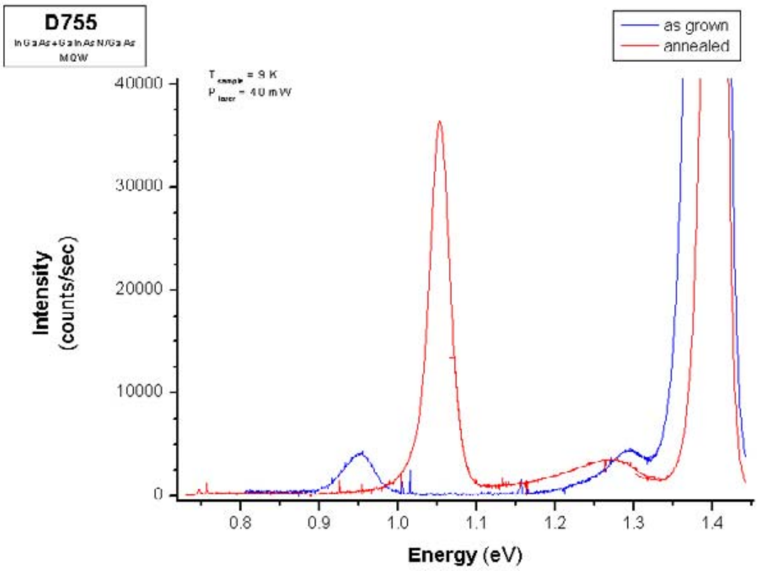

(a)

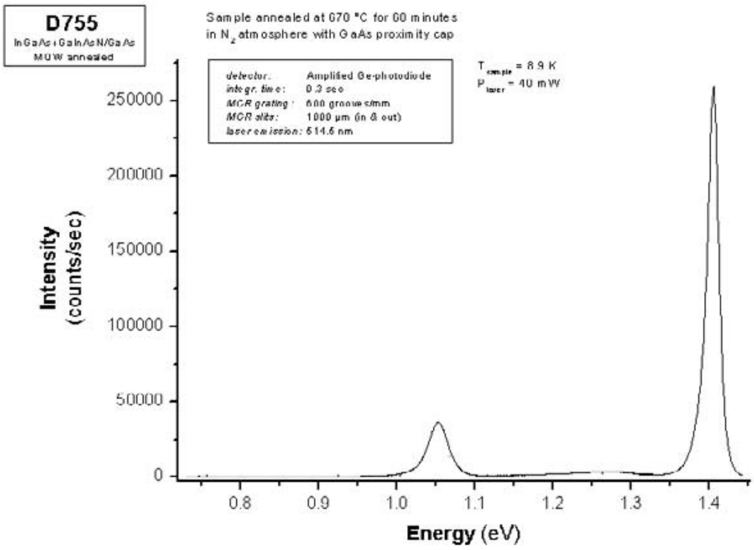

(b)

Fig. 8 PL at 9 K from a GaAs(001) epilayer containing a Ga(1-x)In(x)As(1-y)N(y) quaternary quantum well and a Ga(1-x)In(x)As ternary quantum well of 6.0 nm nominal thickness and x=0.15 fabricated by rf plasma-assisted MBE at TASC. Optical excitation was performed using the 496.5 nm line of an Ar ion laser and 40 mW of cw power. We show results from the as-grown sample (blue line) and from the same sample following a one-hour annealing cycle at 670°C (red line).

We consider the sample of sufficient quality to be employed in a number of projects at TASC and elsewhere. In particular, XSTM and TEM studies of alloy fluctuations and of the effect of annealing are in progress at TASC; time-dependent PL studies as well as optical and electrically -pumped studies of the stimulated emission, are in progress at the University of Lecce; channeling and RBS studies will be performed at the University of Padova.

E.3

In the area of II-VI semiconductors, we performed studies of the native defect density as a function of interface growth parameters, exploiting the new TEM analyitical tools available at TASC to gain a deeper understanding of the interface composition. Epitaxy of high-quality II-VI semiconductor layers on III-V semiconductor substrates is an important process with potential applications ranging from the fabrication of spin-filters in spintronics to the implementation of visible emitters in optoelectronics. The native defect density and, in general, the structural quality of the II-VI/III-V interface are crucial issues for all of the proposed applications. Stacking faults (SFs) nucleating at the II-VI/III-V interface and extending throughout the II-VI epilayers represent the main type of native defects and have been related to the degradation of blue-green emitters. Device lifetimes of several hundred hours have been achieved only by reducing the native SF density below 10^4 cm^{-2}.

It is generally accepted that the initial conditions in which the II-VI/III-V interface is fabricated controls the SF density, but several contrasting protocols have been proposed to minimize the defect density. Exposure of the initial III-V surface to a Zn flux prior to II-VI growth has been considered an essential step by some authors. Other authors have reported that initial II-VI growth in Se-rich conditions was effective at reducing the SF density, while initial growth in Zn-rich conditions would actually *increase* the SF density.

We examined the effect of Zn predosing, Se predosing, Zn-rich initial growth conditions, Se-rich initial growth conditions, migration-enhanced epitaxy (MEE), and related combinations on the native defect density in pseudomorphic ZnSe/GaAs(001) heterostructures. We employed the procedures listed above to fabricate the interface, and assessed the structural quality of the epilayers by etch-pit density measurements and high-resolution XRD. The composition of the ZnSe/GaAs interface was investigated by XPS *in situ* and by cross-sectional TEM. The corresponding band offsets were determined *in situ* by XPS.

Of the different procedures examined only two gave rise to consistent, large reductions in stacking fault densities (to below 10^4 cm^{-2}), namely: a) Zn predosing of the GaAs surface followed by migration-enhanced epitaxy with relatively short periods (3 s); b) Initial fabrication of the interface in Se-rich growth conditions (Zn/Se beam pressure ratio ~0.1), in the absence of *any* predosing of the III-V surface. All other protocols, including all attempts at combining procedures a) and b), proved ineffective or detrimental. Despite the apparent differences, the two optimum protocols were found to yield quantitatively similar defect densities, and qualitatively similar Se-rich interface compositions and band alignments. In particular, TEM and energy-dispersive spectroscopy (EDS) studies revealed in both cases a ternary GaInSe interface composition with a complete As-depletion of the interface.

Z-contrast imaging and the observed interface strain were both found to be consistent with the presence of vacancies on the cation sublattice, as required for charge neutrality within the ternary interface layer. These results proved that existing models (Yao and co-workers) relating low native stacking fault densities to ZnAs-like interface reaction products and high stacking fault densites to Ga_2Se_3-like products are consistently wrong.

Finally, we have initiated a feasibility study of the use of 3d transition metal impurities (Fe, Cr) in II-VI epilayers for the implementation of infrared (IR) emitters exploiting atomic-like d-d intrashell transitions. The relatively large solubity of divalent transition metal impurities in II-VI semiconductors should give these materials an edge relative to III-V materials such as InP:Cr, if the coupling between the atomic-like d-d intrashell transitions and the band edges will provide for a sufficient oscillator strength as a function of temperature an impurity concentration. Also, the possibility that wide bandgap II-VI materials - notoriously degradation-prone in blue-green lasers - will be more resilient for IR emitters in view of the reduced photon energies involved, will have to be tested.

Our initial studies have targeted Fe impurities in ZnSe epilayers, grown by MBE on GaAs buffers. The Fe impurities were deposited using delta-doping protocols in a separate chamber interconnected with the main MBE chambers. The effect of increasing Fe coverages and post-growth annealing cycles is also being addressed.

In Fig. 9 we show PL data recorded at the University of Bari (Scamarcio et al.) from a 100 nm ZnSe epilayer pseudomorphically grown on GaAs(001) with a single Fe delta-doped layer at the center (nominal thickness 0.03 ML), after a post-growth annealing cycle of one hour at 300°C. Optical excitation was performed using the 442 nm and 325 nm lines of a He-Cd laser, 80 mW of cw power, and a Fourier-transform IR spectrometer with a resolution of 2 cm^{-1}.

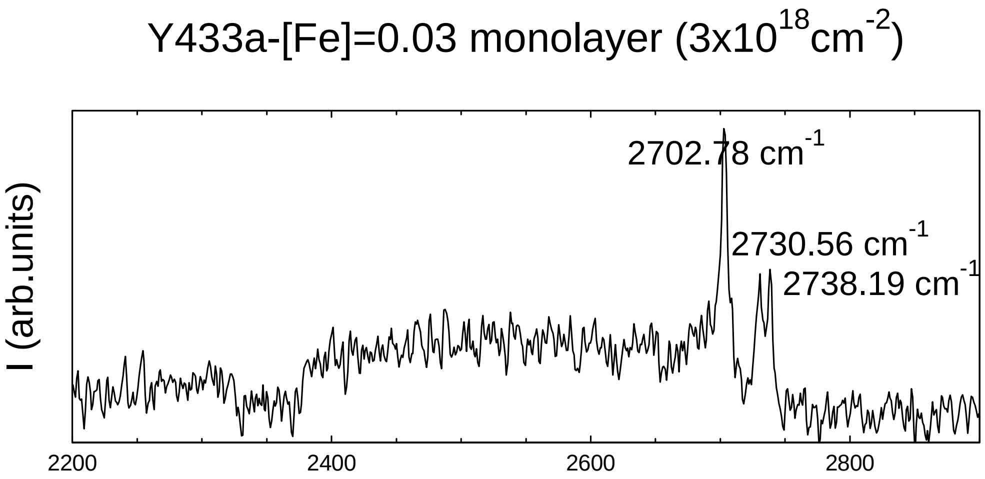

Fig. 9 PL data from a 100 nm ZnSe epilayer pseudomorphically grown on GaAs(001) with a single Fe delta-doped layer at the center (nominal thickness 0.03 ML), after a post-growth annealing cycle of one hour at 300°C. Optical excitation was performed using the 442 nm and 325 nm lines of a He-Cd laser, 80 mW of cw power, and a Fourier-transform IR spectrometer with a resolution of 2 cm^{-1}.

The spectrum in Fig. 9 shows three peaks at 2703 cm^{-1}, 2731 cm^{-1}, and 2738 cm^{-1} that are characteristic of Fe^{2+} states in ZnSe. The spacing (8 cm^{-1} and 28 cm^{-1}) and the relative intensities of the peaks suggest that they derive from the 6-2, 6-3 and 6-4 allowed transitions bweteen level 6 ($^5T_2$) and the spin-orbit split (^5E) levels, by analogy with intra-atomic transitions of Fe in CdTe and ZnSe. The absence of the 6-1 transition is also typical. The broad band in the 2200-2650 cm^{-1} range might be associated with phonon-assisted transitions, since its intensity is affected very strongly by temperature.

Our initial studies suggest that the intensity of the IR emission features is strongly non monotonic with Fe concentration, increasing with increasing impurity concentration to reach a maximum and then decrease at higher concentrations, possibly as a result of the modification of the near-band-edge states character in the concentrated alloy limit.

GRANTS

In 2002 the work of the Materials Division of the TASC-INFM National Laboratory was supported by the following grants and contracts:

COFIN national project "New materials for long-wavelength coherent emitters on GaAs" (A. Franciosi National Coordinator). Includes the University of Lecce and the University of Trieste Theoretical Physics Department. It funds the development of Ga(1-x)In(x)As(1-y)N(y) materials at TASC. [435.000 EUR total over 2 years; 161.000 EUR for TASC]

INFM advanced research project PRA "Cross-sectional scanning tunneling microscopy and spectroscopy of semiconductor nanostructures" (A. Franciosi Co-Principal Investigator; S. Modesti Principal Investigator). Includes the MASPEC Institute of CNR and the University of Trieste Theoretical Physics Department. Among other things, it funds the characterization of semiconductors by means of XSTM and TEM. [422.000 EUR total over 3 years; 273.000 EUR for TASC].

Project 5A, Workpackage 2, Cluster 26 on Advanced Materials (488/92), "Implementation of a center for high resolution applied microscopy" (A. Franciosi Principal Investigator). Among other things, it funds the characterization of semiconductors by TEM, AFM and XSTM.. [981.000 EUR over 4 years].

Optical Technologies Italia S.p.A., "Development of new materials for semiconductor lasers for optical communications". It funds a PhD fellowship for of Ga(1-x)In(x)As(1-y)N(y) MBE. [42.000 EUR over 3 years].

PUBLICATIONS

223. F. Barbo, M. Bertolo, A. Bianco, G. Cautero, R. Cimino, S. Fontana, A. Franciosi, T.K. Johal, S. La Rosa, D. Orani, M. Piccin, R.C. Purandare, S. Rubini, and N. Svetchnikov, "Cross-sectional Photoemission Spectromicroscopy of Semiconductor Heterostruc-tures", in *Nanoscale Spectroscopy and its Applications to Semiconductor Research*, Y. Watanabe, S. Heun, G. Salviati, N. Yamamoto, Eds., Lecture Notes in Physics Vol. 588 (Springer, Heidelberg, 2002), p. 121-130.
224. F. Barbo, M. Bertolo, A. Bianco, G. Cautero, S. Fontana, T.K. Johal, S. La Rosa, R.C. Purandare, N. Svetchnikov, A. Franciosi, D. Orani, M. Piccin, S. Rubini, and R. Cimino, "Cross-sectional Studies of Buried Semiconductor Interfaces by means of Photoemission Microscopy", Appl. Phys. Lett. **80**, 2511 (2002).

225. F. Barbo, M. Bertolo, A. Bianco, G. Cautero, S. Fontana, T.K. Johal, S. La Rosa, R.C. Purandare, N. Svetchnikov, A. Franciosi, D. Orani, M. Piccin, S. Rubini, and R. Cimino, "Photoemission Microscopy Investigation of Buried p-n GaAs Homojunctions and Al/n-GaAs Schottky Barriers", Surf. Rev. Lett. **9**, 249 (2002).
226. F. Boscherini, N. Ferretti, B. Bonanni, D. Orani, M. Piccin, and A. Franciosi, “Silicon Clustering in Si-GaAs -doped Layers and Superlattices”, Appl. Phys. Lett. **81**, 1639 (2002).
227. S. Modesti, A. Furlanetto, M. Piccin, S. Rubini, and A. Franciosi, “High-resolution Potential Mapping in Semiconductor Nanostructures by Cross-sectional Scanning Tunneling Microscopy and Spectroscopy”, Appl. Phys. Lett. **82**, 1932 (2003).
228. A. Colli, E. Pelucchi, and A. Franciosi, “Controlling the Native Stacking Fault Density in II-VI/III-V Heterostructures”, Appl. Phys. Lett. **83**, 81 (2003).
229. E. Carlino, S. Modesti, D. Furlanetto, M. Piccin, S. Rubini, and A. Franciosi, “Atomic Resolution Composition Analysis by Scanning Transmission Electron Microscopy High-angle Annular Dark-field Imaging”, Appl. Phys. Lett. **83**, 14 July (2003).

Surface phase transitions (Research Area F1)

Coordinator:	Silvio Modesti
Staff:	Gustavo Ceballos Roberto Duca Paola Finetti Christophe Nacci

The group is studying a) quasi two-dimensional metals on semiconductor surfaces by STM, photoelectron diffraction and high-resolution photoemission, b) nanostructures in semiconductor by cross-sectional STM; c) functionalized carbon nanotubes by STM. Active collaborations are with the groups led by Franciosi and Rossi at TASC, and by Mariani at S3, Modena. The group is funded by INFM (PRA XSTM) and MIUR (FIRB Carbon based microstructures and nanostructures, PRIN New frontiers of the physics of surfaces, nanowires and nanoclusters)

Valence fluctuations in a quasi two-dimensional metal on Si: Sn/Si(111)-(√3x√3)R 30° ?

1/3 of a monolayer of tetravalent adatoms on Si(111) and Ge(111) forms metallic surfaces. In Sn/Ge(111) and Pb/Ge(111) the low temperature phase is an ordered (3x3) structure with 1/3 of the adatoms risen by about 0.3 angstrom with respect to the others. These kinds of structures have been explained within the one-electron theory, and recently in terms of charge disproportionation. At high temperature the (3x3) phase undergoes an order-disorder transition to a (√3x√3)R30° phase that retains the difference in height between the two kinds of inequivalent adatoms.

The presence of two component in the Sn 4d core level spectra and the valence band photoemission data indicates two inequivalent Sn atoms also in Sn/Si(111)-(√3 x √3). However scanning tunneling microscopy experiments at 6 K and low energy electron diffraction measurements at 70 K indicates that all the Sn atoms have the same position even at low temperature. A possible explanation is that Sn/Si(111) -(√3 x √3) is dynamically disordered, similarly to Sn/Ge(111)) at high temperature. In the case of a dynamic structural distortion slow techniques, such as STM, measure the average position, that may be the same for all the adatoms, while fast structural techniques, such as the photoelectron diffraction (PED), should be able to measure the actual instantaneous position of the inequivalent adatoms without time averaging, as demonstrated in the case of Sn/Ge(111).

We have measured the intensity of the two component of the photoemission peaks of the Sn 4d core levels of the Sn/Si(111)- (√3 x √3)R30° surface at 30 K as a function of the photon energy (150 eV < hν < 550 eV), the emission angle and the defect density at the SuperESCA beamline of the Elettra storage ring. An example of the PED modulation functions for normal emission data from the surface with the lowest defect density are shown in Fig. 1. In contrast to the case of Sn/Ge(111)- (√3 x √3)R30° , where the Sn layer is rippled and the modulation functions of the two components are different, the functions of Sn/Si(111)- (√3 x √3)R30° are the same within the experimental error in all the direction we have measured. The multiple scattering analysis indicates that the Sn-Si bond lengths are 2.70 Å, the bond angles is 51°, and the distance between the Sn atoms and the Si atoms directly below is 2.87 Å for both components. These numbers are in agreement with the values obtained by calculations based on the density functional theory for a undistorted Sn layer.

The angle-resolved photoemission spectra measured on the same system at 30 K are similar to those measured at 300 K. This is again in contrast to the case of Sn/Ge(111)- (√3 x √3)R30°, where the temperature dependence is strong. The measured dispersions of the surface bands do not agree with those calculated either for a flat or for a rippled Sn layer. A fluctuating valence state is a possible explanation of our results.

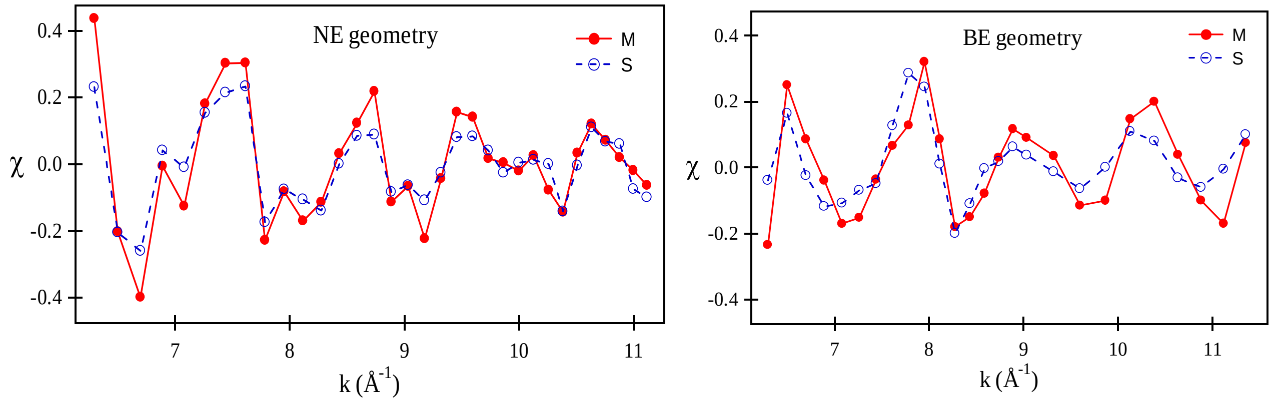

Fig. 1 Modulation functions of the photoemission intensity of the two components of the Sn 4d photoemission peaks as a function of the photoelectron wavevector measured along the surface normal (NE geometry) and along the Sn-Si bond (BE geometry) at 30 K. The small differences between the modulations of the two components are caused by small quantities of a second mosaic phase, and not by differences of bonding geometry.

This work has been done in collaboration with L. Petaccia (Sincrotrone Trieste), L. Ottaviano (INFM unit of L'Aquila) and I. Vobornik (TASC)

The Structure of Functionalized Carbon Nanotubes

The organic functionalization of carbon nanotubes can make their manipulation and integration in new materials and devices easier. It has already been shown that the functionalization can make the nanotubes much more soluble and easy to purify. Work is in progress on the formation of composite materials. One of our aims is the exploitation of the functionalization to bond the tubes to specific sites on a nanopatterned or micropatterned substrate and to integrate them in devices. The structure of the functionalized nanotubes, their electronic properties, the density of the added groups and the length of the tubes after the functionalization are still unknown. We are using scanning tunneling microscopy (STM) and high-resolution transmission electron microscopy (HRTEM) to analyze the structural and electronic modifications induced by the functionalization.

Single wall carbon nanotubes functionalized with ferrocene with a method based on 1,3-dipolar cycloaddition of azomethine ylides have been studied both with STM in ultra-high vacuum and by HRTEM. The ferrocene can easily donate electrons to the nanotubes. The figure shows some of these tubes on an Au(111) substrate. The STM images of these tubes differ from those of the original ones for several aspects. The modified nanotubes tend to form more ordered linear or structures, they are appreciably shorter, they have an apparent roughness caused by the added groups, and the tube-tube distance increases by an amount comparable to the size of the added groups. The motion of the added chemical groups during the image acquisition cause blurring of the details. The images are only preliminary. A more detailed study of the distribution of the added

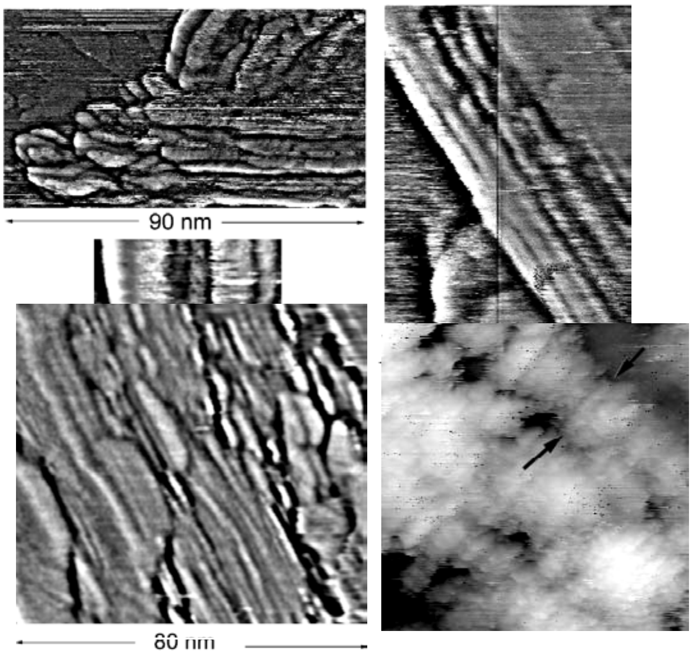

Figure 1. STM topographic images of single wall carbon nanotubes functionalized with ferrocene. The structures along the tubes are caused by the added chemical groups. The size of the image at bottom right is 70x70 nm2, the arrows point to the tips of a single short nanotube.

chemical groups, of the methods for fixing the tubes on the substrate, and of the electronic structure of the new systems is in progress.

This work is supported by the FIRB strategic project “Carbon based microstructures and nanostructures”. It is done in collaboration with M. Prato (University of Trieste) and L. Vaccari (TASC)

.

Publications

S. Modesti, D. Furlanetto, M. Piccin, S. Rubini, A. Franciosi
High-resolution potential mapping in semiconductor nanostructures by cross-sectional scanning tunneling microscopy and spettroscopy; Applied Physics Letters 82, 1932 (2003)

E. Carlino, S. Modesti, D. Furlanetto, M. Piccin, S. Rubini, A. Franciosi
Atomic resolution compositional analysis by scanning transmission electron microscopy high-angle annular dark-field imaging; Applied Physics Letters 83 in press (2003)

Coss-sectional scanning tunneling microscopy and spectroscopy of δ-doped layers, quantum wells and quantum dots in GaAs

S. Modesti,[a] R. Duca, [a] P. Finetti, G. Ceballos, M. Piccin, S. Rubini, and A. Franciosi[a]Laboratorio Nazionale TASC-INFM, S.S. 14, Km. 163.5, 34012 Trieste, Italy
[a] *Dipartimento di Fisica, Universita' di Trieste*

Cross-sectional scanning tunneling microscopy (XSTM) allows studies of the local morphology, composition and electronic structure of semiconductor nanostructures with unparalleled spatial resolution. We have applied this technique to investigate three challenging aspects of current naostructure physics: 1) defects, self-compensation and quantum well formation in Si and Mn layers in GaAs; 2) local alloy fluctuations in InGaAs and InGaAsN quantum wells in GaAs; 3) structure and defects of InAs quantum dots in GaAs.

The technique of δ-doping has an important role in modern technology. It is widely utilized to exceed the bulk solubility limit of important technological dopants in materials systems as diverse as GaAs:Si, GaN:Mg, and ZnSe:N. The nature of the microscopic mechanisms that allow us to obtain in such pseudo-2D structures local free-carrier densities that greatly exceed what can be achieved in the bulk is far from clear. The process of self-compensation, which determines the doping limit achievable, has been variably associated to the formation of isolated point defects, defect complexes, precipitates, or to an amphoteric behavior of same impurity in the high concentration limit. Only indirect information has been gained on this subject, and only for very few materials systems.

Si in GaAs

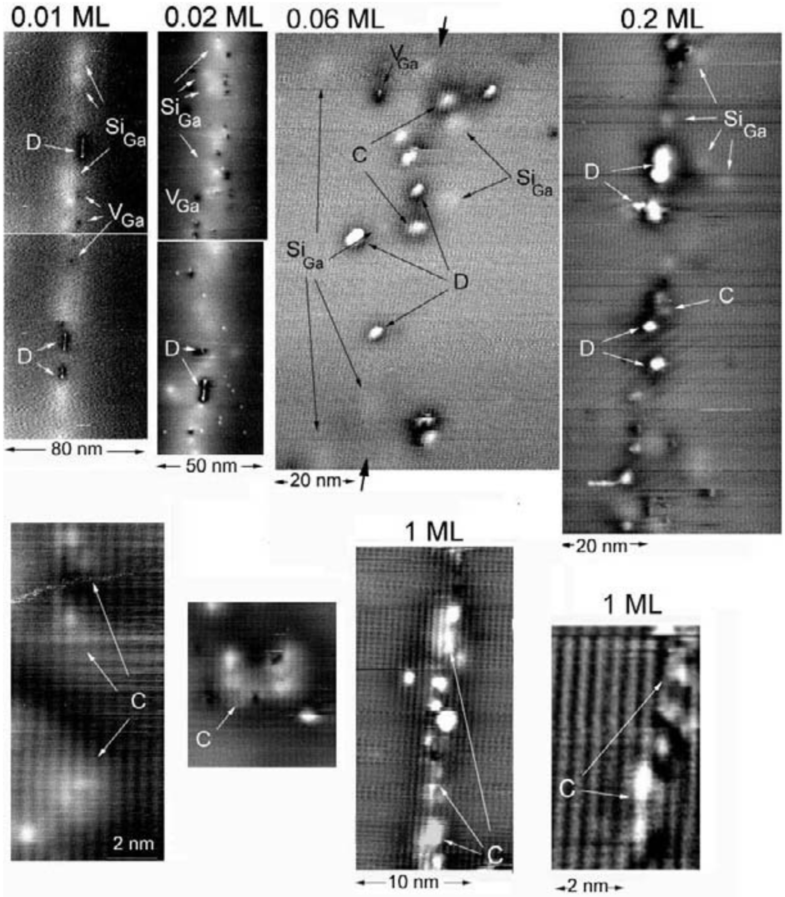

Figure 1. Cross-sectional STM images of layers of Si in GaAs. Si_{Ga} silicon donors, V_{Ga} surface gallium vacancies, C silicon rich regions, D cleavage defects

Fig. 1 shows some of our XSTM topographic images of the intersections of δ-doped layers and quantum wells of Si in GaAs with (110) cleavage surface as a function of the Si surface density. These images show the evolution of the Si layers for increasing concentration, from 0.01 ML up to 2 ML. At 0.01 and 0.02 monolayers of Si only isolated subsurface Si_{Ga} donors, surface Ga vacancies (V_{Ga}) and cleavage defects (D) are present. The surface vacancies form after the cleavage and their number increases with time. The donors are positively charged. At 0.06 and 0.2 ML Si-rich regions (C) –about 1 nm wide-appear. The isolated Si_{Ga} donor density stays constant close to the value reached at 0.02 ML, most of the Si is in the Si-rich regions. At 1 and 2 ML of Si the Si-rich regions form a nearly continuous plane about 2 nm wide (a line in the (110) section). About 1% only of the Si is dispersed as isolated donors outside these planes.

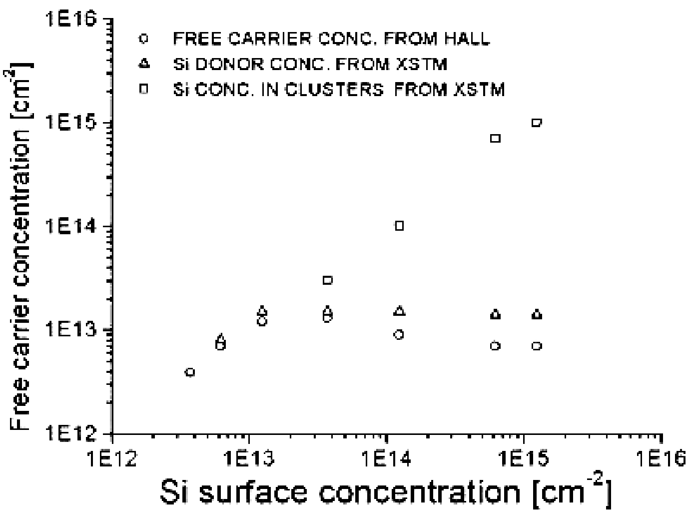

Figure 2. Surface free carrier concentration from Hall measurements (circles), Si_{Ga} concentration (triangles) and Si concentration in clusters (squares) from XSTM data as a function of the nominal Si surface concentration.

.

The density of the isolated Si donors measured by XSTM agrees with the density of the free carriers measured by transport experiments within the experimental errors (see Fig.2). The sum of the Si_{Ga} density and of the density of the Si atoms in the Si-rich regions agrees within the experimental error with the nominal Si density. The density of other defects, including possible Si_{As} acceptors, is about one order of magnitude lower than that of Si_{Ga}. Therefore the main compensation mechanism of Si at high density in δ-doped layers is the formation of the Si-rich regions that capture the majority of the Si atoms at and above 0.06 ML. By comparing the XSTM images with the simulated images of selected Si clusters in GaAs we conclude that most of the Si is in the substitutional Ga sites also in the Si-rich regions.

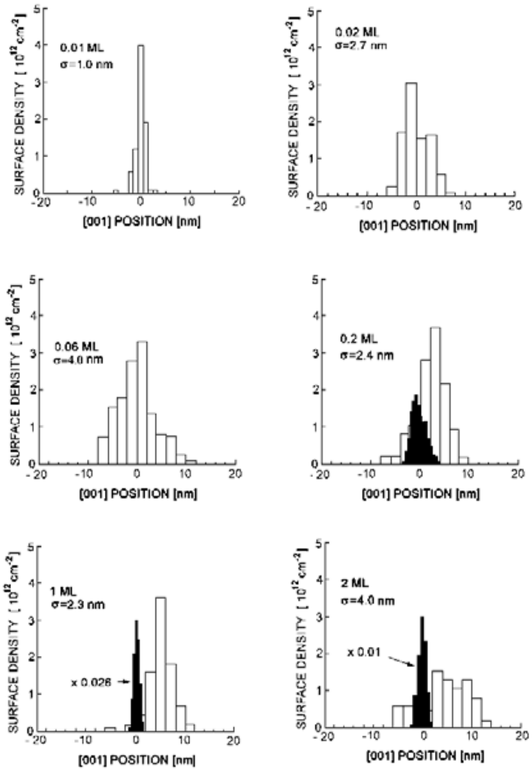

Fig. 3 Distributions of the Si_{Ga} donors (light) and of the Si in the Si-rich regions (dark) along the (001) growth direction for different Si surface concentrations.

Fig. 3 shows the distribution of the Si_{Ga} donors and of the Si in the C regions along the growth direction as a function of the Si surface density. The standard deviation of the Si_{Ga} distribution increase from 0.9 nm to 4 nm from 0.01 to 0.06 ML, decreases up to 1 ML, and increases again up to 4 nm at 2 ML. The width of the distribution is proportional to the Si_{Ga} donor density. The center of the distribution shifts in the growth direction by 2, 4 and 6 nm for n_s=0.2, 1 and 2 ML respectively, with respect to the position of the Si-rich region. We attribute the broadening of the Si_{Ga} distribution for increasing Si_{Ga} density to Coulomb-repulsion-enhanced diffusion of impurities (at the concentration observed at 0.02 ML the Si-Si distance is comparable to the screening length. The shift of the Si_{Ga} distribution with respect to the distribution of the Si clusters in the growth direction is attributed to the electric field present immediately below the (001) growth surface during the growth process ((001) surface band bending) and to partial surface riding. The lower spread of the Si-rich regions C indicates that these regions are less mobile during the growth stage. They mark the original positions of the Si planes.

Tunneling spectroscopy data acquired near and in the bright regions C (Fig. 4) show that the conduction and the valence bands rise in energy up to 0.5 eV in the bright regions with respect to the values measured in the neighboring n-type regions. These regions pin the Fermi level in the middle of the gap through localized states that can be observed at some points of the bright defects. The pinning effect is also observed by measuring the local electrostatic potential by STM with an independent method. DFT-LDA calculations of selected Si clusters show a local density of states with peaks in the gap when the cleavage surface intersects the cluster, in agreement with our experimental results

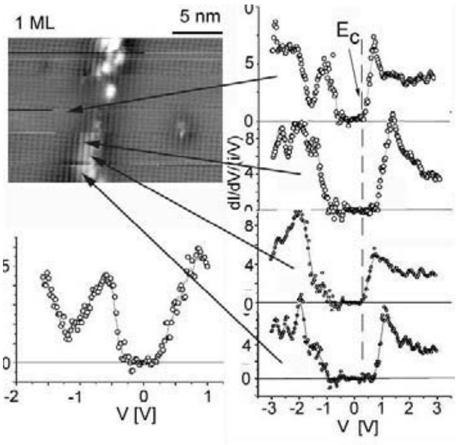

Fig. 4 Scanning tunneling spectroscopy data measured at different positions near and in a Si rich region. Note the shift of the conduction band and the presence of localized states in the gap.

$Mn_xGa_{1-x}As$

$Mn_xGa_{1-x}As$ is a recently discovered diluted ferromagnetic semiconductor with a Curie temperature T_C of about 100 K for x=0.06. It has potential applications in spintronics. In order to increase T_C is necessary to increase the hole concentration and the Mn concentration. However self-compensation and phase-separation effects have prevented till now to approach RT. We are trying to overcome these effects and to find their cause by using the δ-doping technique.

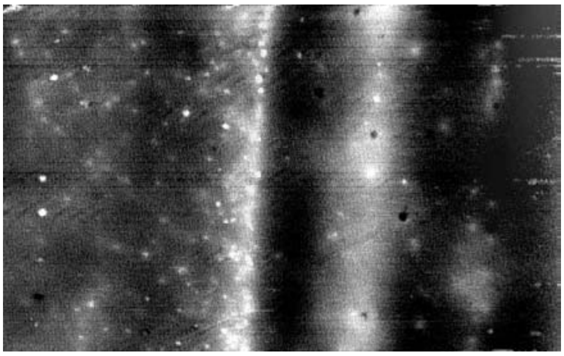

Figure 5. XSTM topographic image of three δ-doped layers of Mn in GaAs spaced by 50 nm. The surface concentrations are 0.02, 0.05 and 0.2 ML from right to left.

Figure 5 shows the XSTM topographic image (170 x 100 nm) of three δ-doped layers of Mn in GaAs with surface Mn concentration of 0.02, 0.05 and 0.2 ML. Images like this are used to measure the number of ionized Mn acceptors, of other Mn related defects, their spread, and the associated electrostatic potential. The acquisition of the data and their analysis is in progress.

Alloy fluctuations in InGaAs and InGaAsN

We are addressing the issue of alloy fluctuations in InGaAs and InGaAsN alloys and QWs grown by MBE on GaAs. GaAsN alloys have been theoretically predicted to exhibit a giant bandgap bowing, with a

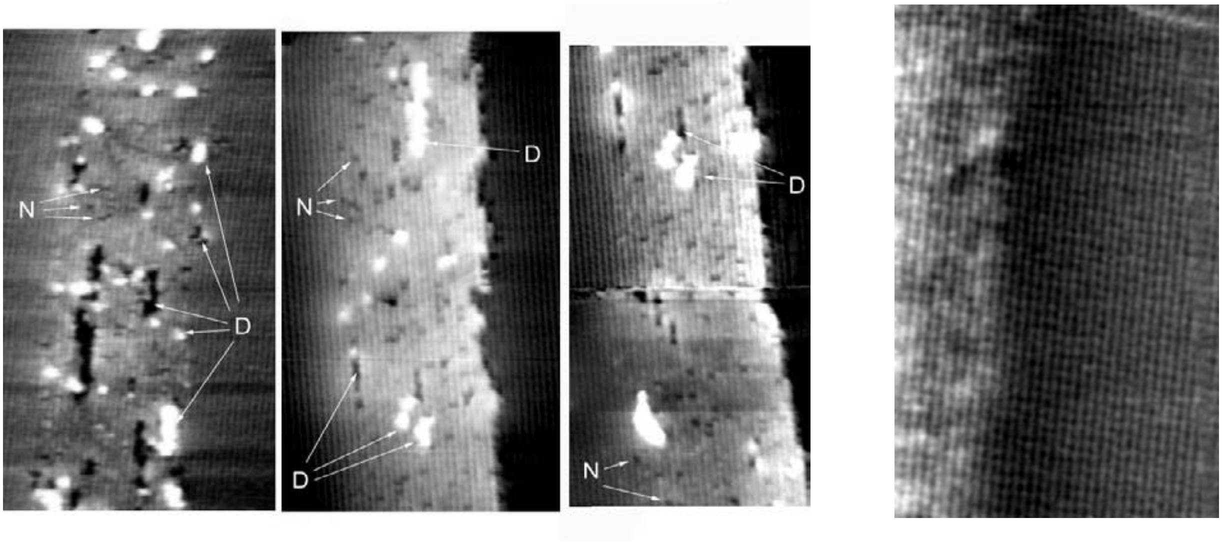

Fig.6 XSTM images of an $In_{0.15}Ga_{0.85}As_{0.97}N_{0.03}$ quantum well (left and center) and of an InGaAs quantum well (right). D are cleavage defects, N are isolated N atoms in the first and third atomic layer. The bright As atoms are those bound to In

bandgap and lattice parameter in the intermediate alloy composition range. These results are potentially opening the way to the implementation of InGaAsN emitters lattice-matched to GaAs operating at 1.3 and 1.55 µm. We are addressing the size, distribution and local potential of the alloy fluctuations, as a function of alloy composition and growth and annealing parameters, through a combination of XSTM, XSTS and cathodolominescence, both in the SEM and in the TEM mode. Comparison of the alloy fluctuations parameters determined by microscopy with those inferred from the optical studies in progress will allow us to ascertain the role of alloy fluctuations in determining the QW optical properties.

Figure 6 shows an XSTM image of a quantum well of $In_xGa_{1-x}As_{1-y}N_y$ (x=0.15, y=0.03) in GaAs, the "dark atoms" correspond to the positions of N atoms in the first and third atomic layer, the "bright atoms" correspond to the positions of In atoms mainly in the second atomic layer. We are acquiring a set of images large enough to extract statistically significant data on the distribution and correlation of the components of the alloy. Strong short distance correlations in the positions of the N atoms are already evident.

InAs quantum dots in AlGaAs

We have measured the distribution of the sizes and shapes of the quantum dots in AlGaAs by XSTM with atomic resolution (see Fig. 7). We are analyzing the distribution of the lattice defects inside the dots and around them. This study is preliminary to the main goal that is the investigation of tunneling spectra of single quantum dots in the matrix by STM.

This work is supported by the INFM Advanced Research Project 2001 XSTMS This project coordinates the activity on this subject of the research lines F1 and E1 at TASC, the of the INFM research unit of Trieste (M. Peressi, X. Duan, S. Baroni), and the IMEM-CNR, Parma (G. Salviati)

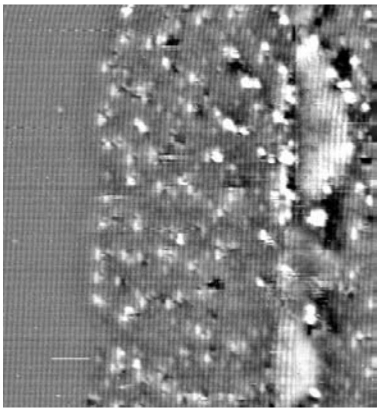

Fig. 7 Cross-sectional STM topographic images of two quantum dots (at the right) in an AlGaAs layer. The GaAs substrate is at the left. The size of the image is 38 x38 nm^2.

Publications

S. Modesti, D. Furlanetto, M. Piccin, S. Rubini, A. Franciosi, High-resolution potential mapping in semiconductor nanostructures by cross-sectional scanning tunneling microscopy and spettroscopy
Applied Physics Letters 82, 1932 (2003)
E. Carlino, S. Modesti, D. Furlanetto, M. Piccin, S. Rubini, A. Franciosi
Atomic resolution compositional analysis by scanning transmission electron microscopy high-angle annular dark-field imaging Applied Physics Letters 83, in press (2003)

INVITED TALKS

S. Modesti
Structure and electronic properties of nanostructures in GaAs by cross-sectional scanning tunneling microscopy and spectroscopy 2nd International Workshop on Nano-scale Spectroscopy and Nanotechnology, Tokyo, November 25-29 2002
E. Carlino High spatial resolution transmission electron microscopy studies of semiconductor heterostructures 6th Multinational Congress on High Microscopy, Pula, Crotia, June 1-5 2003

SURFACE STRUCTURE GROUP (He-Atom Scattering and ALOISA Beamline, F2 Area)

Francesco Bruno	**Gregor Bavdek**
Albano Cossaro	**Dean Cvetko**
Luca Floreano	**Roberto Gotter**
Alberto Morgante	**Fulvio Ratto**
Alberto Verdini	**Fernando Tommasini**

The Surface Structure Division (SSD) pursues the study of structural and morphological properties of surfaces, adsorbates and thin solid films. The SSD has been traditionally devoting much effort to study the surface thermodynamics and kinetics (phase transitions, growth and ordering). To properly address these scientific issues, the study of the correlation between structural and electronic properties is mandatory. As a consequence, for the SSD a guideline in the instrumentation development is the necessity to implement complementary techniques (structural and spectroscopical investigation tools) in the same experimental apparatus. The SSD is responsible for the INFM ALOISA beamline at the Elettra Synchrotron and for an apparatus for He Atom Scattering (HAS), currently connected to the ALOISA branchline. Both experimental apparati represent the state of the art in their respective field.

The ALOISA beamline has been designed with the aim of providing the INFM community with a unique instrument able to exploit most of the experimental techniques available at a Synchrotron source like Elettra for the study of surfaces and thin films, namely grazing incidence surface X-ray diffraction (XRD), photoelectron diffraction (PED), photoemission (XPS) and absorption spectroscopy (XAS), Auger-photoelectron coincidence spectroscopy (APECS). Thanks to its innovative design, ALOISA hosts several photon and electron detectors/analyzers in UHV conditions. The detectors are mounted on two rotating frames that, together with the rotation of the whole experimental chamber, allow one to explore the solid angle above the sample for any orientation of the surface with respect to the X-ray beam polarization.

The HAS apparatus is a very compact instrument for elastic and inelastic He scattering, characterized by a "clean" pumping system (turbo pumps at every differential pumping stage), a high precision 6-degrees of freedom manipulator and high resolution quadrupole. He scattering is certainly the most surface sensitive technique, since its thermal energy He atoms (20-100 meV) are scattered back by the outer surface charge density about 3 Å above the atomic planes. Its large cross-section for surface defects, together with the neutrality of the probe, makes HAS the ideal tool for investigating surface phase transitions and growth processes. At the beginning of year 2003, the HAS apparatus has been connected to the ALOISA branchline with the aim of adding photoemission spectroscopy capability to the diffractive technique.

As responsible of the ALOISA beamline, the SSD carries out about two dozens of experiments per year, that are selected by an international committee. All of the experiments are performed as direct collaborations between the SSD and the guest users, however there are a few fields in which the SSD is also leading and coordinating the research activity. Namely, surface phase transitions, metal film heteroepitaxy, organic molecule growth and coincidence spectroscopy are the main research lines coordinated by the SSD at both the ALOISA beamline and HAS apparatus.

Multiple phase transitions at 5/3 ML Pb/Ge(001)

In the past few years a large experimental effort has been devoted to the study of the low coverage metal phases on semiconductor surfaces since they are expected to display strong electron correlation effects, such as metal to semiconductor transition and low temperature magnetic ordering. The SSD studied in much detail the 1/3ML Sn/Ge(111) phase, which was initially reported to undergo a surface charge density wave driven phase transition from a (3x3) to a (√3x√3)R30°, but we finally concluded the transition to be a genuine order-disorder one [4,5,6]. More promising seems to be the (001) surface of Ge, since it displays a variety of Pb induced reconstructions in the monolayer range. Starting from a covalent bonding of the (2x2) Pb phase up to 0.5 ML, higher order reconstructions with increasing metallicity may be met at higher coverage. The c(4x8), ((2,1)(0,3)) and incommensurate c(4x8)-i symmetry phases are encountered as the Pb atom density in the 2D overlayer increases. The ((2,1)(0,3)) phase at 5/3 ML is on the border line between the low coverage covalent bonding configuration and the high coverage metallic one. This phase was very recently found to undergo a low temperature 2D phase transition to a lower symmetry ((2,1)(0,6)) phase in which a displacive mechanism seems to be involved. For a better understanding of the phase transition we studied by HAS and XRD the temperature behaviour of its order parameter.

At 120 K the substrate displays a ((2,1)(0,6)) surface symmetry. We have taken the diffracted peak profile of the (5/12,1/6) peak as a function of the temperature and observed that its intensity decrease is followed by a gradual peak broadening. From the peak width analysis, a critical temperature of about 170 K with a critical exponent close to 1 has been obtained. This result, together with the absence of any width or intensity variation (a part from the Debye-Waller attenuation) of the diffracted peaks belonging to the ((2,1)(0,3)) RT phase, yields a 2D-Ising order-disorder model of the phase transition. By further increasing the substrate temperature, we observed another reversible transformation into a (2x1) phase symmetry. In this case, we have taken the (1/3,1/3) peak as the order parameter of the ((2,1)(0,3)) phase. From the observed peak width broadening, a critical temperature of about 375 K with a critical exponent ν close to 5/6 has been obtained, i.e. the disordering of the ((2,1)(0,3)) phase is consistent with the 3-state Pott's model. In this case, the diffracted peaks of the high temperature phase display a change of their Debye-Waller attenuation across the transition. This effect might be due to the anisotropic domain wall scattering, but a change of the surface charge corrugation should be also taken into consideration. Further experiments by XRD rod scans (probing the vertical structure of the surface) are currently being pursued to check the possibility of a displacive character of this ((2,1)(0,3)) to (2x1) phase transition.

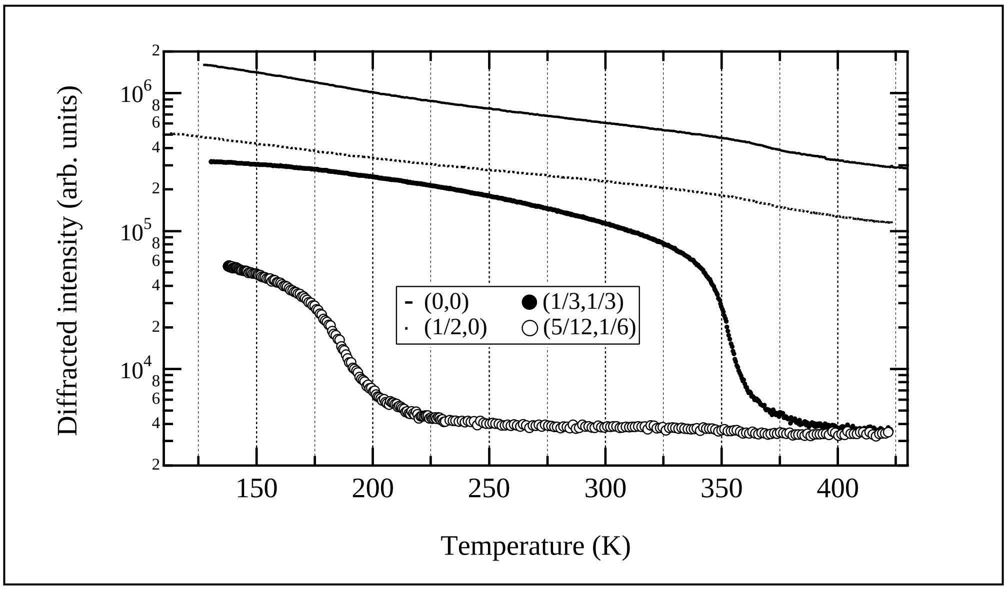

He diffracted intensity as a function of temperature for a few Bragg's peaks. The (5/12,1/6) peak is characteristic of the ((2,1)(0,6)) phase and reversibly disappears beyond 180 K. The (1/3,1/3) peak is characteristic of the ((2,1)(0,3)) phase and reversibly disappears beyond 350 K, where the surface is left in a (2x1) symmetry. The other peaks are unaffected by the first transition, while a change of their Debye-Waller attenuation is observed at 350 K.

2D growth of Pb(111) on Ge(001) and Ge(111)

Room temperature deposition of Pb on semiconductor surfaces always lead to cluster growth due the high mobility of Pb atoms which yields an up-hill atom flow at the Pb cluster edges. Lowering the substrate temperature, 2D growth becomes possible and QSEs are enhanced by the homogeneous film morphology. 2D growth is observed to set in beyond a critical thickness, which depends on the substrate surface and temperature. The existence of a critical thickness has been recently explained by a model based on a detailed energy balance between charge quantum confinement, charge transfer at the interface and stress. Although not quantitative, this electronic growth model qualitatively predicts the oscillatory behavior of the Pb(111) surface relaxation with a bi-layer periodicity, which we effectively observed for Pb/Ge(001). Due to the variable number of quantum well states falling below the Fermi level as a new Pb layer is added, we observed strong variations of the in-vacuum spilling of the surface charge density. This is reflected in an apparent variation of the surface step height as large as 15% in the HAS determinations, while the structural variation, as measured by x-ray diffraction, was found to be two to three times lower. This variable relaxation was found to affect also the dispersion of the acoustic phonon branch, i.e. the elastic force constant coupling the topmost layer to the film beneath. [28]

Very recently, we focussed on the Pb(111) growth on Ge(111), which yields a different morphological behavior with respect to the Ge(001) substrate. In fact, we found a lower critical thickness for the onset of layer-by-layer growth while the overall roughness was found to be higher than on Ge(001) at the same temperature. Layer-by-layer growth oscillations set in after the deposition of 3 ML and the momentum scan analysis also indicates an oscillatory change of the surface step height. Apparent deviations from the Pb(111) bulk interlayer spacing up to 10% have been observed by HAS with a bi-layer periodicity.

We have also studied in detail the very neat change to a double layer regime of growth observed between 7 and 8 monolayers (ML). As the deposition is continued, the HAS reflectivity oscillations switch to a bi-layer periodicity. At the same time the momentum scans indicate the appearance of a third uncovered layer. Interestingly, two of these layers are always found to have a similar filling, one of them with a very small portion of uncovered area, thus confirming the bi-layer regime of growth.

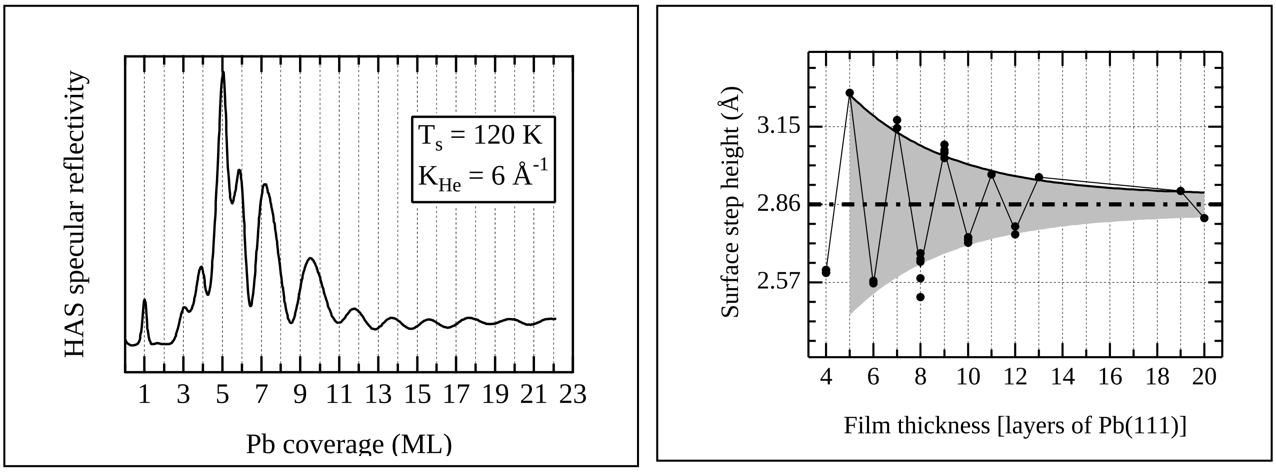

Left panel: HAS specular reflectivity, taken during Pb deposition on Ge(111) at 120 K, shown as a function of the amount of deposited Pb. The Pb coverage as been normalized to the quartz microbalance deposition rate, also taken during deposition. Right panel: the surface step height obtained by momentum scan analysis is shown as a function of the Pb film thickness. Only the data points obtained for layers with large filling have been reported. The shadowed area is a guide to the eye to show the gradual recovery to the bulk interlayer spacing (indicated by the dashed line at 2.86 Å) after many layers.

Thermally reversible transition from pseudomorphic to fcc structure of thin Fe films on $Cu_3Au(100)$

in collaboration with M. Canepa, S. Terreni, L. Mattera (INFM unit of Genova)

In the past two years the SSD has devoted much experimental effort to the study of the structural evolution of thin metal films grown in situ. Most studies focussed on the deposition of magnetic metals on non-magnetic metal surfaces. This route demonstrated the possibility to fabricate thin films with magnetic properties different from the bulk ones. In particular, Fe is displaying the most complex behavior since it can be stabilized in structural phases displaying antifferomagnetic, superferromagnetic, non-magnetic or layered magnetic behavior depending on its lattice cell volume and shape.

By complementary use of XRD and PED, we described in fine detail the complex structural evolution of Fe films grown on $Cu_3Au(100)$ as a function of the Fe thickness. At room temperature (RT), the film grows pseudomorphic to the substrate up to a critical thickness of 4 layers, where a new Fe structure is observed. The latter is found to fall onto the epitaxial line of ferromagnetic fcc Fe, i.e. it is an fct phase. A tetragonally distorted bcc structure is only observed after the deposition of 15 Å, this bct structure [also growing on its (100) surface but rotated by 45˚ with respect to the substrate lattice] is observed to coexist with the fct one over a wide thickness range (up to 25 Å). [19]

This system also displays a complex thermal behavior. We have shown that the deposition of 1 ML at low temperature (LT) leads to the formation of bi-layer nanoislands of uniform size (10 nm). By annealing at 400 K, the nanoislands irreversibly switch to a three-layer structure without surface segregation. [20]

Most interesting is the thermal behaviour of the fct phase. At the critical thickness of about 8 Å, the fct phase transforms into the pseudomorphic one by heating the sample beyond a critical temperature of 380-390 K. The transition is fully reversible. By measuring the XRD rod scans of the pseudomorphic structure above and below Tc, we have seen that the pseudomorphic phase is formed by 4 layers. The pseudomorphic phase is observed even at the lowest attainable temperature (150 K), thus phase coexistence is always present below Tc. Moreover the number of pseudomorphic layers does not change throughout the transition, while the occupancy of each layer is effectively reduced below Tc. The transition thus proceeds by lateral growth of the domains of one phase into the other.

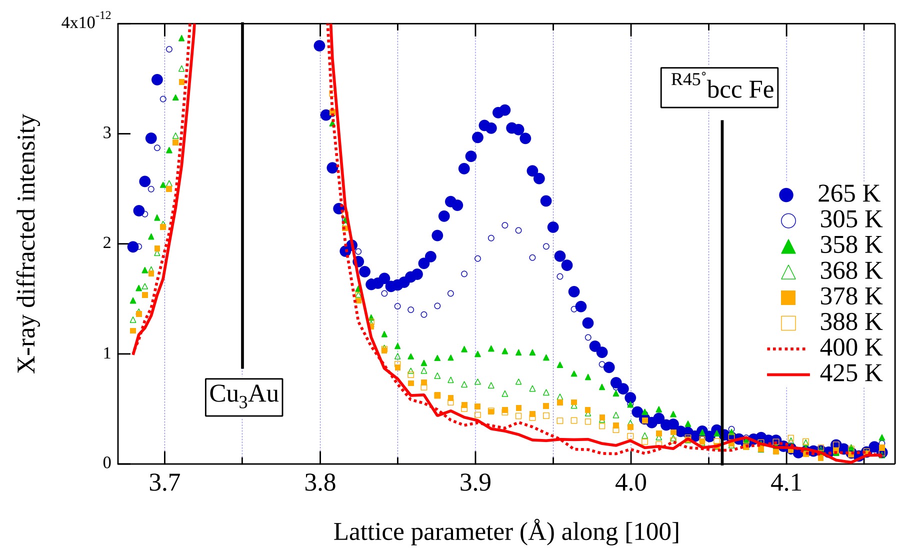

In plane X-Ray Diffraction of the (2,0,0) diffraction peak taken at fixed scattering geometry by varying the photon energy for a few substrate temperature. The photon beam impinges the surface at grazing incidence, forming an angle θ = 45˚ with respect to the fcc(100) planes of the direct lattice. The data are shown as a function of the $Cu_3Au(100)$ lattice spacing along the [100] substrate direction (corresponding to the [1-10] direction of R45˚-bcc Fe). The diffraction patterns have been taken for the same Fe film at a thickness of about 8 Å. The vertical heavy lines correspond to the lattice of the antiferromagnetic fcc substrate and of the bcc(100) lattice, rotated by 45˚.

L-Cysteine Self Assembled Monolayers (SAMs) on Au surfaces

in collaboration with R. Rolandi, O. Cavalleri and M. Canepa (INFM unit of Genova)

L-Cysteine [$HSCH_2CH(NH_2)COOH$] (Cys) is one of the most useful biomolecules to prepare bio-active surfaces for its capability to form covalent bonds with transition metals by the sulflhydryl moiety. As a natural component of proteins, it bridges proteins to solid surfaces. In forming molecular films on transition metals, Cys behaves like alkanethiols (AT), whose SAMs are so widely studied to be considered model systems. However, the carboxy and amino groups make Cys more reactive than alkanethiols and open a richer scenario in the metal-molecule and molecule-molecule interaction. The chemisorption of Cys on Au(111) from the liquid phase has been investigated with synchrotron based, high resolution X-ray photoemission spectroscopy.

We report results obtained on pristine as well as on irradiated and annealed samples. Two doublets are detected in the S2p spectral region. One has the $2p_{3/2}$ energy level at about 162 eV and it indicates that Cys is adsorbed as thiolate. The other one has the $2p_{3/2}$ energy level at about 161eV. The intensity of this last doublet depends on the Cys sample purity, on irradiation time and on annealing procedure. Experimental evidences and the comparison with literature data suggest to assign this doublet to atomic sulfur. The comparison of the spectra of pristine, irradiated and annealed samples shows that annealing at moderate temperature (80-140 ˚C) and prolonged irradiation induce the breaking of the carbon-sulfur bonds leaving residual sulfur atom and carbon groups on the gold substrate. This response to irradiation differs from the results recently reported on long chain ATs.

The absence of S 2p components at higher binding energies, related to so-called “unbound” sulfur or disulfide species, indicates that Cys deposition by liquid solution leaves a monomolecular layer in contrast to 3-mercaptopropionic acid [$HS(CH_2)_2COOH$] (MPA) films, where we observed a weak and broad component ($2p_{3/2}$ level at about 163.5 eV), which could result from a S-R-R-SH adsorption configuration as suggested by angle resolved measurements.

In fact, we obtained the formation of a full second monolayer of Cys by UHV deposition on Au(110) at room temperature. In this case two fully separeted S 2p doublets are observed with the $2p_{3/2}$ components at 162 and 164 eV for the first and second monolayer, respectively. The second Cys monolayer is very weakly bound to the first one and is evaporated by short irradiation exposure or mild annealing. Complementary RHEED and XRD measurements also suggest that the substrate anisotropy drives the formation of ordered structure depending on the coverage.

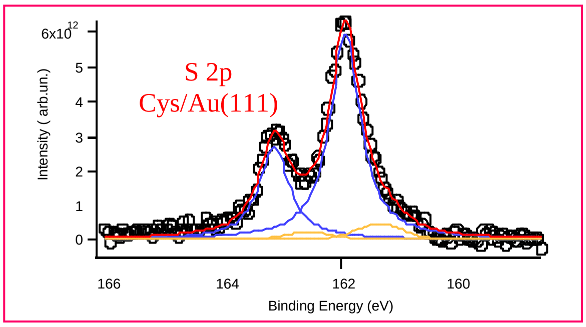

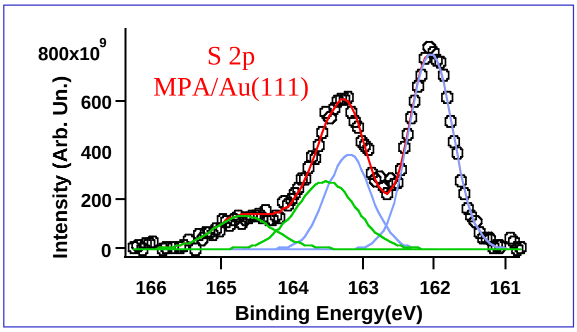

Monolayer of L-Cysteine obtained by liquid solution on Au(111). The $2p_{3/2}$ component at 162 eV indicates Cys to be adsorbated as a thiolate.

MPA deposition by liquid solution on Au(111) leads to the formation of a full monolayer ($2p_{3/2}$ component at 162 eV). Residual 2nd monolayer molecules are left on the surface ($2p_{3/2}$ component at 163.5 eV).

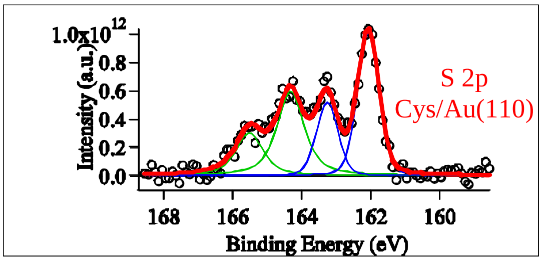

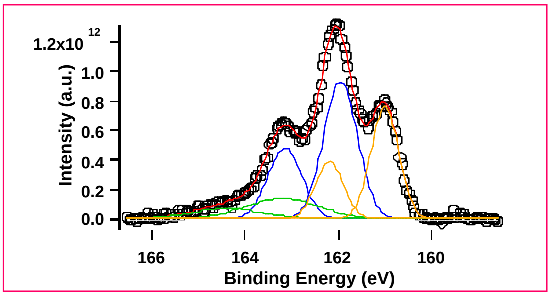

Double layer of L-Cysteine obtained by UHV evaporation on Au(110) at RT. The $2p_{3/2}$ component at 164.2 eV correspond to the second monolayer.

Monolayer of L-Cysteine obtained by liquid solution on Au(111) after irradiation of ≈ $2.5x10^{11}$ (ph/s)/mm^2 for 1h. The $2p_{3/2}$ component at 161 eV is attributed to atomic sulphur generated by S-C bond breaking by irradiation or annealing

Cu-phtalocyanine SAMs on metal surfaces

in collaboration with A. Ruocco, F. Evangelista, F. Offi, G. Stefani (INFM unit of Roma III)

Porphyrins and phtalocianines (PC) are a class of organic molecules that are involved in a wide variety of biological processes, from oxygen transport to photosynthesis, to pigmentation changes. These molecules are characterized by a common structural feature, a macrocycle, which is perfect to bind almost all metal ions like e.g. Zn, Fe, Cu, Ni, Co. Accordingly the properties of the molecule can be changed and appropriately tailored to a particular purpose. Example of applications are gas sensor given the possibility to bind and release gas molecules, application in optoelectronics data storage and solar cells.

We have studied the growth of Cu PC from the submonolayer to the multilayer regime on two different metallic substrates, namely Al(100) and Au(110). The most interesting finding concerns the molecule-substrate interaction. The comparison of the high resolution XPS data and the X-ray absorption results taken on the two substrates indicates a rather different molecule-metal surface interaction in the two cases. In fact, while the multilayer are spectroscopically similar on the two substrates and also to the monolayer on Au(110), the interface layer show a quite different behavior on the Al surface. Satellite features are missing in the C 1s core level spectrum, energy shifts of the Cu 2p levels are present, respect to the Au(110) case and the multilayer, and the main transition line in the Cu L2 edge X-ray absorption spectrum is absent. These findings can be interpreted as due to a stronger interaction of the phtalocianine with Al susbstrate so that the LUMO level of the molecule is filled and not available for electronic transitions.

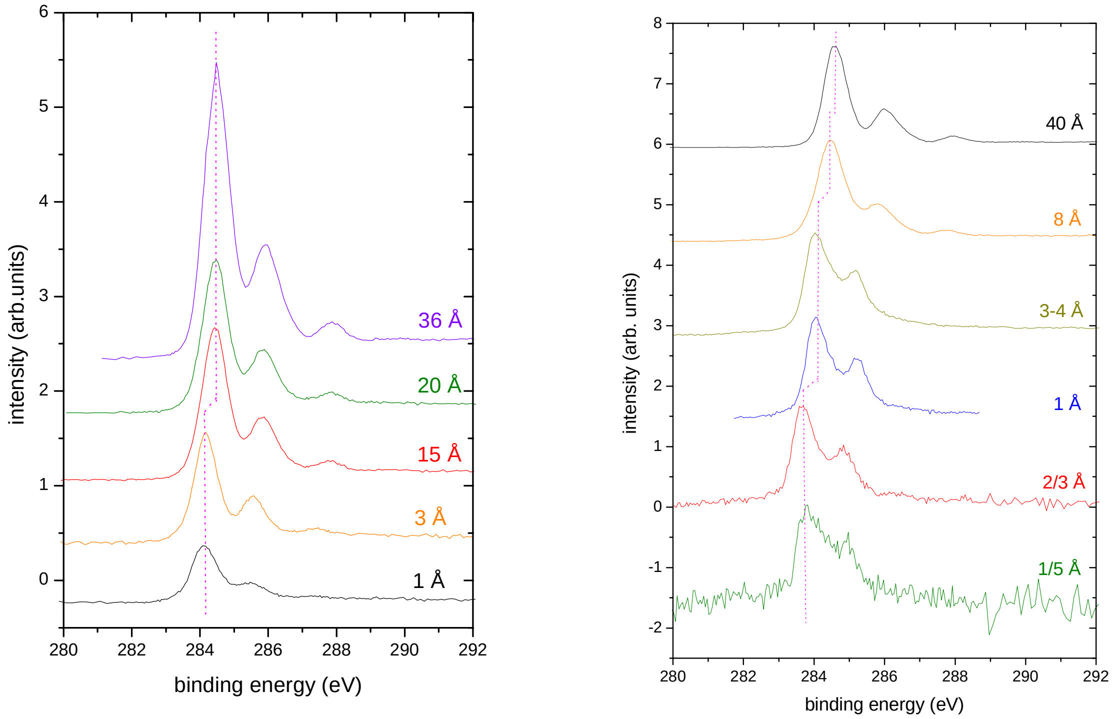

Left panel: C 1s photoemission spectrum from Cu-PC deposited on Au(110) for different thicknesses. The main component at about 284 eV is originated by the Carbon atoms of the aromatic ring, while the secondary component at about 286 eV is originated by the carbon atoms bound to the nitrogen ones. The feature at about 288 eV is the shake-up satellite of the C 1s component at 286 eV. The shake-up satellite, originated by the HOMO-LUMO transition, is observed down to the submonolayer coverage.

Right panel: C 1s photoemission spectrum from Cu-PC deposited on Al(100) for different thicknesses. The shake-up satellite is now observed only in the multilayer thickness range, i.e. the LUMO of the first Cu-PC monolayer is filled by the charge transfer from the Al substrate.

Angle Resolved APECS from Ge(001) surface

In collaboration with R. Bartynski, M. Butterfield (Rutgers University), S. Iacobucci, A. Liscio, A.. Ruocco and G. Stefani (INFM unit of RomaIII)

It is well established that in Auger photoelectron coincidence spectroscopy (APECS) the relationship between the parent photoelectron and the subsequent Auger emission (established by matrix elements and selection rules), achieved by the timing coincidence detection of the two, ensures unprecedented discrimination in separating overlapping spectral features, isolating individual sites in solids and probing their local structure, eliminating uncorrelated secondary electron background and core level lifetime broadening. In angle resolved APECS, we combine these peculiarities with the information contained in the angular dependence of the emitted electron wavefunctions, in order to investigate whether ion alignment effects survive, or are possibly enhanced, in the solid state environment, where the lattice structure dominates the electron scattering.
We have measured the angular distribution of Ge $L_3M_{45}M_{45}$ Auger electrons in coincidence with specific angles of the Ge $2p_{3/2}$ photoelectron [26]. In the Figure, we display the Auger angular distribution as obtained in coincidence with five different directions of the photoelectron momentum. The data points with error bars are the coincidence distribution and the heavy line is a guide to the eye. The thin solid curve is the simultaneously acquired AED pattern. Although these coincidence data have larger error bars than the integrated data, the differences with respect to the AED pattern are now even more pronounced. Systematic changes are observed between the profiles obtained for neighboring analyzer pairs.
Our results show that AR-APECS from solid surfaces provides a new way to perform AED/XPD with enhanced surface sensitivity. If on one side, energy resolved APECS can be used to elucidate the mechanism underlying the core hole generation process and to add insight into the multiplet structure and Auger line shape, on the other side, AR-APECS provides a way to disentangle source function generated effects by diffraction phenomena, i.e. one can explore specific magnetic sublevels in the wave function representing the emitted Auger electron. Finally, we note that AR-APECS, by detecting the coincident photoelectron, preserves the chirality of the ionisation event and then opens the possibility to measure dichroic effects in the Auger emission, thus providing new insight in the study of magnetic systems.

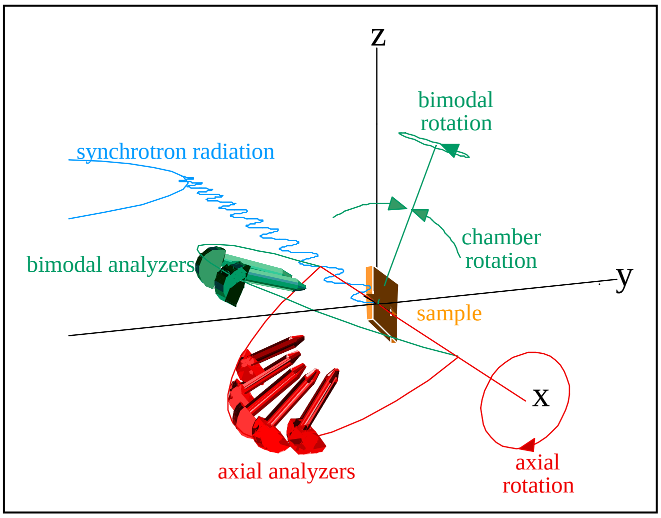

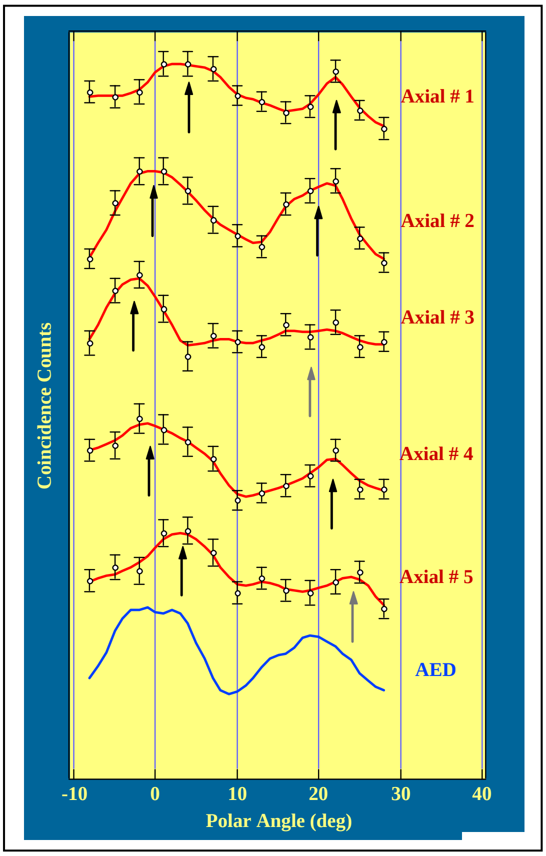

Upper panel: Schematics of the detection setup for coincidence spectroscopy. The Axial spectrometers are used to detect the photoemitted electron, while the corresponding Auger electron is detected by the bimodal spectrometers.
Right panel: Pair-wise AR-APECS angular distributions of Ge $L_3M_{45}M_{45}$ Auger electrons measured in coincidence with Ge $2p_{3/2}$ core photoelectrons along the (001) direction of Ge(001), as detected in each of the five axial electron energy analyzers. The Auger Electron Diffraction (AED) taken is also shown at the graphic bottom.

Instrumentation developments and upgrades

Characterization of the branch-line: in year 2002 the branch line of Aloisa has been characterized. The energy resolution and photon flux correspond to the design values. The He scattering apparatus has been placed at the end of the beamline and first measurements will be carried out during 2003.

New sample manipulator: a new surface manipulator developed in cooperation with the CINEL company, which built the ALOISA experimental chamber, has been designed, the construction has already started and the manipulator has been delivered to us in June 2003. According to the design specifications, the new manipulator has the following main improved characteristics respect to the present VG manipulator:

- Incidence angle variable from 0 to 35 degrees (present range: 0-10)
- Azimuthal and incidence angle resolution better than 4/10000 of degree (presently 4/1000 of degree)
- Higher reliability and reduction of the maintenance costs (presently the rotation are transmitted to vacuum by three in-vacuum Harmonic Drives (HD) which have an average lifetime of 1.5-2 years and cost around 15.000 Euro each.)

New data acquisition system: a complete new acquisition system based on PC and PC boards has substituted the previous one based on Macintosh and VME bus. The new acquisition program allows most types of measurements to be run automatically. Options for complex multiple scans, which comprise variation of all possible sample and detectors angles and photon and electron energy, have been included. The switch of the monochromator from the high energy to the low energy mode, which is a complex and potentially dangerous operation, is now computer controlled.

Users specialized equipment: an INFM program finances the acquisition of new pieces of equipment, which are needed for carrying out particular types of experiments of interest of group of users. Two of these projects have involved Aloisa. A photodiode with large area and high energy resolution for the measurement of fluorescence yield at the K edge of low Z material has been tested on the beam-line. The detector is LN2 cooled and mounted on a holder, which allows reaching a working distance from the sample of a few centimeters to collect photons from the largest possible solid angle. Experiments have been carried out at the C K-edge and at the N K-edge of semiconductor samples. This detector opens the possibility of measuring high resolution absorption spectra of low concentration low Z materials.

A molecular beam source to be connected to the preparation chamber of Aloisa has been also recently tested. The source has been designed in particular to deposit organic molecules that have a low vapor pressure at room temperature avoiding contamination of the preparation chamber. The source has been successfully tested with L-cysteine, a prototypical functional molecule.

New electron energy analyzers: presently 7 electron energy analyzers are mounted on the experimental chamber. The analyzers, developed by the ALOISA group, are hemispherical with mean radius of 33 mm, an acceptance angle of 1 degree. 2 analyzers are mounted on a frame with two angular degrees of freedom (Bimodal frame) and are routinely used for polarization dependent photoemission spectroscopy and Photoelectron Diffraction (PED). The other 5 analyzers, which are mounted on a rotatable frame with only one angular degree of freedom (axial frame), are used for coincidence spectroscopy. We plan to substitute the 7 analyzers with 2 specialized ones. A 66 mm mean radius hemispherical will be mounted on a modified version of the bimodal frame. This analyzer will preserve the high angular resolution of the present ones, necessary for the polarization dependent PED experiments, but will mount a multi channel detector which will allow fast energy resolved PED experiments. This analyzer has been already ordered to the CINEL company.

A second energy analyzer has been designed to be mounted on the experimental chamber. Since the chamber can rotate around the beam axis, this analyzer will allow performing polarization dependent spectroscopes, both valence band and core level, Auger yield absorption spectroscopy, polarization dependent resonant photoemission and Auger to be combined with coincidence spectroscopy. It will be a 130 mm mean radius hemispherical analyzer with the maximum angular acceptance compatible with a large working distance imposed by manipulator dimensions. The analyzer design has been developed in cooperation with a research group of Milano Politecnico, who will perform high energy photoemission experiment exploiting the wide energy range of the Aloisa monochromator.

Publications

2002

[1] P. Luches, C. Giovanardi, T. Moia, S. Valeri, F. Bruno, L. Floreano, R. Gotter, A. Verdini, A. Morgante, A. Santaniello, "*Epitaxy of ultrathin CoO films studied by XPD and GIXRD*", Surf. Rev. Lett. **9** (2002) 937.

[2] S. D'Addato, P. Luches, R. Gotter, L. Floreano, D. Cvetko, A. Morgante, A. Newton, D. Martin, P. Unsworth, P. Weightman, "*Variations in the lifetime of 3d hole states in ultrathin Fe films grown on Cu(100) deduced from the LMM Auger spectra of Fe*", Surf. Rev. Lett.. **9** (2002) 709.

[3] A. Goldoni, C. Cepek, R. Larciprete, L. Sangaletti, S. Pagliara, L. Floreano, R. Gotter, A. Verdini, A. Morgante, Y. Luo, and M. Nyberg, *C70 adsorbed on Cu(111): metallic character and molecular orientation,* J. Chem. Phys. **116** (2002) 7685.

[4] S. Tacchi, F. Bruno, G. Carlotti, D. Cvetko, L. Floreano, G. Gubbiotti, M. Madami, A. Morgante, and A. Verdini, *Structure and magnetism of Fe/Cu(110) thin films*, Surf. Sci. **507-510 (C)** (2002) 324.

[5] F. Bruno, L. Floreano, A. Verdini, D. Cvetko, R. Gotter, A. Morgante, S. Terreni, M. Canepa: *"Study of the isotropic contribution to the analysis of photoelectron diffraction experiments at the ALOISA beamline"*, Journal of Electron Spectroscopy and Related Phenomena **127** (2002) 85.

[6] F. Bruno, G. Panaccione, A. Verdini, R. Gotter, L. Floreano, P. Torelli M. Sacchi, F. Sirotti, A. Morgante, and G. Rossi: *"Surface and Bulk contribution in magnetic linear dichroism in the angular dependence from ferromagnetic transition metals"*, Phys. Rev. B **66** (2002) 024417.

[7] F. Bruno, S. Terreni, L. Floreano, D. Cvetko, P. Luches, L. Mattera, A. Morgante, R. Moroni, A. Verdini, and M. Canepa: "*From pseudomorphic to orthomorphic growth of Fe films on Cu3Au(001).*", Phys. Rev. B **66** (2002) 045402.

[8] A. Verdini, L. Floreano, F. Bruno, D. Cvetko, A. Morgante, F. Bisio, S. Terreni and M. Canepa, "*From bi-layer to tri-layer Fe nanoislands on Cu3Au(001)*", Phys. Rev. B **65** (2002) 233403.

[9] G. Stefani, S. Iacobucci, A. Ruocco and R. Gotter: *Electronøelectron coincidence spectroscopies at surfaces,* J. Elec. Spectrosc. Relat. Phenom. **127** (2002) 1.

[10] S. Iacobucci, M. Sacchi, F. Sirotti, R. Gotter, A. Morgante, A. Liscio and G. Stefani, *L2L3V Coster Kronig decay in Fe, Ni and NiO: the near edge region.*, J. Elec. Spectrosc. Relat. Phenom. **127** (2002) 71.

[11] G.C. Gazzadi, F. Bruno, R. Capelli, L. Pasquali, S. Nannarone, *Structural transition in Fe ultrathin epitaxial films grown on Ni(111)*, Phys. Rev. B **65** (2002) 205417.

[12] F. Bruno, R. Gotter, A.Morgante, A. Verdini, G. Panaccione, M. Sacchi, F. Sirotti, P. Torelli, *Magnetic properties of ultrathin Co/Fe(001) and Fe/Co/Fe(001) systems as probed by Linear Magnetic Dichroism in the Angular Distribution of photoelectrons*, Physica B, in press.

[13] R. Gotter, S. Iacobucci, A. Ruocco, and G. Stefani: *Electron-electron coincidence experiments: from atoms to solids*, in *Correlations, polarization, and ionization in atomic systems*, ed. by Don H. Madison and Michael Schulz (AIP Conference Proceedings, New York 2002) Vol. 604, p. 52-63.

2003

[14] R. Gotter, A. Ruocco, M.T. Butterfield, S. Iacobucci, G. Stefani, and R.A. Bartynski, "*Angle resolved Auger-photoelectron coincidence spectroscopy (AR-APECS) of the Ge(100) surface*", Phys. Rev. B **67** (2003) 033303.

[15] L. Giovanelli, C. Cepek, L. Floreano, E. Magnano, M. Sancrotti, R. Gotter, A. Morgante, A. Verdini, A. Pesci, L. Ferrari, and M. Pedio, "*The molecular orientation of C_{60} on Pt(111) at room temperature and the high temperature graphitization*", Appl. Surf. Sci. **212-213** (2003).

[16] L. Floreano, D. Cvetko, F. Bruno, G. Bavdek, A. Cossaro, R. Gotter, A. Verdini, A. Morgante, "*Quantum size effects in the low temperature layer-by-layer growth of Pb on Ge(001)*", Prog. Surf. Sci. **72** (2003) 135.

[17] F. Bondino, E. Vesselli, A. Baraldi, G. Comelli, A. Verdini, A. Cossaro, L. Floreano, and A. Morgante, "*Molecular orientation of CN adsorbed on Pd(110)*", J. Chem. Phys. **118** (2003) 10735.

[18] L. Sangaletti, S. Pagliara, F. Parmigiani, A. Goldoni, A. Morgante, L. Floreano, V. Aguekian, "*Giant resonant photoemission at the Mn 2p-3d absorption threshold of $Cd_{1-x}Mn_xTe$*", Phys. Rev. B **67** (2003) 233201.

[19] T. Pardini, C. Cepek, R. Larciprete, L. Sangaletti, S. Pagliara, L. Floreano, A. Verdini, A. Morgante, F. Parmigiani and A. Goldoni, "*Sodium doping of a C_{70} single layer adsorbed on Cu(111) surface*" Surf. Sci., in press.

Inverse Photoemission Laboratory (Research Area F3)

Co-ordinator: M. Pedio, Participant: N. Mahne

The F3 Inverse Photoemission Laboratory is under commissioning, being approved as research area in 2002. It is focussed on study by Inverse Photoemission Isochromat technique, performed by a Geiger Müller detector and a home made electron gun. The apparatus will be used for angular resolved Inverse photoemission measurements (KRIPES). The UHV system includes tools for other electron spectroscopies studies, such as a CMA analyser (AES, EELS) , a Kelvin Probe for work function measurements at surfaces, a LEED for structural probes and the typical facilities for preparation of clean surfaces and interfaces.

The Inverse Photoemission technique provides unique information on the electronic properties of empty states, i.e. the total Density of States in conduction band, including its energy position and dispersion. Empty states measurements can also be performed by other techniques that are related to the Local Density of empty electronic States, as near edge X-ray absorption fine structure, depending on element and the edge.

The comparison between the different techniques will give a complementary information on these different topics from clean surfaces, interface formation and chemisorption.

The scientific activity will be oriented to topics affordable by the study of empty states. Some of the research activity is related also to topics performed at the BEAR beamline, whose staff the coordinator of F3 belong to. Empty states will be addressed by two complementary and connected framework: Inverse Photoemission and X-ray absorption. The latter will be performed mainly at BEAR beamline at ELETTRA.

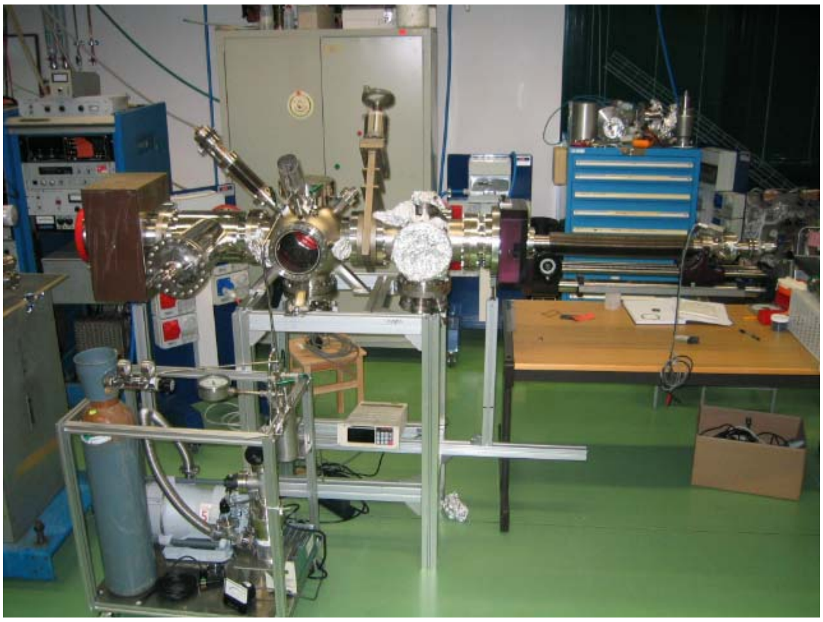

Fig. The IPES apparatus, under commissioning.

The the Inverse Photoemission new lab scientific topics unclude:

Interaction of large molecules with ordered surfaces studies by Inverse Photoemission and X-ray absorption. In particulat the modification of the empty molecular states during deposition and chemisorption will be measured. The data will be analysed also with the help of simulation programs.

The structural part will also be performed by Surface X-ray diffraction in collaboration with Dr. R. Felici OGG unit in Grenoble.

Examples: linear molecules (for example Octane) and carbon molecules (C60, endohedral fullerenes) on metal surfaces.

Growth of ordered SiC thin films on Si substrates by C60 precursors. Collaboration with Prof. Sancrotti, Dr. C. Cepek

Study of transition metals interfaces with SiC(100) substrates.

Acknowledged is the co-operation with a number of international groups (Prof. D.D. Sarma, Solid State Physics Institute, Bangalore, Dr. R. Cimino INFN Frascati and CERN Geneve, Dr. R. Felici OGG Esrf, Grenoble, Prof. M. Sancrotti TASC and Un. Cattolica Brescia) in the domain of surface and material science.

In 2002 a project within Ministero degli esteri in collaboration with Prof. Sarma has funded the staying of a researcher for the commissioning of the lab.

Proposed Projects are:
Participation to the “SICWISE-SiC based bandgap semiconductor devices for IST applications” EU Network, Coordinator Prof. Mikael Oestling, Kungl Takniska Hoegskolen, Dept. of Microelectronics and Information Technology, Kista, Sweden.
Participation to the Biosensors based on Silicon Carbide via controlled surface engineering (BioSiC), FET open, project of European Community, F6. Coordinator Dr. A. Catellani.

Publications

A.Pesci, C. Cepek, M. Sancrotti, L. Ferrari, M. Capozi, P. Perfetti, **M. Pedio** "SiC(111) growth by C_{60} decomposition on Si(111)" Surf. Sci. **482-485**, 829 (2001).
X. Torrelles, J. Rius, W. Moritz, A.Hirnet, **M. Pedio**, R. Felici,P. Rudolf, M. Capozi, F. Boscherini, S. Heun, B. H. Mueller, "Real examples of surface reconstructions determined by direct methods" J. Physics: Condensed Matter 14, pp.4059-4074 (2002).
L. Aversa, R. Verucchi, G. Ciullo, A. Boschetti, L. Ferrari, P. Moras, **M. Pedio**, A. Pesci, S. Iannotta, "Characterization of SiC grown on Si (111) by supersonic C_{60} beams", *Diffusion and Defect Data Part B - Solid State Phenomena*, **82-84**, 523 (2002).
L. Giovanelli, C. Cepek, L. Floreano, E. Magnano, M. Sancrotti, R. Gotter, A. Morgante, A. Verdini, A. Pesci, L. Ferrari, and M. Pedio “Molecular Orientation of C_{60} on Pt(111) Determined by X-Ray Photoelectron Diffraction” Applied Surface Science, 9747, 1, 2003

Annealing Temperature Dependence of C_{60} on Silicon Surfaces: Bond Evolution and Fragmentation

M. Pedio, F. Borgatti, A. Giglia, N. Mahne, S. Nannarone, A. Pesci, C. Cepek, E. Magnano , G. Bertoni , E. Spiller , M. Sancrotti, L. Giovannelli, L. Floreano, R. Gotter , A Morgante

The fragmentation of C60 has been studied by Inverse Photoemission and XAS techniques C_{60} molecules interacting with Si(100) and Si(111) surfaces. Ordered SiC films characterized by low energy electron diffraction patterns can be grown by depositing C60 molecules on a Si substrate kept at a temperature above 1000 K in UHV conditions. The Inverse photoemission measurements performed in situ show the presence of a state in conduction band that is related to the C-Si bond and whose intensity is related to the morphology of the grown SiC film.

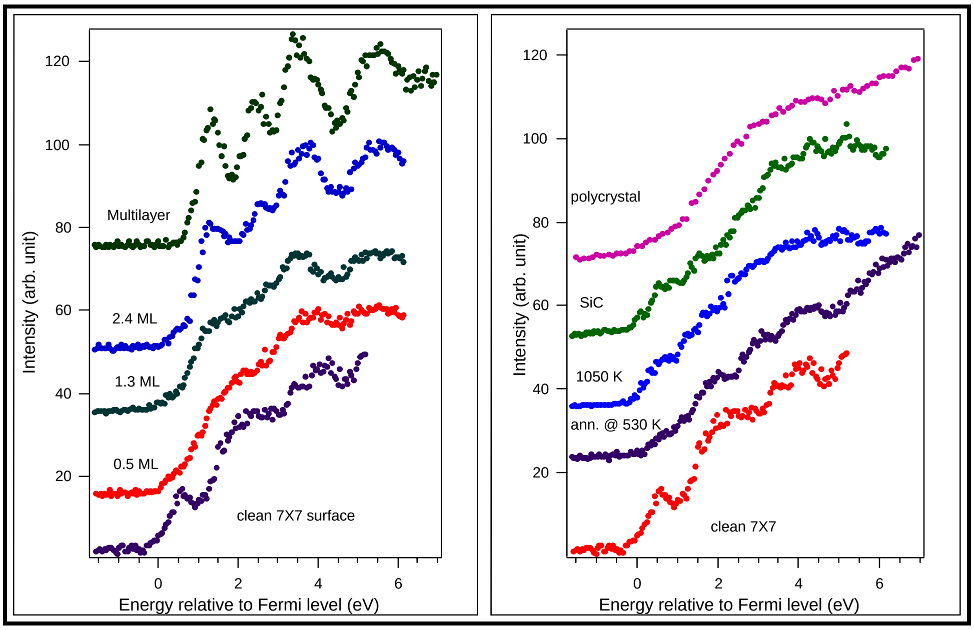

Figure: Evolution of Inverse Photoemission Spectra for the multilayer and the C_{60}/Si(111) system after different annealinf treatment, taken at normal incidence. [A. Pesci, et al., Surf. Sci. **482-485**, 829 (2001)]

The near-edge X-ray absorption spectroscopy (NEXAFS) study of C K-edge of C_{60} molecules interacting with Si(100) and Si(111) surfaces was performed tuning the probing depth and studying polarization dependence, the NEXAFS results enlighten the evolution of the molecular states after thermal treatment, up to the fullerene fragmentation and SiC formation. The NEXAFS spectra of a single layer of C_{60} deposited at 670 K onto both surfaces show a strong C_{60}-substrate interaction, confirming literature results and a polarization dependence of the spectra can be detected. This behaviour is similar to the results obtained on C_{60} covalently chemisorbed on Al surfaces. Annealing of the C_{60}/Si systems at 1050 K induces fullerene fragmentation and leads to SiC nucleation. We found, for both substrates, that fullerene fragmentation starts at the C-Si interfaces, involving the C atoms lying close to the Si substrate with a subsequent increase of C-Si bonds at the fragmentation stage.

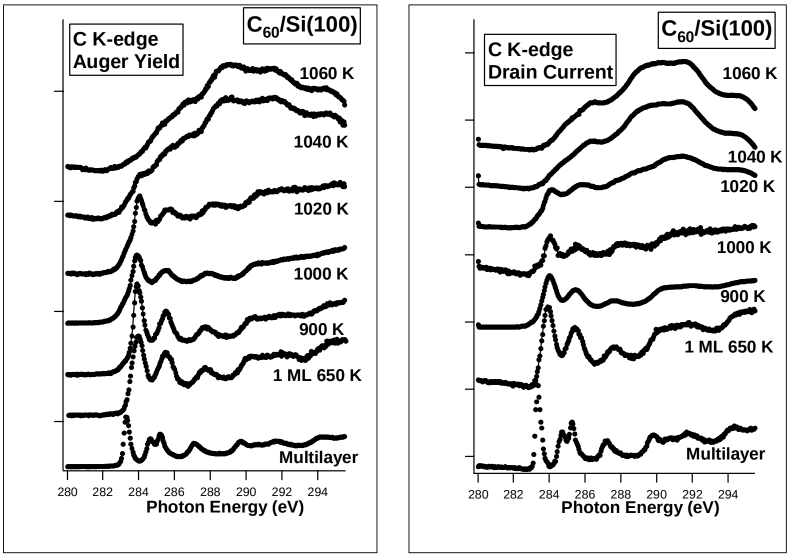

Figure: Evolution of the C K-edge NEXAFS spectra for the multilayer C_{60} and 1 ML of C_{60}/Si(100) system after different annealing treatment as measured simultaneous in two detection mode: the most surface sensitive Auger Yield (left) and Drain Current (right). The Temperature is indicated in Kelvin. Thick C_{60} film (multilayer) is shown for comparison.

The NEXAFS C K-edge results on both C60/Si(100) and C60/Si(111) systems during annealing show that the outer molecular states of the C_{60} cage endure up to annealing temperature as high as 1040 K. These residual fragment molecular states are orbitals directed normal to the surface.
Cooperation: F4 research area, INFM-ALOISA, INFM-BEAR

C_{60} interacting with Pt(111) as studied by photoelectron diffraction and X-ray surface diffraction

C. Cepek , M. Sancrotti , L. Verdini, L. Giovannelli, L. Floreano , R. Gotter , A Morgante
M. Pedio, A. Pesci, F. Borgatti and R. Felici

C_{60} was deposited on Pt(111) and annealed at different temperatures. Fullerene bind covalently with Pt substrate atoms.The changes induced by adsorption on its electronic properties were studied by inverse photoemission spectroscopy. The structural properties of the single C60 monolayer were investigated by low-energy electron diffraction. The two domain hexagonal single monolayer was analysed by X-ray photoelectron diffraction (PhD) at ALOISA beamline [L. Giovannelli et al. Applied Surface Science 2003] and grazing incidence X-ray diffraction at ID-32 Beamline ESRF. PhD analysis show that the C60 molecules in the H2 reconstruction are bond with the six-carbon rings phasing the Pt(111) substrate.with the C-C bonds perpendicularly oriented with respect to the direction of the close packed atom rows.
Grazing incidence X-ray diffraction analysis show that the fullerene cage absorption leads to the vacancy od a Pt atom. The figure shows an artistic view of the molecular orientation of C60 as found by Grazing incidence X-ray diffraction data analysis.

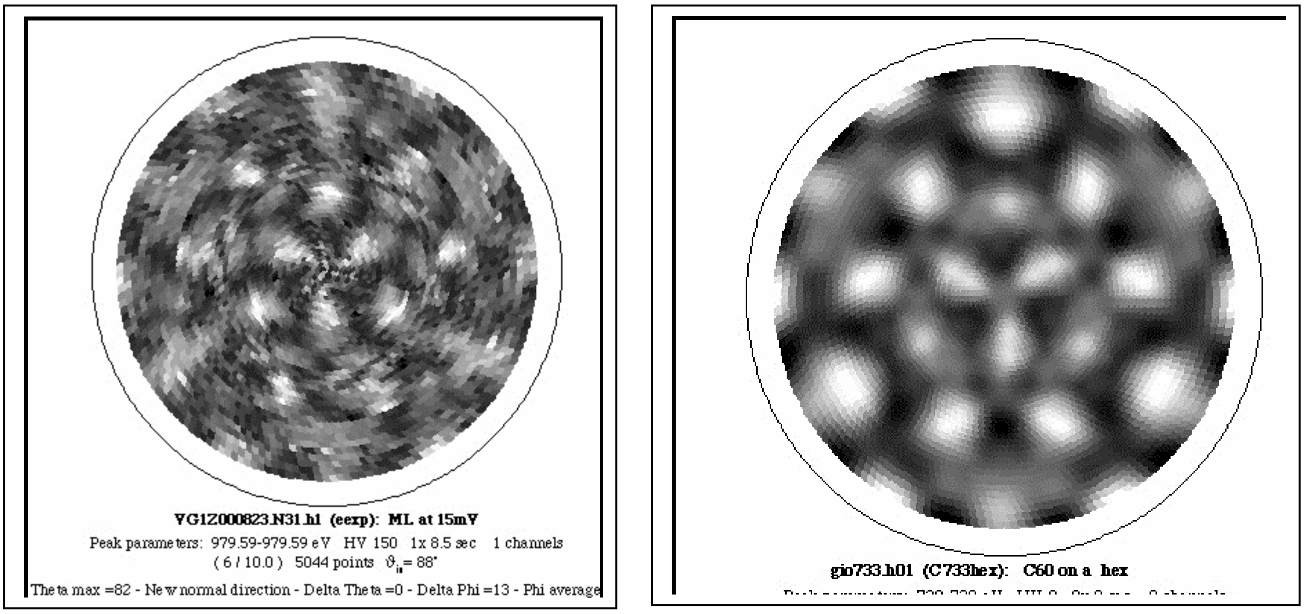

Fig. Stereo graphic projection in grey scale (white corresponding to the maximum intensity) of : (a) the experimental C 1s PhD pattern and (b) calculated Singls Scattering Cluster calculation pattern for a C60 molecule facing hexagon toward the surface.

The overlayer H2 reconstruction is commensurate with respect to the bulk as indicated by previous LEED studies. The surface cell has p3 symmetry and includes 13 Pt bulk cells. The fullerene induces vacancies in the underlying Pt top-most layer. The C60 molecules lie on top of the vacancies while the other Pt atoms show small local relaxations. The data fitting is sensitive to the fullerene orientation indicating that C60 is related to the substrate mostly through its hexagonal faces.

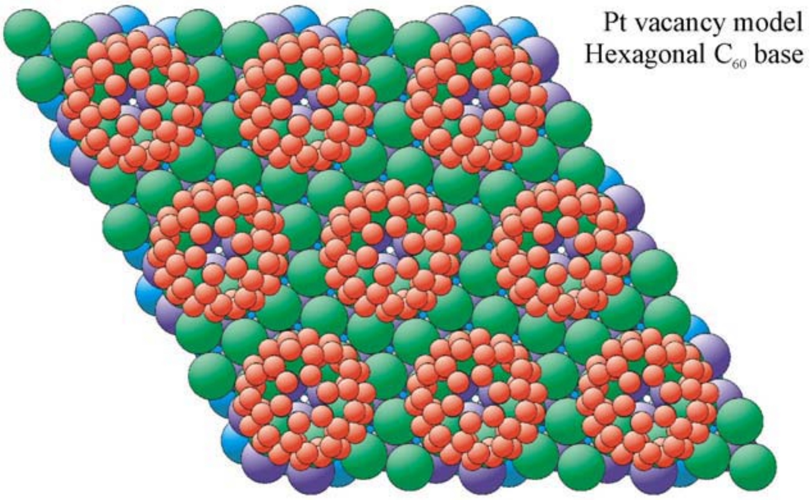

It is worth noting that decomposition of C_{60} takes place on Pt(111) above 560 K respectively and is kinetically limited reaction. These structural results give strong indication of the rehybridization of the π states of fullerene bonded to Pt(111) substrate as found by Inverse photoemission measurements and shown in the following figure. H2 reconstruction of C60 on Pt(111) can be considered as a very strongly chemisorbed precursor state for decomposition.

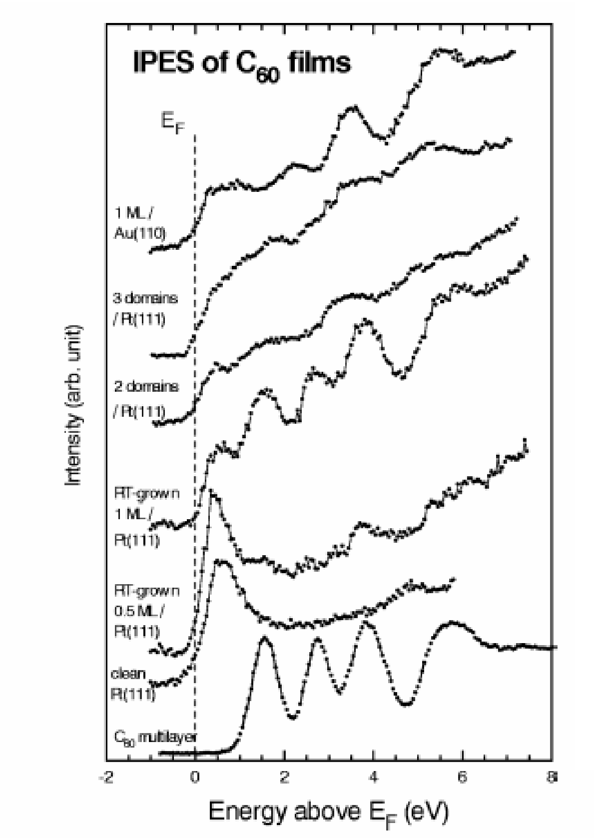

Figure to the left: Inverse photoemission spectra for different C_{60} overlay- ers on Pt(111). The spectra for the chemisorbed 1 ML
C 60 /Au(110) (top) and for the multilayer of C_{60} (shifted 0.12 eV) on the same Au(110) (bottom) are plotted for comparison [*M. Pedio et al.* / *Surface Science 437 (1999) 249–260]*.
Cooperation: F4 research area, INFM-ALOISA, OGG-ESRF

Nano-sized Objects and Thin Films (Research Area F4)

Co-ordinator: Massimo Sancrotti
Staff: Giovanni Bertoni, Cinzia Cepek, Elena Magnano

The research activity of this area is primarily devoted to study the electronic structure and the atomic arrangement of surfaces, interfaces, and thin films, encompassing fullerenes, semiconductors, cluster-assembled overlayers.

Concerning fullerenes, a wide investigation of the properties of ultra thin C_{60}-based films deposited onto single crystal surfaces has been pursued. Growth conditions favoring the formation of C_{60}-based superstructures in good epitaxy with the substrate have been found in a number of cases and special attention has been devoted to explore the properties of such C_{60}-based ultra thin films as a function of temperature. C_{60} was also used as a precursor for the growth of SiC onto the Si(111) surface. Strictly related to the topic of fullerenes is the activty onto carbon-based thin films produced in situ via cluster-assembling. In this context, one of our spectrometers has been equipped with UHV-compatible supersonic cluster source, designed by P. Milani *et al.*. This allowed us to study *in situ* the early stages of growth carbon clusters deposited onto selected surfaces.

Recently, the investigation of carbon nanotubes growth has been initiated, special emphasis being devoted to nanopatterned substrates provided to us by the beam line INFM-LILIT. Most of this research will be funded by the MIUR-FIRB project *Carbon-Based Microstructures and Nanostructures*.

Triggered by the high T_c superconductivity properties of MgB_2, we started a research aiming at growing *in situ* MgB_2 as a result of molecular beam epitaxy on a single crystal of Mg(0001). This enables us to evaluate *in situ* a number of structural and electronic structure properties of the thus-grown samples.

Proprietary research has also been pursued funded by a number of industrial grants, encompassing a) the development of plasma-based surface treatments for the functionalization of polymer-based materials to be used for packaging; b) the growth of carbon-based coatings obtained via Plasma Enhanced Chemical Vapor Deposition for prosthetic implants; c) microscopy analysis of polymer-based materials for food packaging.

The equipment of the research group includes a wide variety of electron spectroscopies (UPS, XPS, AES, EELS) and structural probes (LEED). A sizeable part of the work is also performed via access to international synchrotron radiation facilities (LURE, France; NSLS, U.S.A.; ELETTRA, Italy; BESSY I, Germany; SRS, U.K.; ESRF, France). Also acknowledged is the co-operation with a number of international groups in the domain of surface and interface science (Zürich Universität, CH; Universita' di Roma *La Sapienza*, Italy; Universita' di Genova, Italy; Universita' di Milano, Italy; LURE, France; NSLS, U.S.A.; ESRF, France).

Growth of Multi-Wall and Single-Wall Carbon Nanotubes with *In-Situ* High Vacuum Catalyst Deposition

C. Cepek, G.Bertoni, and M. Sancrotti

In the last few years, carbon nanotubes (CNTs) have attracted a great interest, due to their unique electronic and mechanical properties [1]. Among the CNT synthesis techniques, the chemical vapor deposition (CVD) allows the growth of high quality CNTs at a large scale [1-6]. In this case, a metal catalyst is usually needed for the CNTs synthesis and, by choosing the appropriate growth conditions (i.e. catalyst nature and thickness, precursor gases, and growth temperature), it is possible to obtain single- or multi-wall carbon nanotubes with controlled average diameter and length. In particular, by reducing the catalyst film thickness, it is possible to reduce the nanotubes diameter, and single-wall carbon nanotubes (SWCNTs) can be obtained, even if they are generally mixed with multi-wall carbon nanotubes (MWCNTs) [7].

Since 2002 our group is studying the controlled growth of CNTs via CVD and PECVD with the aim of the integration of CNT in electronic devices. The research activity has been performed in collaboration with the INFM beamline LILIT, which provides patterned substrates. We have studied the effect of oxidation of the catalyst in the growth of CNTs and we have found an efficient procedure for the synthesis of multi- and/or single-wall carbon nanotubes. The method is based on CVD process using acetylene as precursor gas and starting from a catalyst film deposited under high vacuum (HV) conditions (base pressure: $\sim 10^{-8}$ mbar) just before the CVD process. No hydrogen, ammonia or any other time-consuming pretreatment of the catalyst film are needed. This reduces the total time (i.e. catalyst film preparation and CVD process) for CNTs synthesis to 5-20 min, which has to be compared to the typical time needed in the other methods based on a supported catalyst film (i.e. several hours [3]). For a deeper understanding of the role of the catalyst and of its oxidization state, we have compared the CVD growth of carbon nanotubes on metallic and oxidized Fe and Ni films. Our results show that, when the catalyst is oxidized, only an amorphous carbon film grows, consisting of carbon-coated particles and some embedded carbon nanotubes. If the film is not oxidized, it is possible to grow the nanotubes also when the catalyst thickness is as low as $\approx$1nm and, in this case, the grown nanotubes are only single-wall.

Collaborations: F. Romanato (INFM- LILIT beamline ELETTRA, Trieste, Italy); C. Bottani, A. Li Bassi, C. S. Casari (Politecnico di Milano, Italy)

[1] See for example: *Carbon Nanotubes: Synthesis, Structure, Properties, and Applications,* Ed. by M.S. Dresselhaus, G. Dresselhaus, Ph. Avouris (Springer, Berlin, 2001)
[2] Y.Y. Wei, G. Eres, V.I. Merkulov, and D.H. Lowndes, Appl. Phys. Lett. 78, 1394 (2001); Y.Y. Wei, G. Eres, Appl. Phys. Lett. **76**, 3759 (2000)
[3] J. Kong, A.M. Cassell, and H. Dai, Chem. Phys. Lett. **292**, 567 (1998); J. Kong, H.T. Soh, A. M. Cassel, C.F. Quate, H. Dai, Nature **395**, 878 (1998)
[4] W.Z. Li, D.Z. Wang, S.X. Yang, J.G. Wen, Z.F. Ren, Chem. Phys. Lett. **335**, 141 (2001)
[5] J.-F. Colomer, C. Stephan, S. Lefrant, G. Van Tendeloo, I. Willems, Z. Kónya, A. Fonseca, Ch. Laurent, J.B. Nagy, Chem. Phys. Lett. **317**, 83 (2000)
[6] E.F. Kukovitsky, S.G. L'vov, N.A. Sainov, V.A. Shustov, L.A. Chernozatonskii, Chem. Phys. Lett. **355**, 497 (2002)
[7] Y. Homma, Y. Kobayashi, T. Ogino, Appl. Phys. Lett. **81**, 2261 (2002)

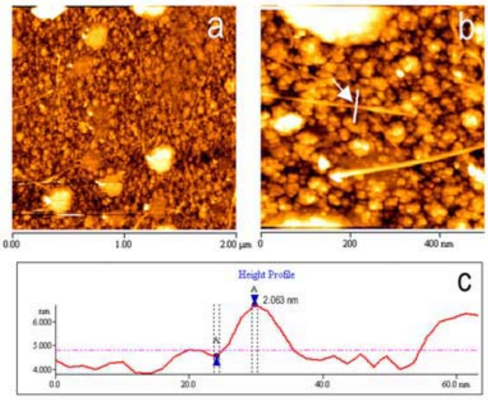

Fig.1: AFM non-contact mode images of the CNTs grown at 650°C on the ~1 nm thick Fe film: (a) 2 µm x 2 µm topographic image. (b) 500 nm x 500 nm topographic image. (c) Height profile for the line indicated by the arrow of Fig. 1b.

Growth of β-SiC(100) on Si(100) with Improved Interface Quality

C. Cepek, E. Magnano, G. Bertoni, and M. Sancrotti

In spite of all the efforts done by the scientific community, nowadays only few SiC-based devices are realized, because of the high difficulties to grow single-crystals and single-polytypes with sufficiently high quality for electronic applications [1]. High cost single-crystal wafers of 4H and 6H hexagonal SiC have been available since several years, but only recently it has been possible to grow epitaxially the cubic form 3C-SiC on Si substrates. Among all, the C_{60} and Si co-deposition growth method has been successfully used to synthesize 3C-SiC films on Si substrates [3]. By the appropriate choice of the Si and C fluxes, it is possible to reduce the silicon atoms effusion from the substrate, which is responsible of a large number of defects and voids formation, and the thus-grown samples show better crystalline and interface qualities with respect to others grown with more standard methods. In addition, by using only Si and C_{60}, no extra chemical species are present in the precursors substances (H-free SiC layer). However, the preparation conditions do influence the microstructure of the growing SiC, and the thus-grown samples still showed pits of pyramidal shape near the Si/SiC interface and holes on the surface. These samples have been grown in a rather high growth and base pressures (≈1x10^{-7}mbar and ≈1x10^{-8}mbar, respectively), which did not enable to obtain well-ordered, flat, and defect-free clean Si substrates. Actually the quality of the substrate on which the SiC film is grown is a clue point to obtain good quality films and interfaces. In fact, generally the morphology of thin films reflects the morphology of the substrate, and the number of defects of the grown film is related to the number of defects of the substrate surface. It results that the growth on atomically flat and defect-free surfaces is a necessary starting point to obtain good quality interfaces.

Our group studied the heteroepitaxial growth of SiC on Si(100), by using C_{60} and Si as precursors, focusing particular attention to the SiC-Si(100) interface quality. We spanned over a wide range of parameters that influence the growth process, including the substrate deposition temperature, the relative effusion fluxes of C_{60} and Si, and the clean Si(100) surface quality. We found that the quality of the SiC/Si(100) interface strongly depends on the clean substrate quality, the carbon and silicon atoms fluxes, and the substrate growing temperature. Our results indicate that the growth on flat and good quality silicon substrates is a crucial and a necessary starting point to reach good quality SiC/Si interfaces where the SiC film shows the minimum number of defects and higher degree of order.

Collaborations: M. Pedio (TASC-INFM, Trieste, Italy), INFM-BEAR beamline in ELETTRA (Trieste, Italy)

[1] See for example Physica Status Solidi **202** (1997)
[2] K. Volz, S. Schreiber, J.W. Gerlach, W. Reiber, B. Rauschenbach, B. Stritzker, W. Assmann and W. Ensinger, Mat. Sci. & Engineering A **289**, 255 (2000)

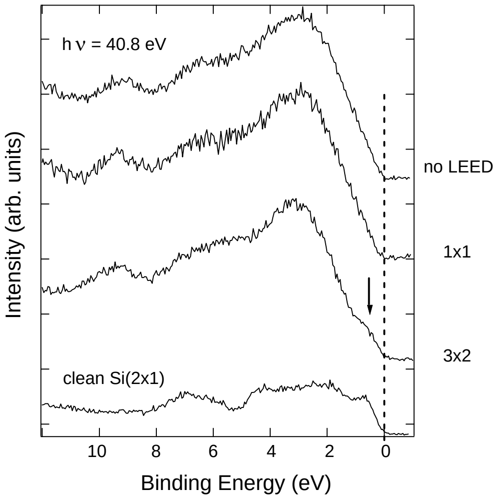

Fig.1: Valence band of the SiC thin films grown in different conditions compared to the clean Si(100)-2x1 surface. The samples presenting the 3x2 LEED pattern show a weak shoulder at ≈0.1eV, which is due to a surface state.

Cluster-Assembled Nanostructured Carbon-Based Films
E. Magnano, C. Cepek, and M. Sancrotti

Low energy cluster beam deposition (LECBD) has recently opened new possibilities as to the synthesis of innovative materials characterized by novel physicochemical and functional properties [1, 2]. These properties are subtly determined by the mass distribution of the precursor aggregates, by cluster-surface interaction and by the degree of cluster coalescence [3]. A variety of systems have been explored so far where the intimate structure can be tailored from the nano- to the meso-scale [1, 2].
The use of LECBD in ultra high vacuum conditions makes it possible to investigate the early stages of cluster deposition in ultra-clean conditions. This allows to address a series of fundamental issues such as the role played by the clusters at the sub-monolayer regime, where the interaction with the substrate is a clue point, in determining the further evolution of thin film growth and its resulting features (roughness, texture development, electronic transport, etc.). In addition, a subsequent fall-out is the investigation *per se* of isolated clusters deposited at surfaces thereby targeting, for example, cluster mobility at surfaces and their chemical reactivity as a function of cluster size, landing energy, substrate temperature, substrate topography, surface defects, etc.. Last but not least, the possibility of fabricating the specimen *in situ* avoiding any undesired contamination makes the interpretation of any experimental response (photoemission, optical, vibrational, etc.) more straightforward and actually reliable. The annealing of carbon clusters with linear, planar and cage structures can represent an alternative to the production of SiC compared to mixed cluster deposition and annealing of fullerenes. In order to produce carbides the use of carbon clusters deposited by LECBD demands appropriate investigation of the temperature-dependent evolution of their physico-chemical properties. We addressed the research on a systematic *in situ* study of the electronic structure of carbon clusters deposited onto Si(100)-(2x1) and Ag(100) surfaces via LEBCD, taking advantage of a very innovative UHV-compatible cluster source developed by the group of P. Milani of the University of Milan, providing supersonic beams of high stability and intensity. The choice of Ag and Si as substrates is suggested by the idea of comparing the deposition of carbon nanoclusters on metal surfaces for which a high mobility of the clusters is expected to the deposition on substrates where the interaction is very strong. A wide set of coverages has been explored on both the substrates. The electronic structure of the thus-obtained samples was characterized via valence band and core level photoemission. Multi-electron excitations were studied by means of Electron Energy Loss Spectroscopy (EELS). In addition, the thermal stability of a thin cluster-assembled carbon film grown onto Si(100)-(2x1) has been investigated and its conversion into a SiC-based film, due to thermal treatment, has been monitored (see Fig. 1).

Recently, it was demonstrated that the supersonic cluster beam deposition is an effective technique for creating structures with high aspect ratio and controlled shape, combining the control of the kinetic energy of the aggregates with high directionality of the beam and high particle fluxes [4].
We studied by scanning electron microscopy (SEM), spatially-resolved Auger electron spectroscopy (SR-AES), and atomic force microscopy (AFM), the thermal evolution of a micro-sized array of carbon dots, fabricated using supersonic cluster beam deposition through a stencil mask on a Si(100) substrate.
The increasing of the temperature induces the diffusion of Si from the substrate into the carbon dots, with the formation of Si-C bonds, starting from the interface dot-substrate and proceeding through the bulk of the dots, up to their top surface. The diffusion of Si is strictly connected to the formation of pits, mostly located at the proximity of the dots. These pits are interpreted as preferential channels for the diffusion of Si from the substrate to the carbon dot. The thermal treatment do not affect the geometry of the pristine pattern resulting in the production of an ordered array of SiC-like micro-sized dots.
Collaborations: F. Siviero, S. Vinati, C. Lenardi, A. Podesta', P. Piseri, E. Barborini, and P. Milani (Universita' di Milano, Italy)

[1] P. Milani, S. Iannotta, *Cluster Beam Synthesis of Nanostructured Materials,* Springer-Verlag, Berlin 1999
[2] C. Binns, Surf. Sci. Rep. **44**, 1 (2001)
[3] P. Jensen, Rev. Mod. Phys. **71**, 1695 (1999)
[4] E. Barborini, P. Piseri, A. Podesta', and P. Milani , Appl. Phys. Lett. **77**, 1059 (2000)

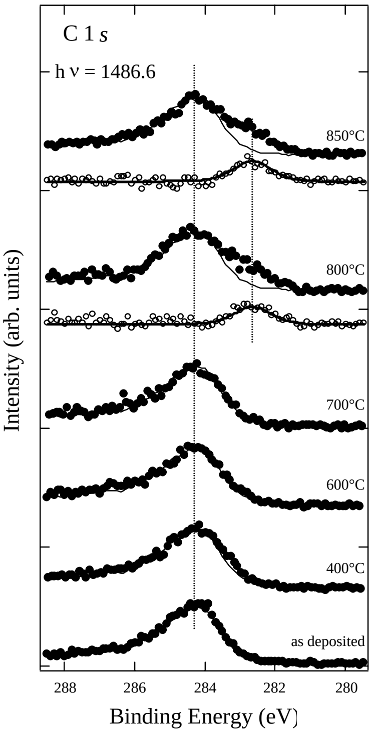

Fig.1 – Evolution of the core level spectra of a thick (≈ 30 nm) nano-structured carbon film as a function of the annealing temperature. The difference spectrum between the annealed sample and the as-deposited one is shown for the two last annealing steps. Formation of a SiC layer is pointed out.

In Situ UHV Epitaxial Growth of MgB_2 Thin Films and Characterization

C. Cepek, R. Macovez, and M. Sancrotti

The recent discovery of superconductivity at 39 K in MgB_2 stimulated an extraordinary research activity to explore the phenomenology and basic mechanism of superconductivity in this material. MgB_2 possesses several unusual and attractive properties. Temperature-dependent electronic anisotropy and multiple superconducting gap structures [1,2] appear to distinguish MgB_2 from a conventional BCS superconductor, and still remain to be explained. A critical step for studying both intrinsic superconducting properties and the possibility to realize superconducting devices based on MgB2 is the controlled growth of high quality epitaxial MgB_2 thin film heterostructures. The growth of MgB2 films has already been reported by several groups [3]. However the reported X-ray data do not show in-plane epitaxy, and there is no clear relationship between the MgB_2 film orientation and the orientation of the substrate.
Since 2002 in the Analytical Division of the TASC laboratory we are studying the possibility to grow thin films of MgB_2 epitaxially on Mg(0001) single crystal by molecular beam epitaxy (MBE), with the aim of the *in situ* study of its electronic properties by means of electron spectroscopies. The Mg-Mg distance in the Mg(0001)

surface is 3.19Å, while the Mg-Mg distance in the MgB_2 planes is 3.08. This lattice mismatch is favorable for an epitaxial growth, however the crystalline MgB_2 growth may be hampered by the reduced temperature that can be reached during the growth due to the extremely high sublimation rate of Mg in UHV conditions. Fig. 1 shows the valence band of thin films of boron epitaxially grown on the clean Mg(0001) surface at different growing temperature, along with the clean Mg(0001) surface spectrum. Although these are only preliminary results, we note the similarity between the spectrum of the sample grown at 250°C and the spectrum measured on a MgB_2 single crystalline grain with a different photon energy (shown in the inset) [4].
Collaborations: A. Goldoni (Sincrotrone Trieste, Italy)

[1] P. Szabo, P. Samuely, J. Kacmarcik, T. Klein, J. Marcus, D. Fruchart, S. Miraglia, C. Marcenat, and A. G. M. Jansen, Phys. Rev. Lett. **87**, 7005 (2001)
[2] F. Giubileo, D. Roditchev, W. Sacks, R. Lamy, D. X. Thanh, J. Klein, S. Miraglia, D. Fruchart, J. Marcus, and P. Monod, Phys. Rev. Lett. **87**, 7008 (2001)
[3] W. N. Kang *et al.*, Science **292**, 1521 (2001); C. B. Eom *et al.*, Nature (London) **411**, 558 (2001); Bu *et al.*, Appl. Phys. Lett. **81**, 1851 (2002)
[4] A. Goldoni et al., Phys. Rev. B **66**, 132503 (2002)

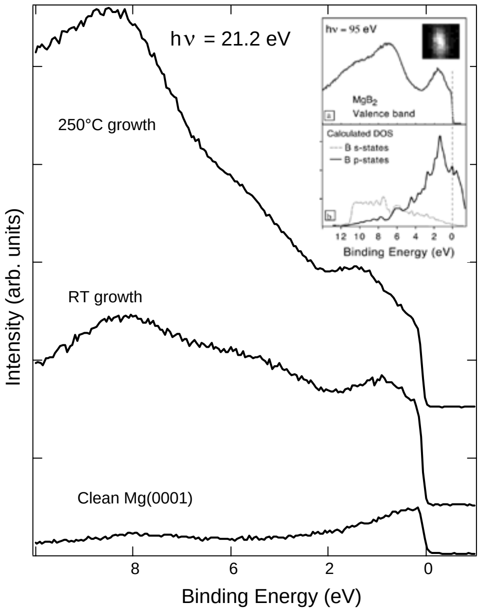

Fig.1: Valence band photoemission spectra of boron films grown on Mg(0001) at RT and 250°C. In the inset is shown the spectrum taken on a MgB_2 single crystalline grain together with the calculated boron density of states [4].

Self-Organization of Ag Islands on Ge(111)-*c*(2x8): A Spectromicroscopy Study (Work done at INFM-UC-Brescia) E. Magnano and M. Sancrotti

Since the late 70's, massive studies have been performed on the semiconductor-metal interfaces from both the experimental and theoretical points of view [1]. Many efforts have been devoted to the study of self-organization processes which opened wide intriguing perspectives in this field.
In this connection, the case of noble metals grown on Si and Ge is of special interest. Actually, for all the three metals (Au, Ag and Cu), coverages of several monolayers (ML) give rise, after annealing, to agglomerated interfaces with the formation of metallic islands reminiscent of the Stransky-Krastanov growth mode. However, in spite of these similarities, the atomic distribution in real space differs significantly depending on the specific noble metal species.
The case of the Ag/Ge interface has been extensively investigated in the past particularly in connection with the fact that an abrupt interface would be expected [2]. In spite of this, a complete understanding of surface phenomena during islands nucleation is still missing.
We have studied the thermal-induced changes of a thick layer of Ag grown on Ge(111) surface, by combining Scanning Electron Microscopy (SEM), Low Energy Electron Diffraction (LEED), Spatially Resolved Auger Electron Spectroscopy (SR-AES), and Atomic Force Microscopy (AFM).
At room temperature, Ag grows on Ge surface as a uniform layer but, as the temperature is raised, it evolves gradually starting from the occurrence of “holes” in the Ag deposit, then proceeding through the formation of dendritic structures and eventually giving rise to the nucleation of regularly shaped and ordered islands (Fig. 1). In these intermediate stages, different surface reconstructions appear, which result to be commensurate either to the Ge or to the Ag surface lattice parameter.

The still open questions of intermixing and segregation of Ge during Ag growth and during the thermal treatments of the grown sample has been studied in detail by following step by step the changes both in the line-shape and in the energy position of the Auger Ge $L_3M_{4,5}M_{4,5}$ and Ag $M_{4,5}VV$ lines.
Collaborations: M. Padovani, G. Bertoni, V. Spreafico, M. Fanetti, L. Gavioli (Universita' Cattolica del Sacro Cuore, Brescia, Italy).

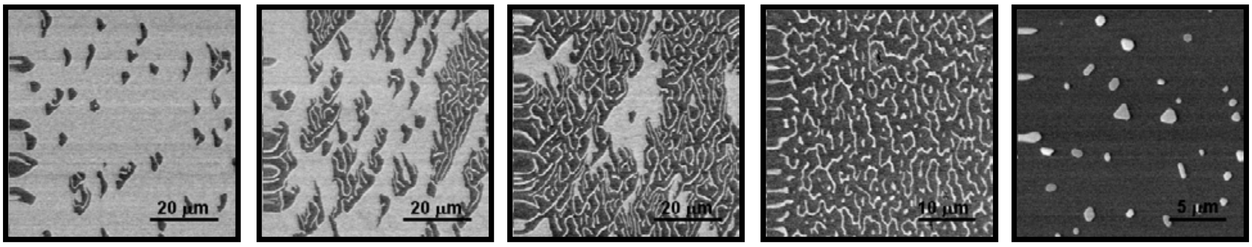

660 K **680 K** **730 K** **760 K** **800 K**

Fig. 1- SEM images of Ag/Ge(111) after annealing at selected temperatures. The gradual extension of the "holes" determines the formation of dendritic structures. At 800 K Ag is condensed in regularly shaped islands.

[1] G. Le Lay, Surface Science **132** (1983) 169; G Le Lay, L. Calliari, M. Sancrotti, and L. Braicovich, Phys. Rev. B **30**, 4885 (1984)
[2] F. L. Metcalfe, J.A. Venables, Surface Science **369**, 99 (1996)

Publications

[1] A.Goldoni, C. Cepek, R. Larciprete, L. Sangaletti, S. Pagliara, G. Paolucci and M. Sancrotti, Core Level Photoemission Evidence of Frustrated Surface Molecules: A Germ of Disorder at the (111) Surface of C_{60} before the Order-Disorder Surface Phase Transition, Phys. Rev. Lett. **88**, 196102 (2002)
[2] A.Goldoni, C. Cepek, R. Larciprete, L. Sangaletti, S. Pagliara, l. Floreano, R. Gotter, A. Verdini, A. Morgante, Y. Luo and M. Nyberg, C_{70} Adsorbed on Cu(111): Metallic Character and Molecular Orientation, Journal of Chemical Physics **116**, 7685 (2002)
[3] A.Goldoni, R. Larciprete, C. Cepek, C. Masciovecchio, F. El Mellouhi, R. Hudej, M. Sancrotti and G. Paolucci, Tracking Thermally Driven Molecular Reaction and Fragmentation by Fast Photoemission: C_{60} on Si(111), Surf. Rev. and Lett. **9**, 775 (2002)
[4] R. Larciprete, S. Lizzit, S. Botti, C. Cepek, and A.Goldoni, Structural Reorganization of Carbon Nanoparticles into Single-Wall Nanotubes, Phys. Rev. B **66**, 121402(R) (2002)
[5] E. Magnano, C. Cepek, S. Gardonio, B. Allieri, I. Baek, E. Vescovo, L. Roca, J. Avila, Maria Grazia Betti, C. Mariani, and M. Sancrotti, Sn on InSb(100)-*c*(2x8): Growth Morphology and Electronic Structure, Journal of Electron Spectroscopy and Related Phenomena **127**, 29 (2002)
[6] I. Vobornik, I. Avramova, L. Giovanelli, G. Panaccione, J. Fujii, S. Vobornik, C. Cepek, M. Sancrotti and G. Rossi, Influence of Impurities on the Density of States at the Fermi Level in the *c*(6x4)-C_{60}/Ag(100) Two-Dimensional Superstructure, Nucl. Instr. and Meth. in Phys. Res. B **200**, 1 (2003)
[7] E. Magnano, C. Cepek, M. Sancrotti, F. Siviero, S. Vinati, C. Lenardi, P. Piseri, E. Barborini, and P. Milani, *In Situ* Growth and Thermal Treatment of Nanostructured Carbon Produced by Supersonic Cluster Beam Deposition: An Electron Spectroscopy Investigation, Phys. Rev. B **67**, 125414 (2003)
[8] R. Larciprete, S. Lizzit, C. Cepek, S. Botti, and A. Goldoni, Thermal Reactions at the Interface between Si and C Nanoparticles: Nanotube Self-Assembling and Transformation into SiC, Surf. Sci. **532-535**, 886 (2003)
[9] T. Pardini, C. Cepek, R. Larciprete, L. Sangaletti, S. Pagliara, R. Gotter, L. Floreano, A. Verdini, A. Morgante, F. Parmigiani and A. Goldoni, Metallic Phases of a C_{70} Single Layer Adsorbed on Cu(111) Doped with Sodium, Surf. Sci. **532-535**, 892 (2003)
[10] G. Bertoni, C. Cepek, and M. Sancrotti, Temperature-Dependent Interaction of C_{60} with Ge(111)-*c*(2X8), Appl. Surf. Sci. **212-213**, 52 (2003)
[11] L. Giovanelli, C. Cepek, L. Floreano, E. Magnano, M. Sancrotti, R. Gotter, A. Morgante, A. Verdini, A. Pesci, L. Ferrari, and M. Pedio, Molecular Orientation of C_{60} on Pt(111) Determined by X-Ray Photoelectron Diffraction, Appl. Surf. Sci. **212-213**, 57 (2003)
[12] E. Magnano, C. Cepek, M. Sancrotti, F. Siviero, S. Vinati, C. Lenardi, E. Barborini, P. Piseri, P. Milani, Thermally Induced Changes in Cluster-assembled Carbon Nanocluster Films Observed via Photoelectron Spectroscopy, Appl. Surf. Sci. **212-213**, 879 (2003)
[13] M. Padovani, E. Magnano, G. Bertoni, V. Spreafico, L. Gavioli and M. Sancrotti, Ag Island Nucleation on Ge(111)-c(2x8), Applied Surface Science **212-213**, 213 (2003)

Contributions to Conferences

Goldoni A., Cepek C., Larciprete R., El-Mellouhi F., Masciovecchio C., Sancrotti M. and Paolucci G., *Thermally Induced Reactions and Fragmentation of Fullerenes on Si(111)*, 21st European Conference on Surface Science, Malmö, Sweden, June 2002

Magnano E., Cepek C., Padovani M., Sancrotti M.**,** Siviero F., Vinati S., Milani P., *ThermallyIinduced Changes in Carbon Nanocluster Films Observed via Photoelectron Spectroscopy*, 11th International Conference on Solid Films and Surfaces, Marseille, France, July 8-12, 2002

Bertoni G., Cepek C., Sancrotti M., *Temperature Dependent Interaction of C_{60} with Ge(111)-c(2x8)*, 11th International Conference on Solid Films and Surfaces, Marseille, France, July 8-12, 2002

Giovanelli L., Cepek C., Floreano L., Magnano E., Sancrotti M., Gotter R., Morgante A., Verdini A., Pesci A., Ferrari L., and Pedio M., *Molecular Orientation of C_{60} on Pt(111) Determined by X-Ray Photoelectron Diffraction*, 11th International Conference on Solid Films and Surfaces, Marseille, France, July 8-12, 2002

Padovani M., Magnano E., Bertoni G., Spreafico V., Gavioli L., and Sancrotti M., *Ag Island Nucleation on Ge(111)-c(2x8)*, 11th International Conference on Solid Films and Surfaces, Marseille, France, July 8-12, 2002

Magnano E., Gardonio S., Allieri B., Baek I., Vescovo E., Betti M. G., Mariani C., and Sancrotti M., *Synchrotron Photoemission Study of the Growth of Sn on InSb(100)*, 11th International Conference on Solid Films and Surfaces, Marseille, France, July 8-12, 2002

Cepek C., Schiavuta P., Magnano E., Prato S., Troian B., and Sancrotti M., *C_{60} and Si Co-Deposition on Si(100)-2x1: A New Method to Obtain Epitaxial 3C-SiC with Good Interface Quality*, E-MRS Spring Meeting, Strasbourg, France, June 2002

Vobornik I., Avramova I., Giovanelli L., Panaccione G., Fujii J., Vobornik S., Cepek C., Sancrotti M. and Rossi R., *Influence of Impurities on the Density of States at the Fermi Level in the c(6x4)-C_{60}/Ag(100) Two-Dimensional Superstructure*, E-MRS Spring Meeting, Strasbourg, France, June 2002

Pedio M., Cepek C., Magnano E., Bertoni G., Giovannini S., Spiller E., Sancrotti M., Borgatti F., Floreano L., Gotter R., Morgante A., Giglia A., Mahne N. and Nannarone S., *C_{60} Precursor SiC Formation on Silicon Surfaces: Thermal Fragmentation and Bonds Evolution as Detected by NEXAFS*, 3rd National Workshop on Silicon Carbide, Torino, Italy, March 28-29, 2003

Pedio M., Borgatti F., Giglia A., Mahne N., Nannarone S., Giovannini S., Cepek C., Magnano E., Bertonii G., Spiller E., Sancrotti M., Floreano L., Gotter R., Morante A., *Annealing Temperature Dependence of C_{60} on Silicon Surfaces: Bond Evolution and Fragmentation as Detected by NEXAFS*, 12th X-Ray Absorption Fine Structure Conference, Malmö, Sweden, June 2003

Padovani M., Magnano E., Bertoni G., Spreafico V., Panetti M., Gavioli L. and Sancrotti M., *Ag Island Nucleation on Ge(111)-c(2x8): A Spectromicroscopy Study*, INFMeeting, Genova, Italy, June 23-25, 2003

Cepek C., Magnano E., Bertoni G., Sancrotti M., Borgatti F., Giglia A., Pedio M., Paiser E., Felici R., *3C-SiC Ordered Film Obtained by Codeposition*, INFMeeting, Genova, Italy, June 23-25, 2003

Magnano E., Padovani M., Spreafico V., Panetti M., Sancrotti M., Podesta' A., Barborini E., Piseri P., and Milani P., *SiC-like Micropattern on Si(100)*, INFMeeting, Genova, Italy, June 23-25, 2003

Gavioli L., Padovani M., Fanetti M., Pasca D., Betti M. G., Sancrotti M., *Self-Organization of Pentacene Molecules on the Cu(119) Surface*, ICFSI Conference, 2003

Invited Talks

1) Sancrotti M., *Ultra thin fullerene-based films: Electronic structure and molecular arrangement*, 9th Joint Vacuum Conference, June 16-20, 2002, Schloß Seggau, Leibnitz, Austria (**PLENARY**)

2) Sancrotti M., *Carbon-Based Nanostructures*, 22nd Course of the International School of Solid State Physics, July 14-20, 2002, Erice, Italy

3) Sancrotti M., *Ultra thin fullerene-based films: Electronic structure and molecular arrangement*, 5th Micro Colloquium Microstructures, December 5-7, 2002, Paris, France

4) Sancrotti M., *Photoemission Spectroscopy*, Scuola di Dottorato in Ingegneria dei Materiali, November 27, 2002, Politecnico di Milano, Italy

5) Sancrotti M., *Defects and Doping Effects on the Single Layer of C60 Molecules Adsorbed on Ag(100)*, 203th Electrochemical Society Meeting (ECS), April 27-May 2, 2003, Paris, France

6) Sancrotti M., *Surface Science Experimental Methods*, Scuola Nazionale di Fisica della Materia, September 15-19, 2003, Torino, Italy

7) Sancrotti M., *Ultra thin fullerene-based films: Electronic structure and molecular arrangement*, Congresso Societa' Italiana di Fisica, September 17-22, 2003, Parma, Italy

Laurea Thesis

Spiller E., Proprietà Morfologiche ed Elettroniche di Nanostrutture Monodimensionali Autoassemblate: K/InAs(110), Universita' Cattolica del Sacro Cuore, Sede di Brescia, Supervisor M. Sancrotti, April 2003

PhD Thesis

Bertoni G., Carbon-Based Nanostructured Films, Universita' degli Studi di Milano, Supervisor M. Sancrotti, December 2002

Structure and Reactivity of Metal Surfaces (Research Area F5)

Coordinators: Giovanni Comelli,Renzo Rosei
Staff: Cristina Africh, Alessandro Baraldi, Erik Vesselli, Friedrich Esch

Introduction

The group activity is focussed on determining the structure of transition metal surfaces in the presence of adsorbates and coadsorbates, with respect to their chemical reactivity. We are interested in how adsorbates interact on a surface, how they modify the substrate, how the substrate structure influences reactivity and what the elementary steps in simple catalytic reactions are. To this purpose, we use a LEED/XPS apparatus for structural determination by diffraction techniques and a Variable Temperature Scanning Tunneling Microscope for direct imaging of the surfaces at an atomic scale. Further experiments are periodically performed at the Elettra beamlines, in particular at the SuperESCA.

The experiments are often complemented by DFT calculations of external groups.

Activity (2002-2003)

The group has been in charge of the "Fast STM" project, aimed at increasing the STM time resolution in the tens of milliseconds regime, and of the "Molecular beam" project, devoted to integrate a supersonic molecular beam in the SuperESCA system. Both projects have been successfully completed.

Major scientific interest has been the use of microscopy (STM) and spectroscopy (XPS) techniques for the study of the dynamics of surface processes. Particular attention has been devoted to the formation of dense oxygen layers on transition metal surfaces, the determination of the reaction mechanism for simple catalytic reactions and the characterization of surface structure in complex adsorbate systems.

The group participates in several national and international scientific projects, either in progress (INFM-PAISS, INFM-PURS, MIUR-COFIN, MIUR-FIRB, FVG-SRP) or under examination (EU-FP6-IP, MIUR-CE, MIUR-FISR).

Publications (2002-2003)

- C. Africh, F. Esch, G. Comelli and R. Rosei, *Reactivity and Deconstruction of the (1x2)-Rh(110)*, J. Chem. Phys. **116**, 7200 (2002).
- A.F. Lee, R.M. Ormerod, K. Wilson, R.M. Lambert, A. Goldoni, and A. Baraldi, *A fast XPS investigation of NO-promoted acetylene cyclotrimerisatin on Pd(111)*, Surf. Sci. **501**, L165 (2002).
- R. Lindsay, E. Michelangeli, B.G. Daniels, T.V. Ashworth, A.J. Limb, G. Thornton, A.Gutierrez-Sosa, A. Baraldi, R. Larciprete and S. Lizzit, *Impact of defects on the surface chemistry of ZnO(000-1)-O*, J. Am. Chem. Soc., **124**, 7117 (2002).
- E.D.L. Rienks, J.W. Bakker, A. Baraldi, S.A.C. Carabineiro, S. Lizzit, C.J. Weststrate and B. Nieuwenhuys, *Interaction of nitric oxide with Pt(100). A fast X-ray photoelectron spectroscopy study*, Surf. Sci. **516**, 109 (2002).
- Ph. Hofmann, Ch. Sondergaard, S. Agergaard, S.V. Hoffmann, J.E. Gayone, S. Moreno, G. Zampieri, S. Lizzit and A. Baraldi, *Unexpected surface sensitivity at high energies in angle-resolved photoemission*, Phys. Rev. B **66**, 245442 (2002).
- A. Baraldi, L. Rumiz, M. Moretuzzo, M. Barnaba, G. Comelli, S. Lizzit, G. Paolucci, R. Rosei, F. Buatier de Mongeot and U. Valbusa, *A Supersonic Molecular Beam for Gas-Surface Interaction Studies with Synchrotron Radiation*, J. Vac. Sci. Technol. A **20**, 683 (2002).
- L. Savio, L. Vattuone, M. Rocca, F. Buatier de Mongeot, G. Comelli, A. Baraldi, S. Lizzit, and G. Paolucci, *Formation of Channels for Oxygen Migration Towards Subsurface Sites by CO Oxidation and Growth of the Surface Oxide Phase on Ag(001)*, Surf. Sci. **506**, 213 (2002).
- G. Paolicelli, A. Fondacaro, A. Ruocco, A. Attili, G. Stefani, G. Ferrini, M. Peloi, F. Parmigiani, G. Banfi, G. Cautero, R. Tommasini, G. Comelli and R. Rosei, *A Novel Apparatus for Laser-Excited Time-Resolved Photoemission Spectroscopy*, Surf. Rev. Lett. **9**, 541 (2002).
- F. Bondino, G. Comelli, A. Baraldi, S. Lizzit, F. Esch, A. Locatelli, A. Goldoni, R. Larciprete, G. Paolucci and R. Rosei, *Angle-Scanned High Resolution Photoelectron Diffraction: from Clean Surfaces to Complex Adsorption Systems*, Surf. Rev. Lett. **9**, 741 (2002).
- F. Bondino, G. Comelli, A. Baraldi, R. Rosei, S. Lizzit, A. Goldoni, R. Larciprete and G. Paolucci,

Photoelectron Diffraction Study of the Low-temperature, Low-coverage Oxygen Layer on Rh(110), Phys. Rev. B **66**, 075402 (2002).

- L. Vattuone, L. Savio, M. Rocca, L. Rumiz, A. Baraldi, S. Lizzit and G. Comelli, *Real–Time XPS Investigations of the Impact–Energy Dependence of* C_2H_4 *Adsorption on Ag(100)*, Phys. Rev. B **66**, 085403 (2002).
- J.M. Ripalda, E. Román, L. Galán, I. Montero, S. Lizzit, A. Baraldi, G. Comelli, G. Paolucci and A. Goldoni, *Core Level Spectra of Amorphous Carbon Nitride*, J. Chem. Phys. **118**, 3748 (2003).
- A. Baraldi, G. Comelli, S. Lizzit, M. Kiskinova and G. Paolucci, *Real Time XPS of Surface Reactions*, Surf. Sci. Rep. **49**, 169 (2003)
- A. Baraldi, S. Lizzit, A. Novello, G. Comelli and R. Rosei, *Second-Layer Surface Core–Level Shift on Rh(111)*, Phys. Rev. B. **67**, 205404 (2003)
- J. Onsgaard, S.V. Hoffmann, P. Møller, P.J. Godowski, J.B. Wagner, G. Paolucci, A. Baraldi, G. Comelli, A. Groso, *Adsorption of* CO_2 *and Coadsorption of H and* CO_2 *on Potassium-Promoted Cu(115)*, ChemPhysChem **4**, 466 (2003).
- F. Bondino and G. Comelli, *Analysis of the Angular Distribution of Soft-x-ray Photoelectrons: a Tool for Surface Structure Determination*, J. Electr. Spectr. Relat. Phenom. **129**, 171 (2003).
- F. Bondino, E. Vesselli, A. Baraldi, G. Comelli, A. Verdini, A. Cossaro, L. Floreano, A. Morgante, *Molecular Orientation of CN Adsorbed on Pd(110)*, J. Chem. Phys. **118**, 10735 (2003).

Conference Contributions (2002-2003)

1. *F. Bondino, G. Comelli, A. Baraldi, S. Lizzit, A. Goldoni, R. Larciprete, R. Rosei,* Structure of the Low-Coverage Oxygen Layer on Rh(110), *ICSFS-11, Marseille (France), 2002.*
2. *K. C. Prince, C. Castellarin Cudia, G. Comelli, Saw Wai Hla, Z. Sljivancanin, B. Hammer, A. Baraldi, and R. Rosei,* Temperature Dependent Mechanisms of the CO+O Reaction on Rh(110), *ICSFS-11, Marseille (France), 2002.*
3. *G. Comelli, C. Castellarin Cudia, Saw Wai Hla, Z. Sljivancanin, B. Hammer, A. Baraldi, K.C. Prince, and R. Rosei,* The CO+O Reaction on the Rh(110) Surface, *NANO-7/ECOSS-21, Malmö (Sweden), 2002.*
4. *A. Baraldi, "Surface Core Level Shift on Metal Surfaces: from Structural Determination to Chemical Reactions", MAX-Lab Seminar, Lund, 2002* ***(invited)****.*
5. *C. Africh, S. Marchini, F. Esch, G. Comelli, and R. Rosei,* NH_3-NO Complex Formation on Pt(111) Studied by STM, *NANO-7/ECOSS-21, Malmö (Sweden), 2002.*
6. *G. Comelli*, Analysis of the Angular Distribution of Soft-X-Rays Photoelectrons: a Tool for Surface Structure Determination, *The 22nd Werner Brandt Workshop, Namur (Belgium), 2002* ***(invited)****.*
7. *F. Esch, C. Africh, S. Marchini, G. Comelli, R. Rosei,* The Formation of a NO-NH_3 Complex on Pt(111): an STM Study, *INFMeeting, Bari (Italy), 2002.*
8. *F. Esch, C. Africh, S. Marchini, G. Comelli, R. Rosei,* Fast STM for the Study of Surface Processes: NO/NH3 Interaction on Pt(111), *INFMeeting, Bari (Italy), 2002.*
9. *F. Bondino, G. Comelli, A. Baraldi, S. Lizzit, A. Goldoni, R. Larciprete, G. Paolucci, R. Rosei,* Quantitative Structure Determination of the Low-Temperature, Low-Coverage Oxygen Layer on Rh(110) by means of Photoelectron Diffraction, *INFMeeting, Bari (Italy), 2002.*
10. *L. Savio, M. Rocca, L. Rumiz, A. Baraldi, S. Lizzit, G. Comelli,* Real time XPS Investigation of the Impact Energy Dependence of C_2H_4 Adsorption on Ag(100), *Workshop on "Towards an understanding of simple catalytic reactions", Trieste (Italy), 2002.*
11. *G. Comelli, F. Bondino, A. Baraldi, E. Vesselli, R. Rosei, A. Goldoni, S. Lizzit, C. Bungaro, S. de Gironcoli, S. Baroni,* NO Adsorption on Rh(100), *Workshop on "Towards an understanding of simple catalytic reactions", Trieste (Italy), 2002.*
12. *A. Baraldi, S. Lizzit, G. Comelli, M. Kiskinova, G. Paolucci, R. Rosei,* Surface Core Level Shift on Metal Surfaces: from Structural Determination to Chemical Reactions, *Workshop on "Towards an understanding of simple catalytic reactions", Trieste (Italy), 2002.*
13. *F. Esch, M. Corso, C. Africh, G. Comelli and R. Rosei,* Two Step Reaction on a Nanostructured Surface, *Workshop on "Towards an understanding of simple catalytic reactions", Trieste (Italy), 2002.*
14. *F. Esch, C. Africh, A. Spessot, G. Comelli and R. Rosei,* Fast STM for the Study of Surface Processes, *INFMeeting, Genova (Italy), 2003.*

15. *L. Vattuone, A. Gerbi, M. Rocca, U. Valbusa, F. Pirani, D. Cappelletti, F. Vecchiocattivi, A. Baraldi, L. Petaccia and L. Rumiz,* Molecular beam study of the interaction of the aligned ethylene molecules with O2-Ag(001), *INFMeeting, Genova (Italy), 2003.*
16. *F. Esch, C. Africh, M. Corso, G. Comelli and R. Rosei,* Reactivity of a strained surface, *INFMeeting, Genova (Italy), 2003*
17. *R. Rosei,* Measuring the local reactivity of surfaces, *IV Convegno Nazionale sulla Scienza e Tecnologia dei Materiali, Ischia (Italy), 2003* ***(invited)***.
18. *C. Africh, M. Corso, F. Esch G. Comelli and R. Rosei,* Reactivity of a strained, segmented surface, *ECOSS-22, Prague (Czech Republic), 2003.*
19. *C. Africh, M. Corso, F. Esch G. Comelli and R. Rosei,* Two step reaction on a strained surface: H_2 + (10x2)-O/Rh(110), *STM'03, Eindhoven (Netherlands), 2003.*
20. *F. Esch, C. Africh, S. Marchini, G. Comelli and R. Rosei,* NO-NH_3 complex formation on Pt(111) studied by STM, *STM'03, Eindhoven (Netherlands), 2003.*

Reactivity of a strained, segmented surface: O/Rh(110)

C. Africh, G. Comelli, M. Corso, F. Esch and R. Rosei

High coverage, compressed oxygen structures, which often form on transition metal surfaces, can be regarded as the link between adsorbate systems and oxide phases. The study of their reactivity is therefore important for the understanding of the catalytic activity of oxidic surfaces. On Rh(110), a metastable, oxide-like, reconstruction has been found, where the high local oxygen coverage induces a strain, which leads to the formation of segmented Rh chains. The Rh atoms, which are ejected during the formation of the segments, nucleate and form islands in which the surface is not reconstructed. The surface is thus composed by coexisting reconstructed (segmented) and unreconstructed areas (Fig.1).

This adsorption system represents a perfect example on which the effect of strain and segmentation on reactivity can be studied. We investigated the reactivity of the (10×2)-O surface towards hydrogen at different temperatures and on various length scales.

When exposing the surface to hydrogen, the water formation reaction proceeds unambiguously in two distinct steps (Fig.2). In a first step a reaction front propagates on the surface, removing one oxygen atom of every couple in the (10×2)-O configuration. The strain is immediately released (thus demonstrating that it is due to the high local O coverage) and the surface relaxes to a more stable configuration with the remaining O atoms bound in threefold sites in a zig-zag fashion. Only in a second reaction step also this second half of oxygen is reacted off from the segment ends on. The strain release during the first reaction step opens up free adsorption sites for hydrogen dissociation in the segmentations; the second step starts therefore homogeneously on the surface from the segmentations on.

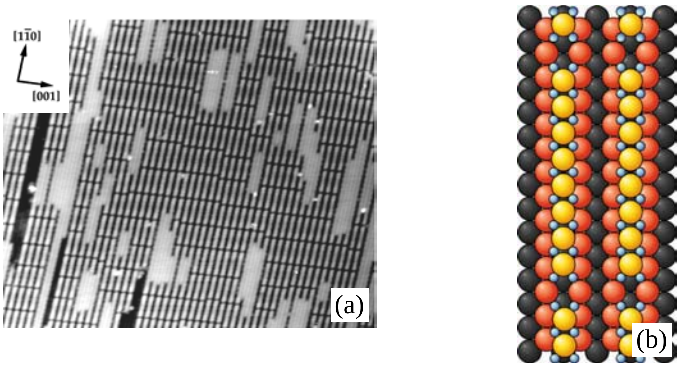

Fig.1: STM image (40 nm × 250 nm) of the surface and model of the segmented (10×2)-O structure.
Oxygen atoms (small blue circles) occupy symmetrical threefold sites along the Rh rows. Because of the high local O coverage, the metal atoms are moved from their original position (thus increasing the interatomic distance), so that two atoms out of ten are ejected.

At RT the reaction nucleates at jagged steps and the front propagates with an elliptical shape, faster along the $[1\bar{1}0]$ direction, and is not affected by the presence of defects and steps (Fig.3). When lowering the temperature, the anisotropy diminishes and a new kind of nucleation centres starts to compete. What is common to all nucleation centres is the presence of unreconstructed areas (which are intrinsically part of the (10×2)-O surface) close to defects.

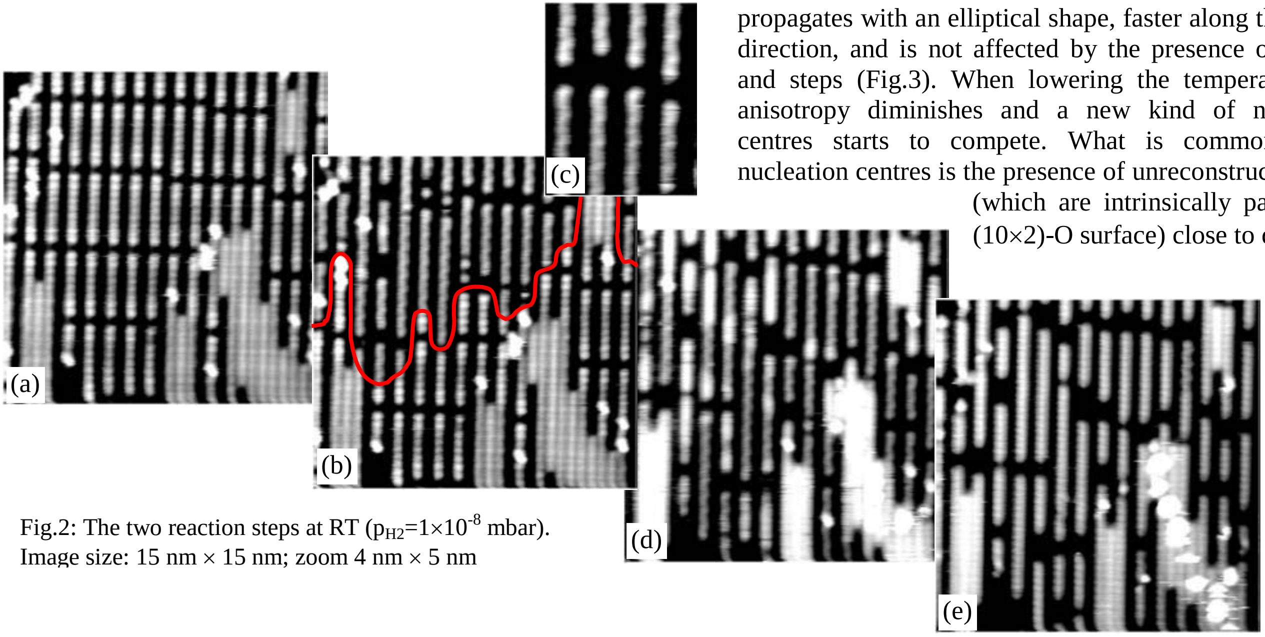

Fig.2: The two reaction steps at RT ($p_{H2}=1\times10^{-8}$ mbar).
Image size: 15 nm × 15 nm; zoom 4 nm × 5 nm

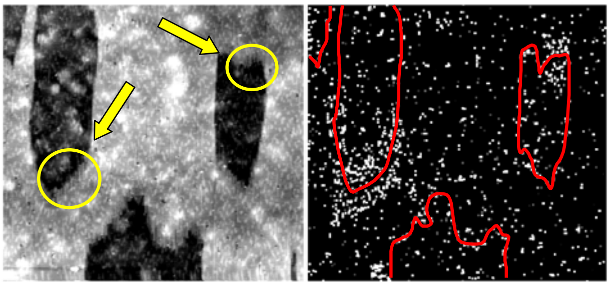

Fig.3: Reaction front at RT. On the left, nucleation centres are indicated on a topographical image. On the right, topographical features have been removed and the contrast has been enhanced in order to highlight the front; here the steps are indicated by red lines. Image size: 0.5 µm × 0.5 µm

Fast STM for the study of surface processes

F. Esch, C. Africh, A. Spessot, G. Comelli and R. Rosei

The time resolution of conventional STM measurements is limited to about 10 s/image, due to the limitation of the feedback loop in constant current measurements. This limits the range of dynamic phenomena that can be observed - like propagating reaction fronts, structural rearrangements upon external perturbations and molecular motion -, which often cannot be slowed down just by reducing the temperature.

In order to improve time resolution by up to 3 orders of magnitude, two approaches have been proposed in literature: *Video STM* (fast imaging in the constant height mode at video frequency) and *Tracking STM* (by locking the STM tip on a specific feature). We have developed in our group and in collaboration with the Instrumentation and Detector Laboratory of ELETTRA a FastSTM module based on the *Video STM* approach, to be used in combination with our commercial VT-STM from Omicron.

We opted for a modular architecture where the FastSTM module is inserted between STM and existing Omicron control hardware (see fig. 1), which is not modified and can be used for standard image acquistion. In this way, the vertical tip control, as well as the lateral drift correction, continues to be performed by the Omicron hardware; only the fast lateral scan and the synchronised current data acquisition are performed by the module. This allows later for full transferability of the FastSTM module to other STM systems or other scanning microscopes.

Besides the development of the FastSTM module, care had to be taken in order to reduce the noise and to increase the time resolution of the current measurement: A new piezo cabling reduced the pickup noise with respect to the original Omicron STM setup by a factor of 3. In combination with the FEMTO preamplifier, a noise reduction down to ≤5 pA_{pp} could be achieved (LN, gain 10^9), which corresponds to an overall noise reduction of a factor of 50 with respect to the original Omicron STM setup.

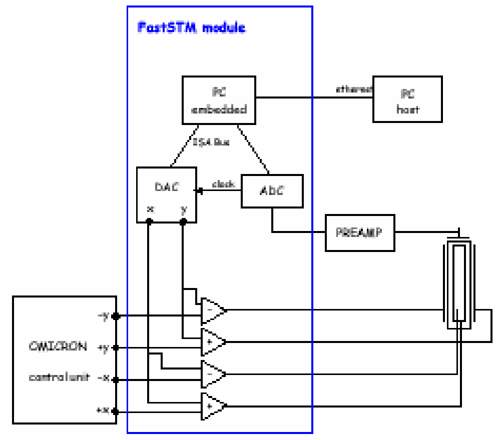

Fig.1: Architecture of the FastSTM module. The modulation in x and y direction is driven by 4 APEX operational amplifiers. They add the output of the DAC board (2 8 bit waveforms and 2 8 bit offsets) to the output of the Omicron control unit Synchronisation with data acquisition (12 bit ADC) occurs via the ADC clock which triggers the DAC.

First FastSTM results, performed on a c(2x8)-O/Rh(110) surface as test structure (see fig. 2), can be summarised as follows:

- the Omicron control system is not perturbed by the insertion of the FastSTM module
- the quality of the acquired images of the Omicron system and of the FastSTM module under same acquisition conditions is comparable in noise and spatial resolution
- the mechanical stability of the commercial Omicron STM is sufficient to obtain atomic resolution under fast scanning conditions
- *Video STM*: time resolutions of 25 ms/image (50x50 pixel), resp. 625 ms/image (250x250 pixel) can currently be achieved (will be enhanced by a factor of 8 after prototype engineering)
- *Tracking STM*: when taking 10x10 pixel images, time resolution with the FastSTM acquisition system can be pushed down to 1 ms/image. An image based tracking approach is feasible and should have the advantage of higher tracking stability with respect to the conventional lock-in/circular dither approach.

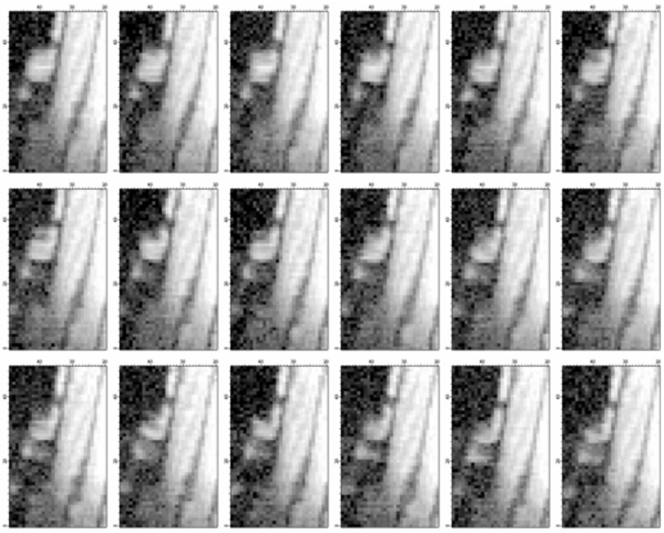

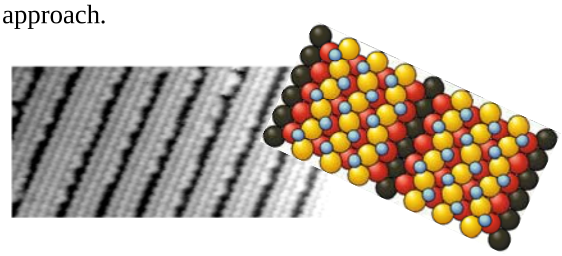

Fig.2: FastSTM image sequence of a c(2x8)-O/Rh(110) surface.

Right: Structural model (blue balls represent O, yellow balls Rh), conventional constant current (above) and constant height image.
17x9 nm^2, 0.5 nA, +0.6 V.

Left: FastSTM sequence taken with 15 ms/image close to a step. Atomic resolution across the missing rows is retained.
3x5 nm^2 (30x50 pix.), 0.5 nA, +0.6 V.

Structure and stability of NO on Rh(100)

F. Bondino, G. Comelli, E. Vesselli, A. Baraldi, A. Goldoni, S. Lizzit and R. Rosei

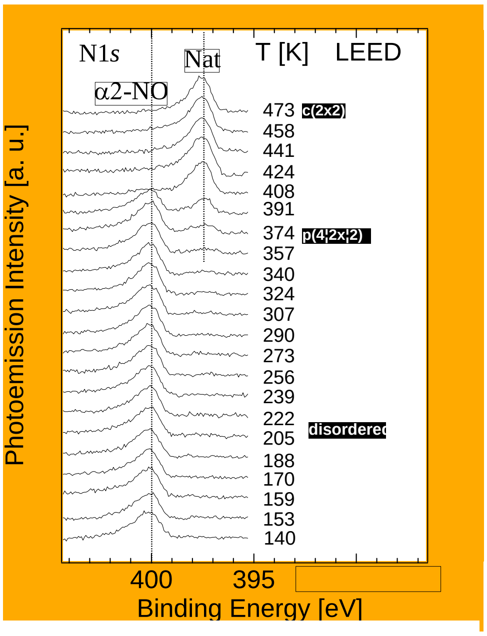

Figure 1: Sequence of selected N 1*s* photoemission spectra with the corresponding observed LEED patterns, measured during the linear-rate annealing of the saturated α2-NO layer adsorbed at 140 K on Rh(100).

Among transition metals, rhodium is particularly selective for N_2 production and effective for nitric oxide reduction, a key chemical reaction for the environment. In order to understand the activity of rhodium in the dissociation of NO, the structure, composition, stability and thermal evolution of NO adsorption layers formed on Rh(100) have been fully characterized using several techniques. Two different NO species are detected on the Rh(100) surface at 140 K by X-ray Photoemission Spectroscopy (XPS). A single NO chemisorbed species (α2) is found at saturation, forming a disordered phase which develops in a new ordered *p*(4x2)R45° Low Energy Electron Diffraction (LEED) structure after heating the layer to 373 K (see Fig. 1).

The bonding geometry of α2-NO has been determined by combining polarization-dependent Near Edge X-ray absorption Fine Structure (NEXAFS) and Photoelectron Diffraction (PD). Both the position of the N1s PD forward scattering peak and the angular dependence of the N K-shell absorption spectra provide direct evidence that α2-NO molecules are oriented upright, bonded through the N atoms (see Fig. 2). PD combined to multiple scattering cluster calculations further indicates that α2–NO are adsorbed at a bridge site. Upon annealing of the *p*(4x2)R45°-NO layer the NO molecules dissociate progressively and, above 425 K, a c(2x2) phase consisting of co-adsorbed N and O atoms is observed. At low NO coverage, a different NO molecular species (α1), characterized by ~1.7 eV lower N1s binding energy, is revealed (Fig.3). Considering the change in the total energy of the system when the core electron is removed, in the framework of the Z+1 approximation, a lying-down geometry for α1 is consistent with the sign of the large N1*s* core level shift between α1 and α2. The α1-NO species is observed to undergo dissociation under the 500 eV synchrotron light, whereas α2-NO is stable to irradiation. The different molecular orientations between α1- and α2-NO and, thus, the different electronic coupling to the substrate could be at the origin of the different selectivity in N-O bond breaking of the two NO species.

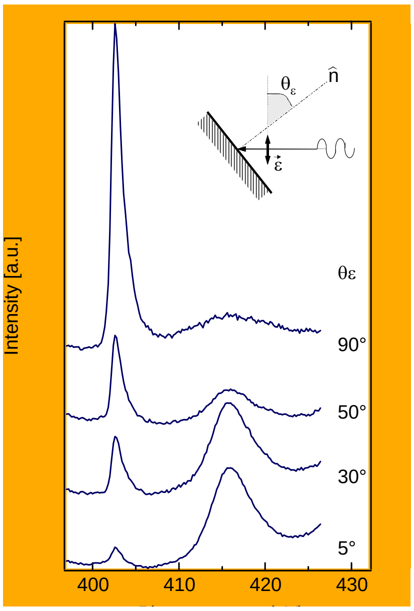

Figure 2: Auger yield N-edge NEXAFS spectra recorded as a function of the light-polarization polar angle at fixed surface azimuthal orientation from a α2-NO saturated

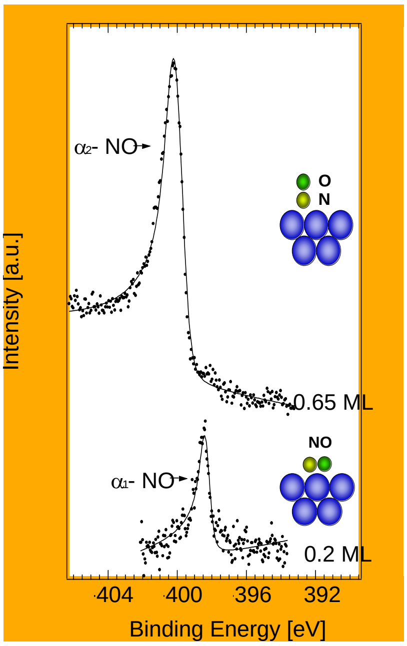

Figure 3: N1s photoemission spectra of the different NO species on Rh(100) at 140 K.

Molecular orientation of CN adsorbed on Pd(110)

F. Bondino, E. Vesselli, A. Baraldi, G. Comelli, A. Verdini, A. Cossaro, L. Floreano and A. Morgante

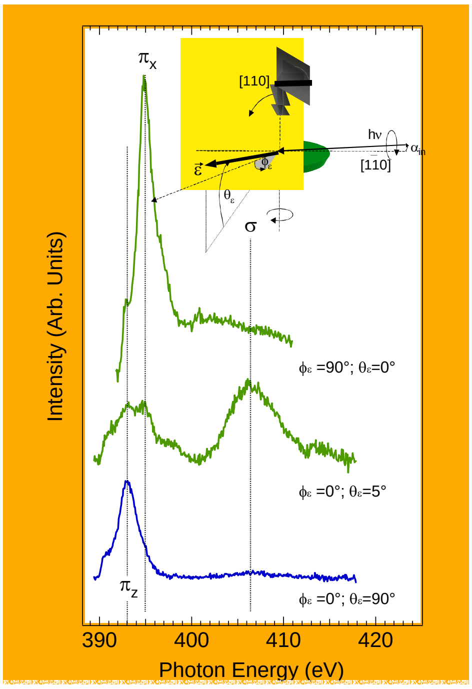

Fig. 1 Comparison of of Auger Yield N K-shell NEXAFS spectra NEXAFS spectra measured for along the [1$\underline{1}$0], [001] and [110] directions.

CN is an interesting molecule having a model character for the surface interactions of organic and polymeric nitriles, where the CN functional groups provide important centers for surface attachment. On metal surfaces in ultra high vacuum environment the CN bonding geometry is rather peculiar. Unlike most adsorbed diatomic molecules and contrary to expectations drawn from co-ordination chemistry, on most metal-vacuum interfaces CN does not bind in the typical end-on geometry, but with the molecular axis essentially parallel to the surface.

By combining polarization-dependent near edge x-ray absorption Fine Structure (NEXAFS) and full-solid-angle x-ray photoelectron diffraction (PED) we have determined the bonding geometry of the C–N molecule in the saturated *c*(2×2) layer on the Pd(110) surface. The experiments were performed at the ALOISA beamline. The N K-edge spectra display a strong dependence on the polar and azimuthal orientation of the light polarization with respect to the sample surface (Fig. 1). A strong forward scattering peak along the [001] direction (ϕ=0°) is present in the full-solid-angle photoelectron diffraction data of the C1s core level (Fig.2).

Both the position of the C1s PED forward scattering peak and the angular dependence of the N K-shell absorption spectra provide direct evidence that the CN molecules are oriented with the molecular axis along the [001] surface direction, at variance with earlier conclusions based on angle-resolved valence level photoemission data. The forward scattering peak in the C1s PED data, combined to single scattering cluster calculations (SSC), further indicates that the N atoms lie above the C atoms, with the C–N molecular axis tilted by 25°±4° with respect to the surface plane. A schematic representation of the CN adsorption geometry as derived from PED and NEXAFS measurements is shown in Fig. 2.

This geometry shows a strong analogy with the results of previous structure determinations of CN adsorbed on Ni and Rh (110) surfaces.

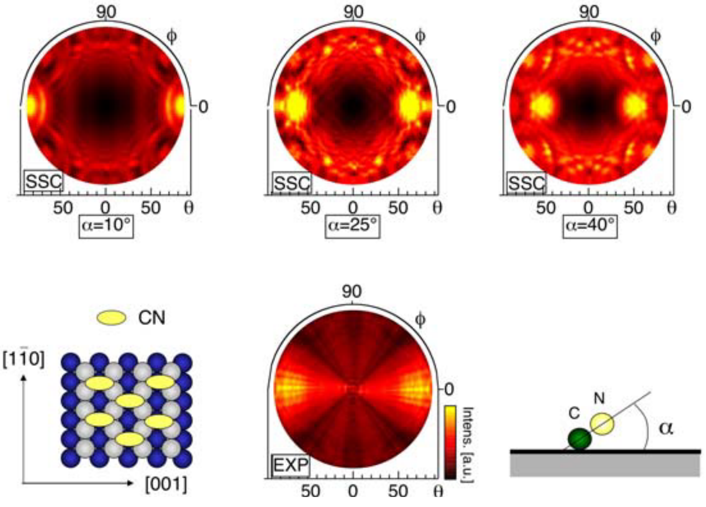

Fig. 2 Full-solid-angle C1*s* PED pattern measured at 947 eV photon energy (bottom) with the PED simulation obtained for a C–N tilt angle of 10°, 25° and 40° from the surface plane (top). Each point in the displayed patterns shows the normalized intensity in a linear grey scale of the C1*s* core level measured at a specific (θ, ϕ) angular position, in a polar coordinate system.

Facility for In-Situ Growth of Complex Oxides and Advanced Characterisation and Experimentation

The goal of this research line is in-situ studies of the surface and interfacial properties of strongly-correlated transition-metal oxides (e.g., cuprates and manganites) by synchrotron techniques. The project has taken concrete form since May 2002 when Dr. B. A. Davidson joined TASC. Since then, progress has been made on 4 different fronts: 1) internal scientific discussion and consensus of the interested groups both at TASC and Elettra; 2) detailed design of the oxide MBE growth system with TASC technical staff; 3) requests for funding; and 4) identification of potential collaborations with the other groups within the INFM that already perform thin-film growth of the targeted oxide materials.

The first step in clarifying a research strategy has been lengthy internal discussion of the experimental and scientific state-of-the-art regarding cuprates and manganites within the materials' growers and the synchrotron radiation communities. This involved a series of informal seminars with personnel from TASC, APE and ALOISA principally. Several of the most important and unresolved problems of the physics of cuprates and manganites have been identified (e.g., non-Fermi behavior and quantum criticality in cuprates, mesoscopic phase separation in both cuprates and manganites, failures of double-exchange model in manganites, to name a few). Oxide MBE growth has been chosen for its superior control of atomic layering and surface engineering as compared to alternative techniques, in consultation with the internal personnel directly involved in future experiments. Dr. Davidson and the technical staff of TASC (Dr. R. Gotter, A. de Luisa) have completed the design of the MBE chamber, and have received preliminary quotes from 4 prospective fabricators (all Italian). All essential subsystems have also been designed, parts specified among competitive vendors and quotations received. Throughout, a distinction has been made between what can be built in-house and what must be bought from outside vendors, to minimize costs. The subsystems include: evaporators (both Knudsen cells and mini ebeam evaporators), Atomic Absorption Spectroscopy [AAS] (together with 1st Researcher F. Martelli at TASC), Reflection High Energy Electron Diffraction [RHEED], manipulator and transfer subsystems [compatible with APE and ALOISA), ozone distillation subsystem, the analytical half of the growth chamber (for the addition of AES, XPS and UPS subsystems in the future, STM, LEED and MOKE are already available on APE) and a novel in-situ transport measurement subsystem integrated into the loadlock chamber. These technical decisions have then permitted us to define a detailed roadmap for building the MBE system that by necessity will be dependent on future successful funding requests.

Analitical TEM Centre for Electron Microscopy

Coordinator: Elvio Carlino
Staff: Vincenzo Grillo
Davide Furlanetto

Introduction

The Centre for electron Microscopy, (CEM) established at TASC INFM National laboratory during 2002, has the mission to represent a TEM facility for the scientific and industrial community and to explore and to develop new TEM methodologies to be applied to the study of the solid state matter. The latter task has to strongly take into account the location of the CME: inside the TASC laboratory and close to the synchrotron storage ring of ELETTRA.

The role of TEM facility is being realized by opening the CEM to the scientific and industrial community. In particular activity under contract has been realized for the Politecnico di Torino, the CNR-IMEM, the Universita' di Ferrara and the Universita' di Camerino. On the industrial side, CME is part of a project named Medea in collaboration with some of the most important industries in the field of semiconducting technologies like ST microelectronic, Philips, Infineon and Motorola.

On the side of the methodologies the following three lines are the most important aspects on which the CEM is committed: Quantitative atomic resolution z-contrast in STEM (also known as HAADF imaging). This is a relevant part of the research line E5: Quantitative high-resolution transmission electron microscopy of strained heterostructure.

HAADF imaging is a field of large interest in which the European community has some delay with respect to USA or Japan. In particular, CME is the first laboratory in Italy to achieve a resolution of 0.14 nm with this approach. It has also demonstrated how (App. Phys. Lett. Scheduled for publication on July 14 2003) HAADF can be used to gauge the Si distribution in GaAs on the atomic scale even without any image simulation. Development of codes for the simulation of HAADF images is in progress. This subject is within the mission of CME to apply and developing “ not conventional” TEM techniques.

-Dichroism in TEM: (collaboration Vienna University and APE beam-line at ELETTRA). The possibility to measure dichroic effect similar to the effect measured by using linear or circular polarized x-ray photons in a synchrotron. One project has been presented to the Austrian Science Fund and another project has been presented to the EU in the VI WP. This subject is within the mission of CME to explore the possible synergies between synchrotron and TEM experiments.

-In situ microscopy (collaboration within TASC). To measure the properties of nanotubes or nanowires stressed by STM tip or by micro electromechanical systems (MEMs) while viewing by TEM. This project is part of a collaborative project FIRB approved during 2002 by MIUR. This subject is within the mission of CME to explore the possible synergies between TEM and the existing know-how at TASC national laboratory.

Activity Report:

1) Installation of new equipment.

-A brand-new TEM has been delivered on February 2002 and the installation of the main equipment has been completed within July (funds project CIPE P5AW2). Attachments to expand the capabilities of the TEM has been acquired by using INFM institutional resources:

Energy dispersive spectrometer, analytical low background double tilt specimen holder, scanning transmission electron microscope (STEM) unit with bright field (BF) detector and high angle annular dark field (HAADF) detector,

The equipment has been tested and the performances are, in some cases, better with respect the ones guaranteed by the manufacturer. This is mainly due to the mechanical, thermal and magnetic stability of the environment in which the TEM has been installed. In particular the CME at INFM-TASC national laboratory has been the first in Italy to achieve a resolution of 0.14 nm in HAADF imaging.

-The TEM specimen preparation laboratory, established during the 2001, is now equipped with brand-new plasma cleaner to remove the hydrocarbon contamination from the TEM specimen and specimen holder prior of inserting in the TEM vacuum (Funds FIRB 2002 on nanostructured carbon). This step is of particular importance when a high intensity electron beam is focused on an area of less than 0.2 nm as during HAADF experiments or during the acquisition of EDS or EELS spectra from a sub-nanometric volume. The specimen preparation laboratory is now committed to find a thinning procedure to achieve better surface roughness with respect the one currently obtained nowadays.

2) Manpower search and acquisition;

On January 2002 a technician dedicated to the TEM sample preparation and to the technical assistance of the TEM instrumentation has started his activity. The specific training of the technician has immediately started and so far he already prepared several state of the art TEM specimens in plan-view and cross-section geometries.

On December 2002 the search for a researcher dedicated to the TEM activities has been successfully concluded and the new researcher started his activity on February 2003. His main activity so far has been in the field of the simulation of HAADF results.

3) Opening of the CEM to the scientific and industrial community;

Scientific proposal can be addressed to the CME by using its web page on the INFM-TASC laboratory web site. The following studies were performed so far under contract:

-High-resolution TEM experiments in phase contrast (HRTEM) to study the structure of a particular grain boundary in Si (Prof. G. Martinelli-University of Ferrara).

-TEM experiments in HRTEM and in diffraction contrast have been performed to study the structure of columnar defects induced by high energy Au ions bombardment on YBCO / CeO_2/ YSZ (001) heterostructures (Prof. E. Mezzetti-Politecnico di Torino);

-High resolution experiment on Au clusters dispersed in polymers (Dr. M. Epifani-CNR-IMEM Lecce).

-In the next month TEM experiments on Ge/GeMn heterostructures grown by MBE will be performed (Prof. N. Pinto University of Camerino).

CME is part of a project named Medea in collaboration with some of the most important industries in the field of semiconducting technologies like ST microelectronic, Philips, Infineon and Motorola. The aim is to study materials to be used to realize masks for the semiconducting UV technology.

4) Application to Italian and European funds for research;

The CEM facility is a national resource for INFM research programs in semiconductor physics (FIRB collaborative program, 72k€), magnetic materials (FIRB collaborative program90k€), carbon nanotubes, nanowires and nanocontacts (FIRB collaborative program, 100 k€).

CEM presented at the end of 2002 to MIUR a project in collaboration with the University of Trieste and the École Centrale du Paris to study the ultimate performances of the electron energy loss spectroscopy (EELS) at the highest spatial resolution (520 k€). This project would hopefully allow to one of the most important international scientist in the field of EELS to join CEM in 2003.

CEM is a core partner for the INFM-PRA 2003 named NANOBIO (60k€);

CEM is a core partner in an approved INFM-PAIS project named HINCANA (45k€)

CEM is a partner in a European project proposal in the framework of MEDEA action of ST microelectronics (160k€);

CEM is part of the European network of excellence named TEMNET;

CEM is part of a project approved by the Austrian Science Fund to study dichroic effects during TEM experiments;

CEM is part of a NEST project presented in the VI EU WP to study dichroic effects during TEM experiments;

CEM has been invited by the Polish Academy of Science to be part of the “Centre of Excellence in nano and micro scale characterization and development of advanced materials” (NAMAM) already approved in the VI EU WP.

5) TEM methodologies:

-Quantitative atomic resolution z-contrast in STEM (also known as HAADF imaging). This is a relevant part of the research line E5: Quantitative high resolution transmission electron microscopy of strained heterostructure. HAADF imaging is a field of large interest in which the European community has some delay with respect to USA or Japan. In particular, CME is the first laboratory in Italy to achieve a resolution of 0.14 nm with this approach. It has also demonstrated how (Appl. Phys. Lett. Scheduled for publication on July 14 2003) HAADF can be used to gauge the Si distribution in GaAs on the atomic scale even without any image simulation (Fig. 1).

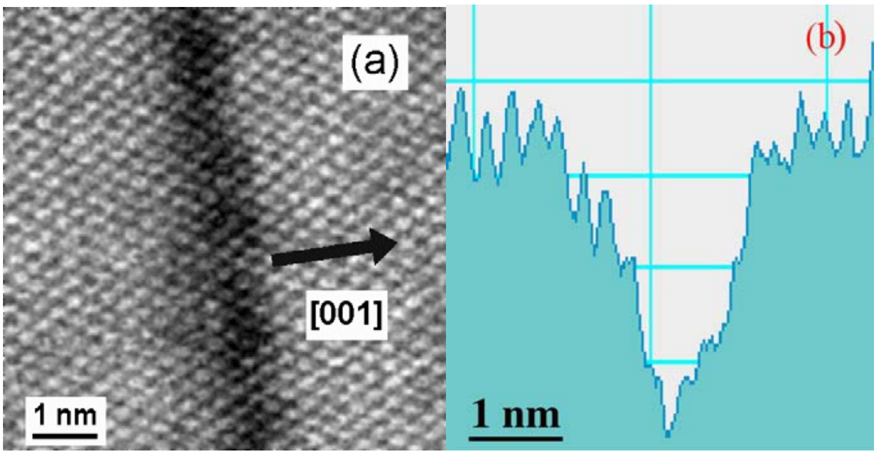

Fig: 1 (a) High-resolution z-contrast HAADF image in [110] zone axis of a Si quantum well. (b) Intensity profile (a. u.) as measured on the image in Fig. 2(a)

On the side of the simulation of the results, software with multislice approach and the frozen phonon approximation is being developing starting from the codes of E. J. Kirkland. The limit of this calculation is in the huge CPU time necessary to get reliable simulation. CME is also developing a new procedure to reduce the calculation time. The coupling of STEM HAADF imaging with high spatial resolution energy dispersive x-ray spectroscopy allows further possibilities in studying materials as demonstrated (Proc. Inst. Phys. Conf. MSM XIII Cambridge (UK) 2003) in the case of the GaAs/ZnSe heterostructure (Fig. 2) where the interface chemistry and structure of low defect density epilayer was addressed.

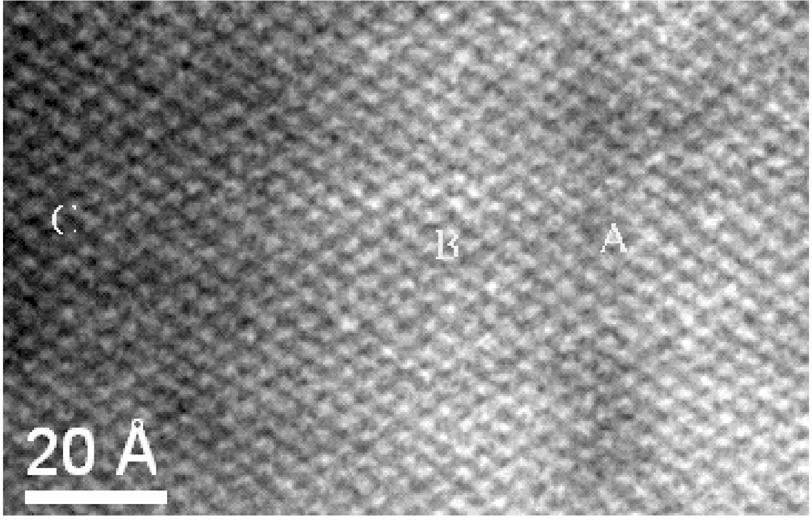

Fig. 2: atomic resolution HAADF image of the GaAs/ZnSe interface

The image contrast at the interface of strained structure in HAADF experiments is strongly related to the experimental condition. This influence allows (Appl. Phys. Lett. Scheduled for publication on July 14 2003) to measure the influence of the strain. This aspect is in the main stream of the aims of the research line E5: Quantitative high-resolution transmission electron microscopy of strained heterostructure.

It is worthwhile to remark how tailored experiments to explore the ultimate performance of TEM can be addressed thank to the synergy with the growth facility at TASC laboratory and, on the other side, how new materials can be tailored thank to the knowledge gathered by TEM.

-Dichroism in TEM: (collaboration Vienna University and APE beam-line at ELETTRA). The project explores the possibility to measure dichroic effect similar to the effect measured by using linear or circular polarized photons in a synchrotron. In fact, powerful methods for characterizing and testing magnetic materials are based on x-ray magnetic linear or circular dichroism (XMLD and XMCD) observed, for examples, in x-ray absorption near edge structures (XANES). The similarities between XANES and energy loss near edge structures (ELNES) in the TEM has long been recognised. In fact linear magnetic dichroism has been already measured in TEM but it is believed that the correspondence of XMCD cannot be performed in a TEM. A recent discovery suggests that, by proper experimental set-up, circular dichroism should be observable in a TEM. A project aimed to demonstrate this possibility has been presented to the Austrian Science Fund and another project has been presented to the EU in the VI WP. These project are the first to address one of the mission of CME that is, to explore the possible synergies between synchrotron and TEM experiments.

-In situ microscopy (collaboration within TASC). The aim is to measure the properties of nanotubes or nanowires stressed by STM tip or by micro electromechanical systems (MEMs) while viewing by TEM. This project is part of a collaborative project FIRB approved in 2002 by MIUR. To this aim a dedicated specimen holder is under construction in the technical support group of the TASC laboratory. The TEM specimen holder will give the possibility to drive an STM or MEMs and also to measure conductivity of nanostructured materials under stress. The structural modification of the materials can be studied in the meanwhile by TEM. This project is a good example of how new TEM experiments can be realised thanks to the know-how at TASC laboratory.

6) Collaboration with Italian and foreign groups:

Universita' di Trieste, Universita' di Ferrara, Universita' di Brescia, Universita' di Trento, Universita' di Lecce, Universita' di Roma, University of Antwerp, University of Vienna, École Centrale du Paris, University of Sheffield, Politecnico di Torino, CNR-IMEM Lecce, CNR-IMEM Bologna, Universita' di Camerino, Universita' di Ancona, University of Krakow, Polish Academy of Science, University of Zagreb

7) Papers, invited lectures and conferences:

Elvio Carlino, Roberto Duca, Davide Furlanetto, and Alfonso Franciosi
The New INFM High-Resolution Transmission Electron Microscopy facility at the TASC National Laboratory, INFM workshop – Genoa- April 2002

Elvio Carlino, Roberto Duca, Davide Furlanetto, Silvio Modesti, Matteo Piccin, Silvia Rubini and Alfonso Franciosi
HIGH SPATIAL RESOLUTION STUDIES OF SI-GAAS -DOPED LAYERS AND SUPERLATTICES
INFM Meeting Rome, June 2002

E. Carlino, S. Modesti, D. Furlanetto, M. Piccin, S. Rubini and A. Franciosi
Atomic resolution composition analysis by Scanning Transmission Electron z-contrast imaging
INFM Meeting Genoa, June 2003

Elvio Carlino; Seminar at TACS meeting titled: TEM activity at CME, Bologna October 2002

Elvio Carlino ;Invited seminar at PICS 913, Challenge in ELNES, École Centrale Paris, titled "Atomic Imaging in ADF STEM coupled with EELS" Paris (F) November 2002

Elvio Carlino; Invited seminar at the University of Wien, Inst. f. Festkörperphysik titled “Magnetic Dichroism with polarization dependent electron spectroscopies and TEM activity at the TASC-INFM national Laboratory” Wien (A) December 2002

E. Carlino D. Furlanetto, A. Colli and A Franciosi; Oral presentation at the conference “XIII microscopy on semiconducting materials” on “high spatial resolution TEM studies of GaAs/ZnSe interfaces grown by different MBE procedures”. Cambridge (UK) 2003

Elvio Carlino Invited seminar at the meeting Chemistry at Elettra” on “TEM activity at TASC-INFM national Laboratory” Trieste (I) April 2003

Elvio Carlino, Invited seminar at the Multinational Congress on Electron Microscopy on “ High spatial resolution transmission electron microscopy studies of semiconductor heterostructures“ Pula (KR) June 2003

Elvio Carlino, Invited chairman at the Multinational Congress on Electron Microscopy in the session of Thin films and Nanostructured materials. Pula (KR) June 2003

Elvio Carlino, Invited seminar at the SISSA on “Transmission Electron Microscopy: how to study the solid state at the highest spatial resolution” Trieste (I) June 2003

Elvio Carlino, Invited lectures on Scanning Transmission Electron Microscopy. SIME-ENEA School on Transmission Electron Microscopy in Materials Science Brindisi (I) October 2003

E. Carlino, S. Modesti, D. Furlanetto, M. Piccin, S. Rubini and A. Franciosi; *ATOMIC RESOLUTION COMPOSITION ANALYSIS BY SCANNING TRANSMISSION ELECTRON MICROSCOPY HIGH-ANGLE ANNULAR DARK-FIELD IMAGING* (Appl. Phys. Lett. Scheduled for publication on July 14 2003)

- E. Carlino D. Furlanetto, A. Colli and A Franciosi

HIGH SPATIAL RESOLUTION TEM STUDIES OF GaAs/ZnSe INTERFACES GROWN BY DIFFERENT MBE PROCEDURES (Inst. Phys. Conf. Ser. MSM XII Cambridge (UK) 2003)

-E. Carlino, S. Modesti and A. Franciosi

High spatial resolution transmission electron microscopy studies of semiconductor heterostructures

Proceedings 6th Multinational Congress on Electron Microscopy. Pula (KR) June 2003. Ed: Croatian society for electron microscopy – Zagreb.

Litography Facility at TASC (LIF@TASC)

Coordinator: Enzo Di Fabrizio

Staff: F. Romanato, S. Cabrini, M. Tormen, L. Businaro, L. Vaccari, M. Altissimo, D. Cojoc, M. Prasciolu, R. Kumar, P. Candeloro, R. Malureanu

2D photonic crystals fabrication.

Photonic crystals (PC) represent one of the most important building blocks towards the achievement of a full-based optics communication technology. At LILIT the study of two-dimensional PCs during year 2002 was mainly devoted to the activity of the PRA project named PHOTONIC. In the following is reported the technical report of the first year.
LILIT Report PRA PHOTONIC First year: June 2003
Realization of waveguide photonic crystals
It was fabricated by MBE (Prof. L. Sorba) a 2 inch wafer a waveguide with the following structure:
200 nm AlGaAs/200 nm GaAs/1.5 micron AlGaAs/substrato. The percentage of Aluminum is 25%.
The patterning of the photonic crystal was done by X-ray lithography.
The first step is the design and fabrication by e-beam lithography of the X-ray Mask. The symmetry of the pattern is triangular with 600 nm pitch and 360 nm dot diameter. In figure is reported the SEM pictures of the mask. The absorber material is Gold 400 nm thick.

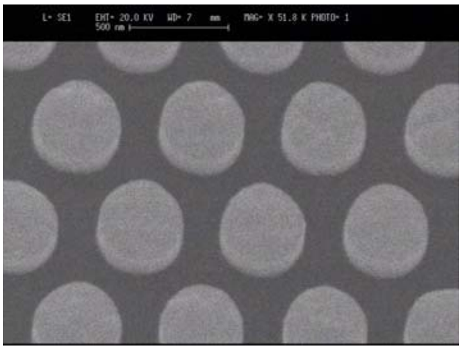

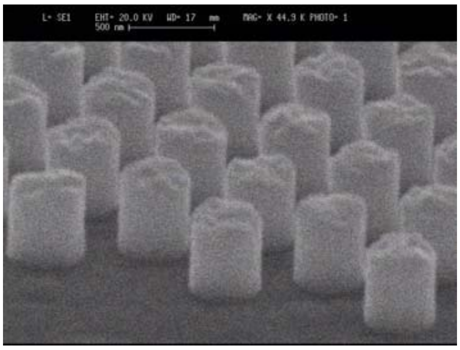

The second step is the pattern replication, by means of X-ray on the waveguide substrate.
The substrate was preliminarily coated by a conductive layer in order to allow the subsequent electroplating growth of 200 nm Ni. This step is necessary because Ni is a good selective mask for RIE proocess for pattern transfer in the waveguide substrate.
In Figure is reported a sample after X-replication and Ni electroplating growth.

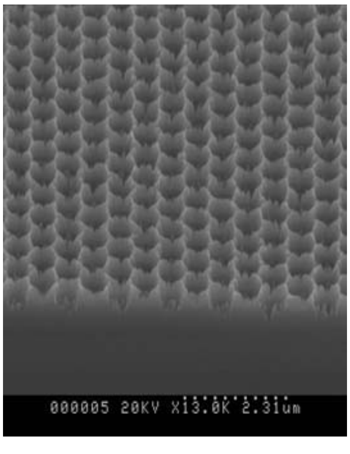

This sample is used in RIE process to transfer the geometry through the waveguide.
We have prepared 11 sample with Ni. The effective area is 400x400 um^2.

In the following figure is reported the results after RIE under the following conditions
$SiCl_4$ 1 sccm
O_2 0,4 scc
Bias: 148 V
Pressure 2 mT
Potenza 12 W
etching time10 min

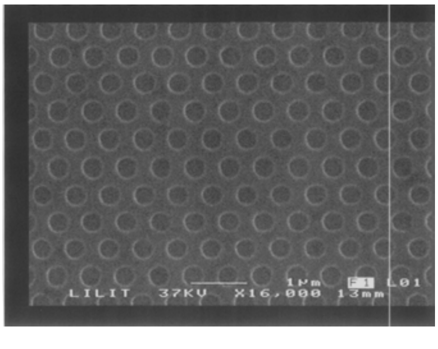

The quality of the patterning in terms of etching and sidewall is good. The roughness seen is due to the Ni mask that in this case was too thin. The new sample to be etched by RIE has a thicker mask and should give a good transfer quality.
Meanwhile it was developed a new process based on Si_3N_4 mask deposited by PECVD on PMMA.
The following pictures show the PMMA pattern: top view and side view.

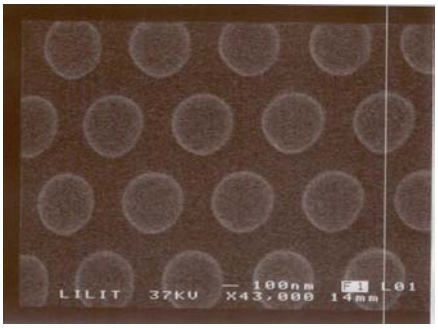

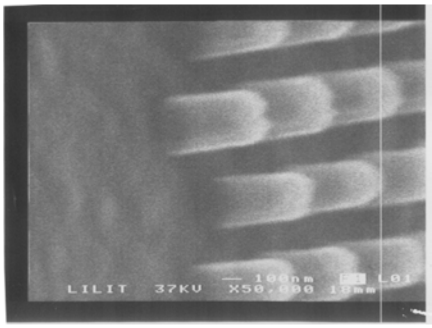

The following figures show the results obtained with $SiCl_4$ RIE on the sample masked by 100 nm of Si_3N_4

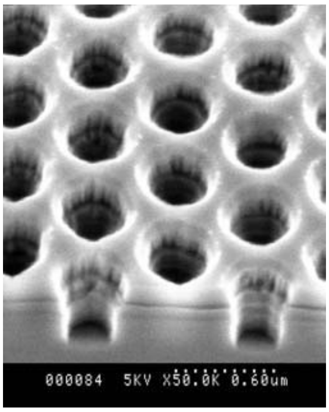

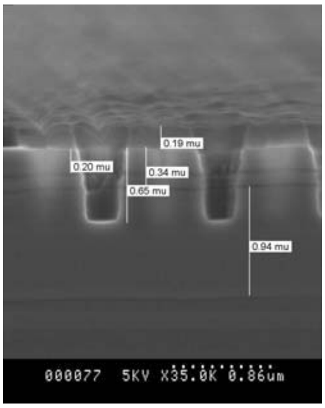

In order to show the future patterning and etching capabilities at TASC we show the high resolution Patterning obtained by the lithographic system dual beam LEO 1540 XB that will be installed at TASC in September 2003. The following pictures show a photonic cryestal on GaAs/AlGaAs substrate with a linear defect and with a dot distance control down to 40 nm. The third picture shows 10 nm line on a 50 nm grating pitch.

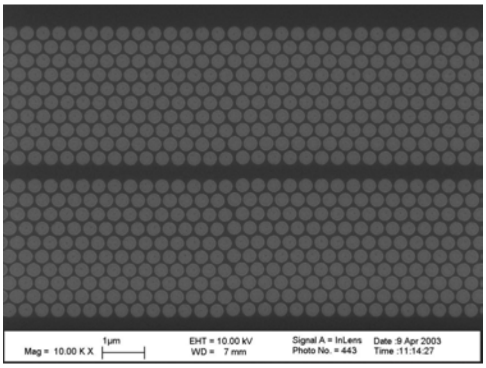

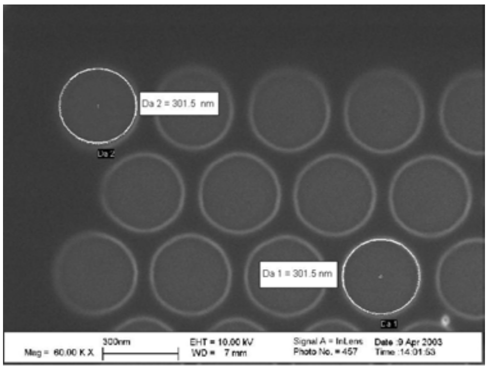

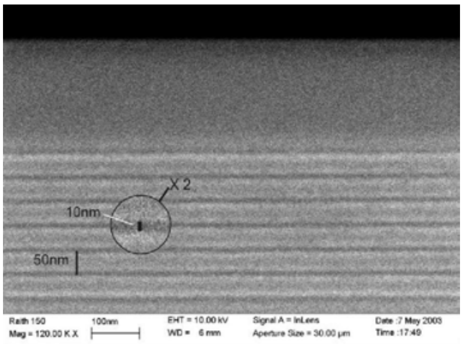

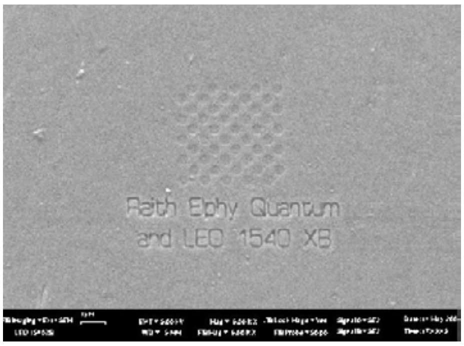

Finally, the following picture show an RIE done by using the Ga ion beam and chlorine gas. Even if the experiment was done by the demo machine at LEO, this can be considered as the first homemade test sample including the RIE process.

About the installation of SiCl4 gas at TASC there was a delay caused by the changing of tender rules. The plant installation was formally assigned on May 19 2003 and the deliver date is end of July 2003.

The following pictures refers to Ni mask, fabricated by X-ray lithography, on the following Bragg mirror architecture, (GaAs Substrate/200nnm GaAs/44.44 nm AlAs/GaAs177.77 nm) repeated 5 times. We produced 6 samples and the etching based on SiCl4 chemistry is in progress.

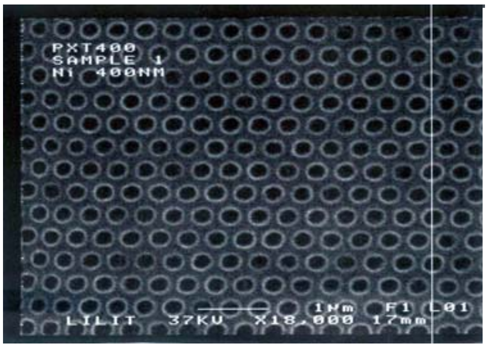

First results of etching SiCl4 on symmetrical guide June 18/2003
RIE AlGaAs : 2 SCCM SiCl4, 0.2SCCM O2, Pw=12 Watts P=2 mT, bias=160 V
RIE GaAs 1sccm SiCl4. 0.4 O2 stesse condizioni

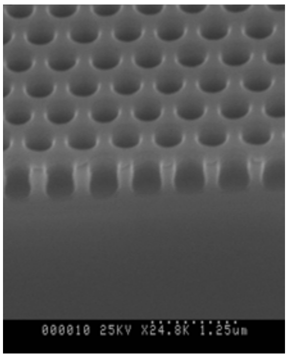

Photonic Crystal 3D

Molding the flow of light represents one of the goal of photonics. Computational experiments showed that a full control can be obtained by allowing light to travel along linear waveguide performed in three-dimensional arrays of material with lattice parameter comparable with the wavelight, also called 3D photonic crystals. The possibility to realize 3D PC and the waveguide path in the material represents a challenge from a fabrication point of view. At present only pioneering fabrication methods have been demonstrated. During last year we worked on the fabrication of 3D periodical arrays, including controlled defects, by means of multi tilt X-ray exposures and e-beam lithography (see the next two pictures). The metallic 3D PC can be used in high frequency region (grater than 100 THz) where the metals become almost completely reflectors. Gold and Nickel 3D photonic crystal with 3fold (Yablonovite) and 4 fold rotation symmetry have been fabricated with a lattice parameter ranging from 3 m to 500 nm. 2fold structures have also been fabricated to explore non symmetric band energy dispersion. The structures are self standing in order to allow reflectance and transmission optic characterization. The total thickness of the 3D PC is of the order of 10 m, a value that allows to achieve a full 3D optical behavior as confirmed by variable angle reflectance measurements (see the next two graphs). Moreover, the developed fabrication technology allows to easily control the design and the realization of defects that represent the key feature to make usable PC as wave guide. In the following pictures are reported 3D lattice where linear defects have been introduced.

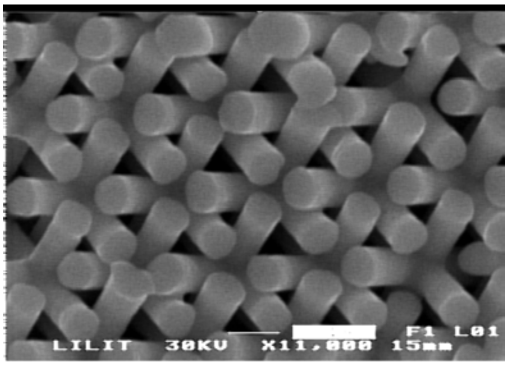

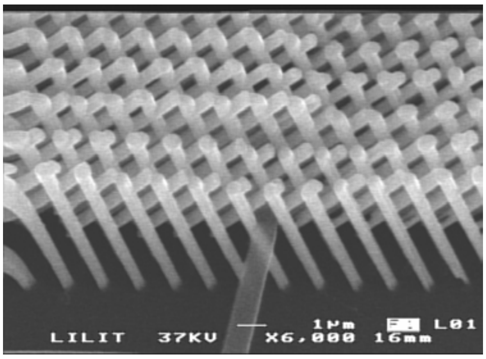

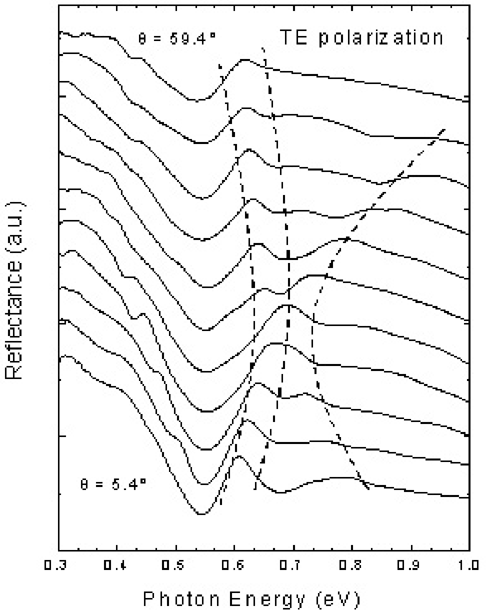

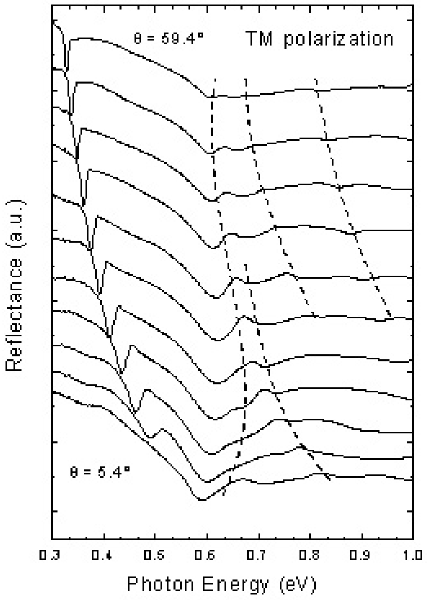

Carbon Nanotubes

The lack of simple and reliable processes to deposit CNTs in a controlled way has severely hindered the fabrication of all kinds of CNT-based device.

Last year activity was focused on the characterization of functionalized CNTs employing microscopy techniques as Atomic Force Microscopy, Scanning Electron Microscopy and Transmission Electron Microscopy. The possibility to exploit these properties to integrate functionalized CNTs in micro electronic mechanical systems (MEMS) has been also investigated. Single wall and multi wall CNTs have been variously functionalized employing a methodology based on 1-3-dipolar cycloaddition of azomethine ylides and conventional nano-technology techniques as e-beam lithography, Reactive Ion Etching, CVD induced by electrons and Electrochemical growth have been employed for the fabrications of MEMS.

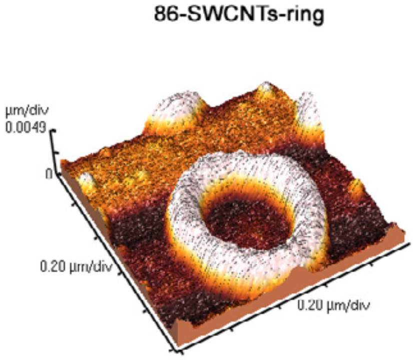

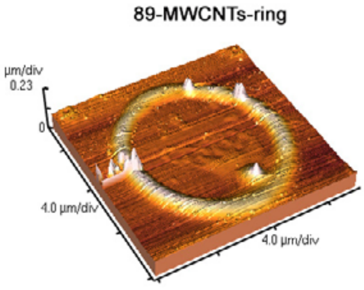

In the above picture are reported two examples of single wall and multiwall ring nanotube investigated by the AFM .

Microcontact printing lithography

Device miniaturization and microelectronics relied on planar lithography and layering of essentially two-dimensional structures. Nowadays, nanotechnology demands to overcome the VLSI scheme and in particular it aims at a fully three-dimensional (3D) patterning. Technological advances in micromechanics, microfluidics, micro- or nano-optics and innovations of the toolset of biology (microfluidic chips for DNA array) and medicine (microsurgical tools, drug delivery) depend in fact strongly on the development of 3D structuring capabilities at the sub-micron scale.

We present results about the combined use of nanoimprint and X-ray lithography..

In the last year the most relevant result was the combination of nanoimprint and X-ray lithography for fabricating non conventional three-dimensional (3D) polymer structures.

The technological potential of this method is demonstrated by pattering with X-ray lithography several different types of structures on an hexagonal array of hemispheres previously obtained by nanoimprinting. The overall profile consists of high aspect ratio trenches and/or pillars modulated by slowly varying 3D structures defined by imprinting.

The combination of this two lithography extends the fabrication to a much wider class of micro- e nano- objects that allows to conceive new device categories.

Fig. 1a shows three patterned regions that contain three possible lithographic combination: NIL, XRL and the overlap of the two. Figure 1b shows that special optical elements containing refractive and diffractive components can be produced

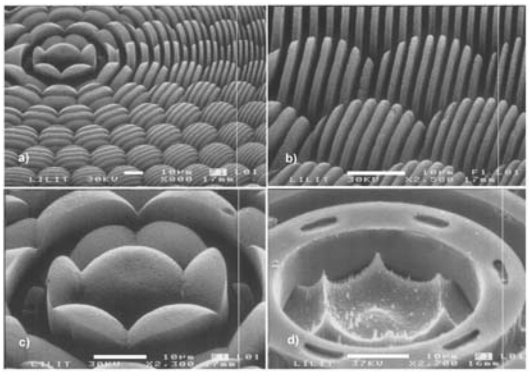

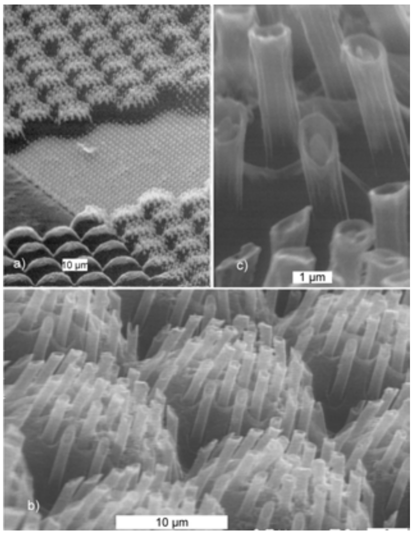

Patterning of magnetic material

In the last decades patterned arrays of magnetic elements such as wires,dots and antidots have attracted a lot of interest both for their potential applications in magnetic data-storage devices and for the investigation of magnetic phenomena in low-dimensional systems. Understanding and controlling their magnetization reversal and domain structure becomes very important in submicron magnetic systems,an interest motivated in part by applications to the magnetic recording industry. However,the use of micro-and nano-structures in magnetic high density recording media and non-volatile random access memories is not trivial.If compared to the case of a continuous film,.Moreover,new effects due to the lateral confinement of the structures occur,
such as the frequency quantization of spin-wave modes.

These latter effects are of great interest also from a fundamental point of view,because many questions remainunclear,such as the details of the magnetization reversal process.

Magnetic arrays of rectangular dots 1100nm´300nm with 200nm spacing (in figure pattern a) and dots 800nm´550nm with 200nm spacing (in figure pattern b) with the nominal thickness of 30 nm in Permalloy ($Ni_{81}Fe_{19}$) material were fabricated using X-ray lithography in combination of lift-off technique. A detailed magnetic characterization of the dot arrays was accomplished by magneto-optical Kerr effect investigations and micro-magnetic simulations, with emphasis given to the dependence of the hysteresis loop of the dots on their aspect ratio (shape anisotropy). In addition, the high frequency dynamical properties were probed by Brillouin light scattering (BLS) showing a marked discretization of the Damon-Eshbach surface spin-wave mode induced by the finite lateral dimensions. The measured frequencies compare fairly well to those calculated by an analytical method which considers spin waves confined in rectangular prisms.

Pattern A

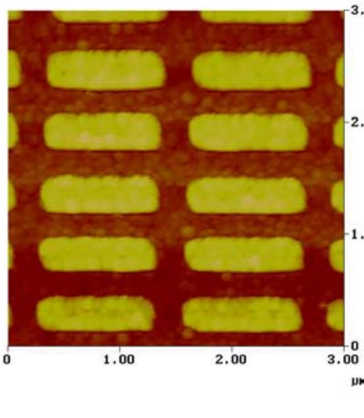

Pattern B

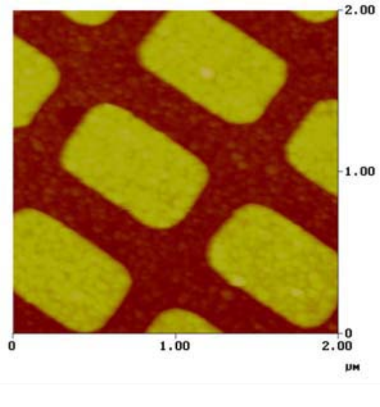

Fabrication of MEMS

There is a great industrial interest in developing microsystems based on silicon technology and making use of fabrication processes suitable for batch production.

A new worldwide impulse is originated by the spatial industry. Space exploration in the incoming millennium will mostly rely on drastically miniaturized spacecraft by today’s standard. A key point for precise orbit and attitude control of nanosatellites, whose typical weight is about 2-3 kilograms, is the development of suitable propulsion systems, weighting few grams and capable of few μN thrust.

The feasibility study of a based on cold N_2 gas propeller microthruster complying these requirements and its prototyping were developed jointly by Mechatronic and INFM.

The microthruster design and its fabrication process were based on the study of theoretical behaviour of the microthruster expansion chamber, on fluid dynamic simulation of the nozzle flow and on technology selection according to the complete integration of the components on silicon carrier.

The microthruster was obtained manufacturing a silicon p-type 2 inch wafer using Electron beam lithography, Reactive ion etching, evaporation techniques and anodic bonding for final packaging. It consists of a 20-micron deep chamber, in which the pressurized nitrogen is introduced, terminating in a supersonic nozzle through which the gas is accelerated. The throat size, on the order of 10 µm, defines the thrust range. The very low roughness of the thrusters walls permit to have low thrust loss: ground tests show that the thrust is roughly 100 µN.

Testing in space is ongoing on the Italian satellite UNISAT2, launched in December 2002. The satellite weight is roughly 10kg, and this platform is suitable for micropropulsion experiments to test the ability microthruster to change the spin speed of satellite

In figure we report the pictures of the microthruster mounted on UNISAT 2 assembled with nitrogen tank, gas supply circuit, proportional control valves, pressure sensors and control electronics. A particular of microthruster is also shown.

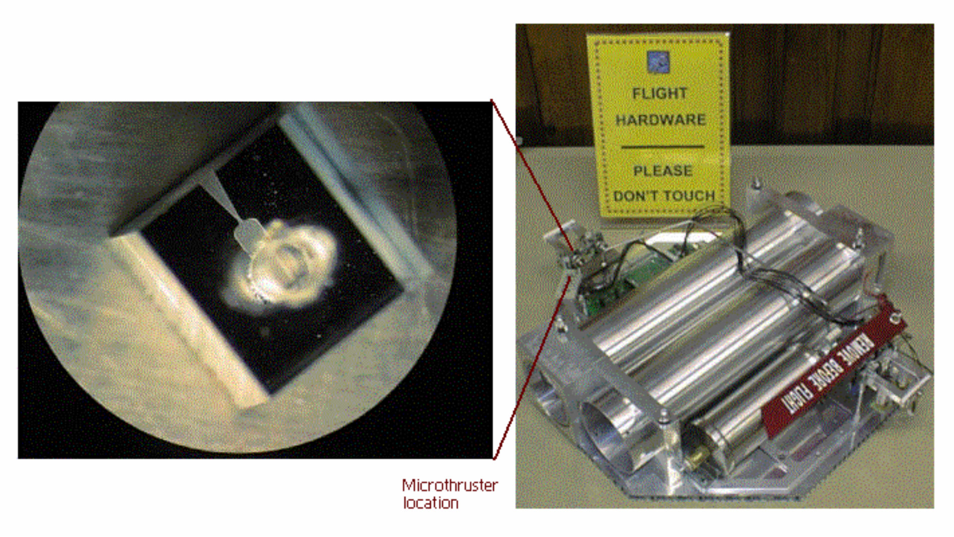

Computer Aided Simulations for MEMS and microfluidic devices

The computer aided methods, such as the Finite Elements Method (FEM) and the Finite Volume Method have known in this decade a widespread diffusion in every field of engineering, such as fluid mechanics, electromagnetism, heat conduction and many more. This flexibility is due to the particular way FEM and FVM use to simplify complex problems: the geometry of the system under analysis (main domain, generally complex in shape) is divided in smaller parts with a simple shape, the subdomains, that can be also called elements in the Finite Elements Method and volumes in the other case.

We use commecial software based on the Finite Elements Method for structural analyses of Finite Volumes to study fluidic environments. With these analyses tools we are able to study the behaviour of a wide category of microdevices, such as aerospace microthrusters, Si_3N_4 membranes (1-2 microns thick), biomedical microdevices for drug delivery. As an example, here we report the simulation of a micromirror and a microfluidic mixer.

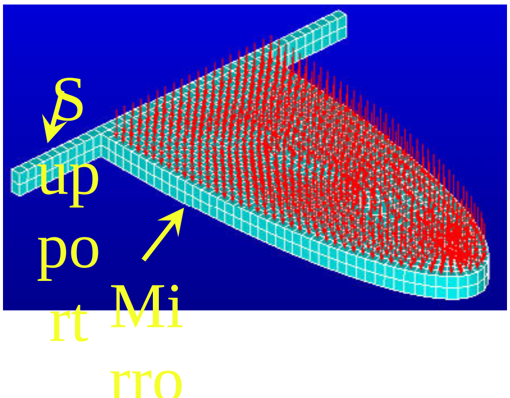

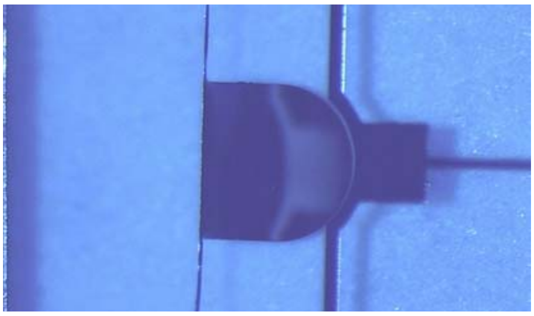

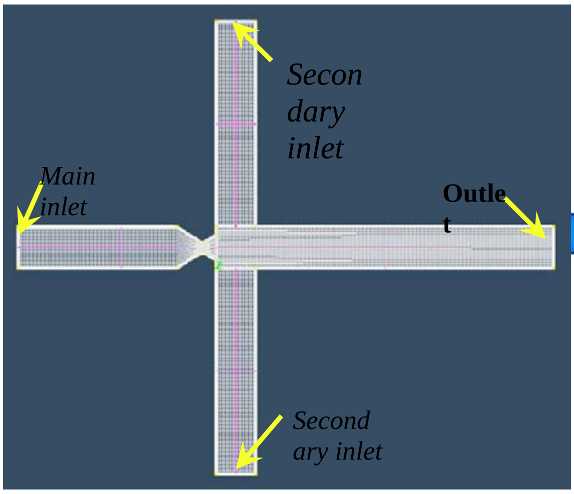

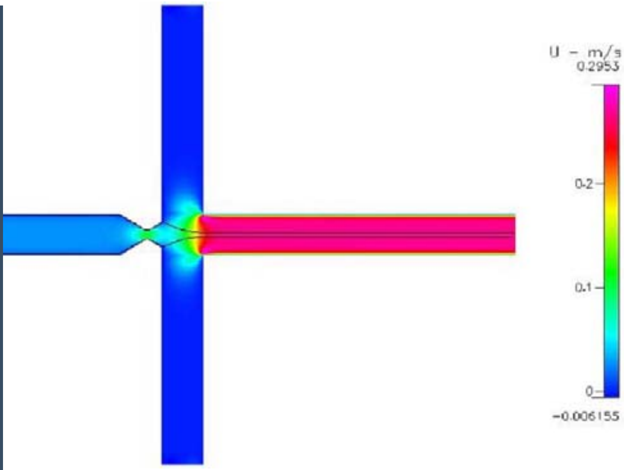

Diffractive optics:design & fabrication

Zone plate for neutrons

During last year the activity was extensively devoted to zone plate and general optical elements that can perform beam shaping, multifocusing in a single an multiple focal plane from visible wavelength up to x-rays and neutrons. The activity includes the design and fabrication.

Regarding the design we developed a complete software, that exploiting several kind of algorithm, such as iterative phase retrieval methods and genetic algorithm, allows to calculate with an high degree of freedom, the intensity distribution on a generic plane when the input field is known.

Despite the traditional view that X-rays cannot be focused, the topic of focusing systems for X-rays has today become an extensive subject. The principal methods employ diffractivemicrostructures that have beeen fabricated by methods mutuated from microelectronic (MOS devices) fabrication technology. For this reason, X-ray microscopy is now a research area inwhich enormous progress has been made in the last years. The advent of the last synchroton generation together with the progress made in the fabrication quality of new optical devices, such as zone plate, are the two main factor that influenced the interest around the microscopy science. There is a similarity between X-ray optics and Neutron optics due to the similarity of the real part of the refractive index. The activity on neutron zone plate is based on the fabrication, by means of electron beam and X-ray lithography of high resolution and high efficiency zone plate for neutrons in the wavelength range between 1 Angstrom and tens of Angstroms. Here we report on the results obtained in focusing a cold neutron beam by means of an optical devices which exploits the Fresnel zone plate (ZP) concept.Presently, a limitation in the neutorn optical element resides in the need for efficient neutron focussing devices. Several tehcniques such as the use of reflective optics have been proposed in the past. Recently innovative applications of neutron radiography and imaging have been presented. We have adopted an approach based on diffractive optics and especially on the Fresnel Zone Plate design. Such lenses allow to fabricate thin systems. More than 20 year ago, it was demonstrated that a phase reversal ZP, that is a Fresnel lens which obeys the equation of thin lenses, can be successfully employed to focus and image a cold neutron beam ($\lambda \approx 20$ Å). It is only in the last decade that progress in nano-fabrication has made possible the production of high-efficiency and high-resolution ZPs for focusing of short wavelength x-rays. We have adopted similar fabrication techniques for the fabrication of neutron focussing lenses. We have reported in a previous communication about the fabrication and test of a large area FZP (5mm in diameter) which could be used for focussing a neutron beam. Here we focus on a different device. This device is a square matrix, 1 cm^2 surface, consisting of 900 zone plates, 300μm in diameter each and with a 1 m focal length at 3 Å. The system is deposited on a silicon substrate. The matrix is designed to focus the neutron beam from a point source into 900 small spots. The thickness of the phase shifter (natural Ni) is 3.5 μm resulting in an aspect ratios of the Ni structures of about ~5. This device was produced at the Elettra Synchrotron Light Source. The Figure 1 shows an optical picture of the whole device together with an SEM image of one of the individual zone plate

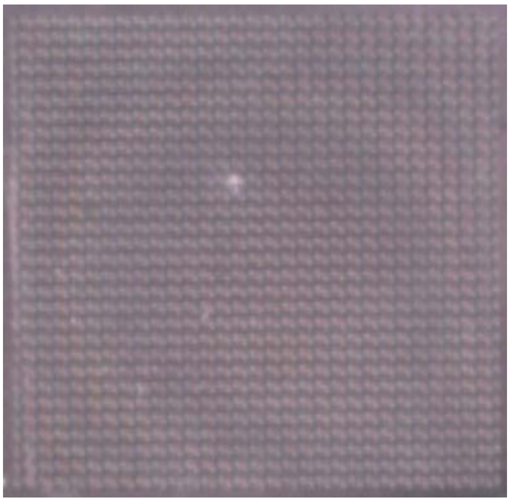

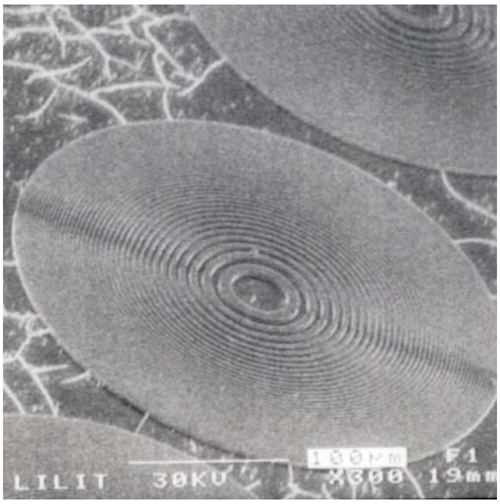

Design and fabrication of lenses on the top of an optical fiber for efficient fiber-to-waveguide coupling by means of Focus Ion Beam (FIB) lithography The purpose of this work is to demonstrate efficient optical coupling between a single mode fiber and a LiNbO3-APE waveguide using a lens fabricated directly on the top of the fiber. Optical critical alignment of the devices along the optical axis. In order to avoid this problem one should integrate the optical element used for coupling with the fiber. Our attempt is to fabricate a spherical lens directly on the top of a cleaved fiber using a lithographic process. This lens should be able to focalize the gaussian beam leaving the fiber, into a plane at a distance of 28 µm from the lens surface. The size of the beam leaving the fiber is of about 10.5 µm while the size of the focused beam is 7.8 µm. To obtain an efficient coupling one should control also the phase of the beam in the focal plane. A plane wavefront provides an efficient matching with the fundamental mode of the waveguide, depicted in figure 1. The design of the lens and the calculations related to the optical fiber-to-waveguide coupling were carried out using our own developed code. The lens profile has been obtained by means of Focus Ion Beam (FIB) lithography. Beside its very high resolution FIB lithography allows us to write the desired pattern on the top of the fiber without spinning a layer of resist, as required by E-beam lithography. The profile of the lens fabricated by means of FIB lithography is shown in figure 2(a,b). As one can see, the shape of the lens is very well reproduced in ten 100 nm thick levels. We have measured also the coupling efficiency using a laser beam with 1550-nm wavelength. The optical coupling using the lens on the top of the fiber is 67 % more efficient than the direct coupling between the fiber and the waveguide.

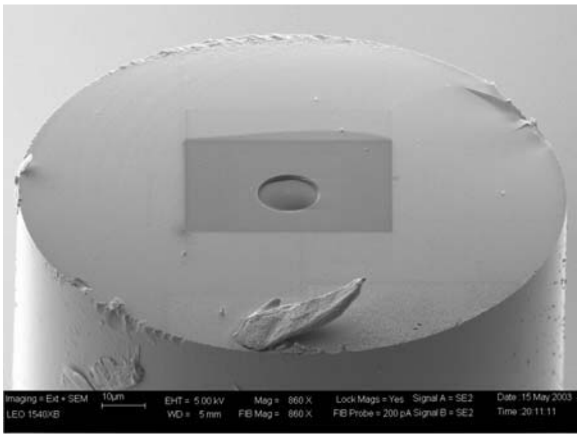

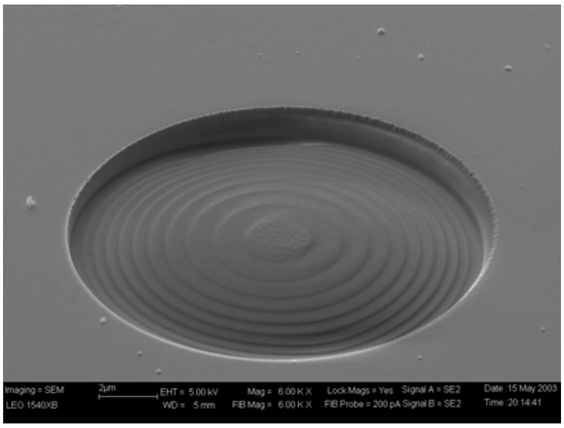

Dynamic multiple optical trapping by means of diffractive optical elements

The goal of this activity is to prove the usefulness of the diffractive optical elements to generate arrays of optical tweezers. A set of micro-particles can be thus trapped in three dimensions and each micro-particle can be then moved independently.

A single-beam optical trap or optical tweezers can be formed by highly focusing a laser beam using a microscope objective with a high numerical aperture. When a moderately powerful laser is focused to a diffraction-limited spot in the specimen plane of a microscope, a steep gradient in light is produced in the focal region. Small dielectric objects, such as latex or silica micro- spheres, or biological material, including cells, chromosomes, and organelles, experience a form of radiation pressure, called the ‘gradient force’, that tends to draw them towards the center of that region. Another form of radiation pressure, usually called the “scattering force”, arises from reflection or absorption of light, and it tends to push objects down along the beam, in the direction of propagation of the light. Stable, three- dimensional trapping takes place when the effect of gradient force is sufficiently large to overcome the effect of the scattering force.

Although optical tweezers have been a valuable research tool since their development in the 1980s, they have remained limited to trapping only one particle per laser beam. One of the most exciting developments in optical tweezers in recent years has been the creation of two- and three-dimensional arrays of optical traps by using diffractive optical elements (DOEs). We have developed our own algorithms and code to design phase DOEs that can transform a single laser beam into an array of independent traps, each with individually specified characteristics, arranged in arbitrary geometrical configurations. These DOE’s were fabricated by means of e-beam lithography in PMMA to generate fixed traps. Recently they were implemented on computer addressed liquid crystal spatial modulators. This allows us to control the configuration of the optical tweezers almost in real time. Experimental results show trapping and dynamic manipulation of multiple silica micro-spheres immersed in water. An array of three traps is shown in figure 1. This is achieved in a first step using one DOE. After trapping them we change the position of only one trap, changing the configuration of the DOE. The corresponding particle is thus displaced in a new position. A circular tray, performed by this particle in 5 seconds is shown in figure 1. An array of five traps is shown in figure 2-a. The trapped particles are kept fixed while un-trapped particles move together with the water surrounding them (figure 2b).

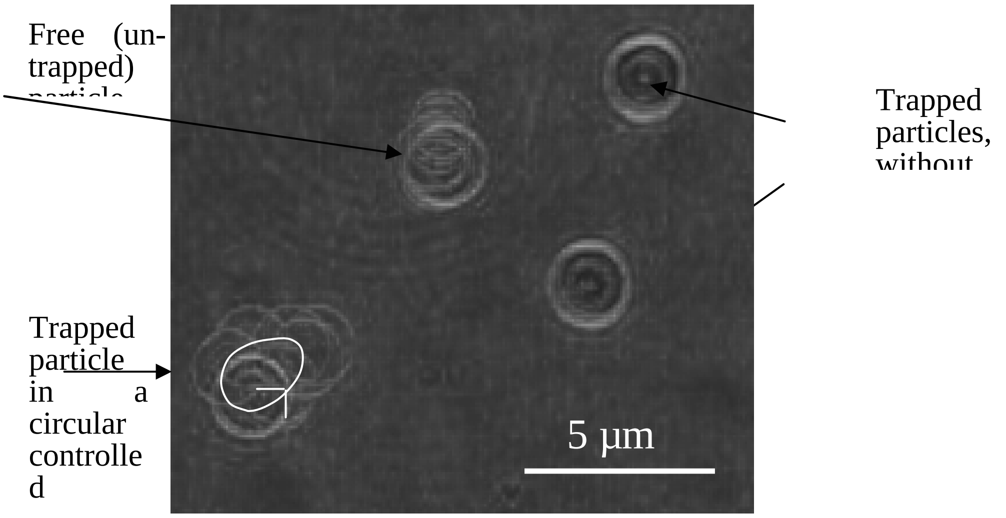

Figura. Multiple trapping of three particles and dynamic trapping inducing a circular movement for one particle (the movement lasts for 5 seconds); the free particle has a Brownian movement

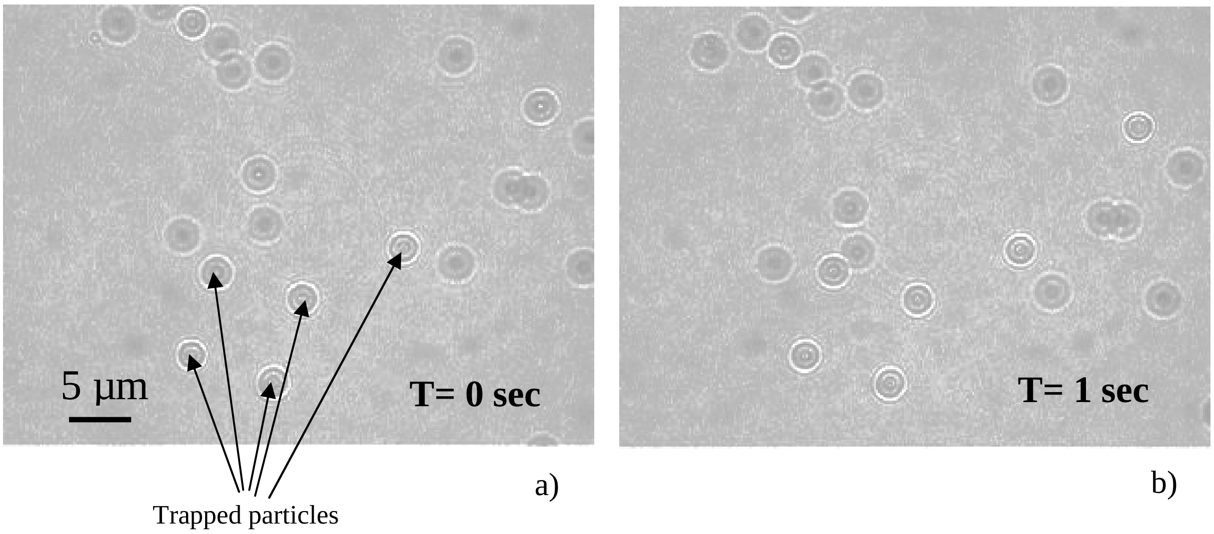

a)

b)

Figura Multiple trapping: an array of five particles is kept fixed while the other particles are displaced together with the environment

AMPLIFON project: Scanner to obtain a 3D Map Inner Canal of Ear

This activity regards the application of a torsional micromirror, fabricated by micromachining technique, to the 3D reconstruction of the ear canal.

The advances in micromachining technology has enabled successful demonstration of novel sensors, actuators, and systems in many diverse application areas such as optics, fluid mechanics, biological and medical science, communications, information storage and more

Micromirrors, which modulate the phase or amplitude of incident light, are becoming integral components in projection display systems, pattern generators in maskless lithography systems, cross connectors in optical communication systems, adaptive optical systems, and switches and optical scanners. Micromirrors can be classed into various categories in accordance to their type of actuation such as, deformable, movable, piston and torsional micromirror by using various mechanism of energy-transduction. Torsional micromirror has advantages in terms of good dynamic responses and is being suited for applications requiring high speeds and large arrays such as in the projection displays of optical cross bar switches. The micromirror showed in figure 1, is integrated in a scanner to produce a digital 3D map of the inner canal of the human ear. This instrument is able to measure the convex surface of a very narrow diaphragm (1.5 mm minimum diameter) with an accuracy of few microns in 2 minutes scanning. The surface reconstructions can be performed following different strategy such as spiral or flipping and rotating the mirror.

In figure 2a) it is shown the raw data for the 3 dimensional digital map obtained by our scanner. Figure 2b) shows the smoothed digital reconstruction of the shell and figure 3c) shows the final shell obtained by the laser stereo-lithography from the digital data.

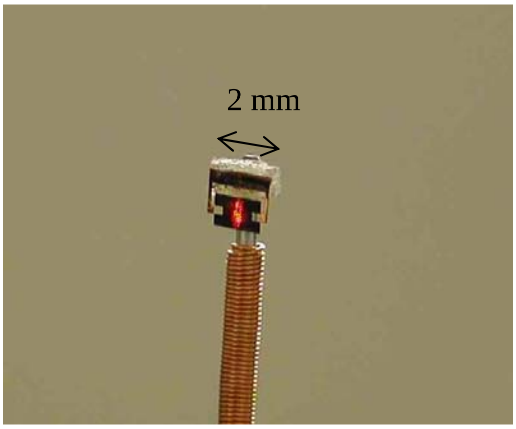

`Figure 1 shows t`*he micro-mirror mounted on a micro-coil. The tilting and can be as large as 30 ° .*

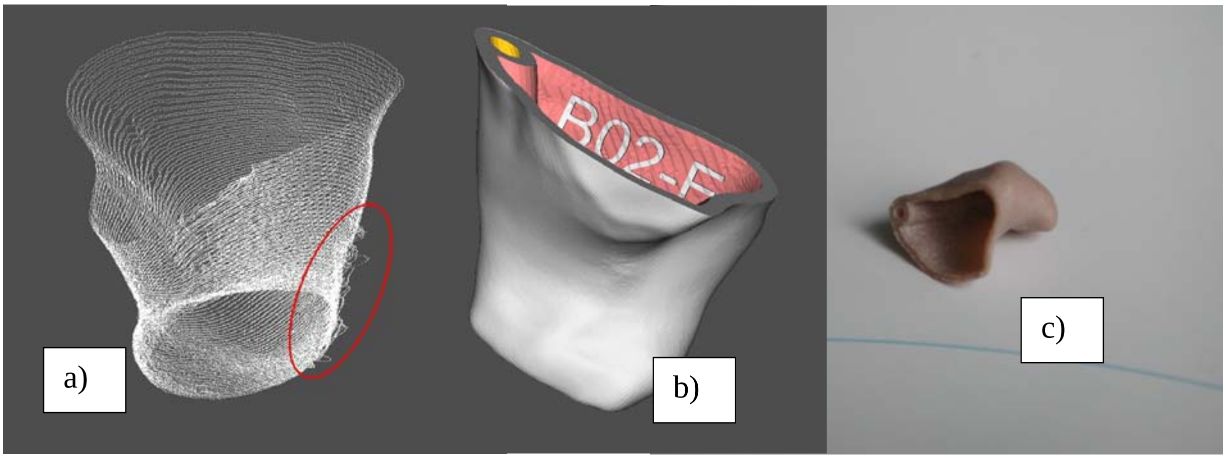

Figure 2 shows the raw 3D digital map obtained by thescanner. b) the smoothed digital reconstruction of the ear canal and c) the final shell obtained from digital data by the laser stereo-lithography.

Most important projects activated year 2002

1) FIRB project “Study, realization and experiment on microsystems for controlled drug delivery in situ” duration 3 years (2.14 M€)
2) FIRB project Miniaturized Systems for Electronics and Photonics duration 3 years (90 K€)
3) FIRB project “Design and fabrication of Optical Tweezers for applications to nanoscience and biotecnology” duration 3 years (250K€)
4) FIRB project “Carbon based microstructures and nanostructures” duration 3 years (350 K€)
5) FISR project “Nanodispositivi ottici a pochi fotoni” Duration 2 years (100 k€)
6) FISR project ” NANOTECNOLOGIE E MICROSISTEMI”. Duration 2 years (90 K€)

List of publications 2002-2003

1) “ Differential interference contrast makes sub-micron X-ray imaging possible for transparent materials Thomas Wilhein , Burkhard Kaulich, Enzo Di Fabrizio, Stefano Cabrini, Fillipo Romanato Jean Susini. JOSA A, Volume 19, Issue 4, 797-806 April 2002
2) “X-ray lithography fabrication of a zone plate for X-rays in the range from 15 to 30 KeV
M. Altissimo, F. Romanato, L. Vaccari, L. Businaro, D. Cojoc, B. Kaulich, S. Cabrini,and E. Di
Microelectronic Engineering 61-62, 173, (2002)
3) “ Design and Fabrication of diffractive optical elements for optical tweezers arrays by means of e-beam lithography”, D. Cojoc, E. Di Fabrizio, L. Businaro, S. Cabrini,F. Romanato, L. Vaccari, M. Altissimo.
Microelectronic Engineering 61-62, 963, (2002)
4) Differential interference contrast x-ray microscopy T. Wilhein B. Kaulich, E. Di Fabrizio, J Susini. Proceedings SPIE 2002 San Diego August 2001 Advanced X-ray optics .
5) Linear optical properties and photonic mode dispersion in GaAs/AlGaAs photonic crystal slabs M. Patrini, M. Galli, M. Agio, L.C. Andreani, D. Bajoni, and G. Guizzetti
L. Businaro, E. Di Fabrizio, and F. Romanato A. Passaseo. Presentato alla International Conference on Superlattices, Nano-structures and Nano-devices (ICSNN 2002) July 22 to July 26, 2002 (Toulouse)
6) Second-harmonic generation measured on a GaAs photonic crystal planar waveguide A.M. Malvezzi, F. Cattaneo, G. Vecchi, G. Guizzetti, L. C. Andreani, *INFM and* F. Romanato, L.Businaro, E. Di Fabrizio, A. Passaseo, M. De Vittorio Presentato alla International Conference on Superlattices, Nano-structures and Nano-devices (ICSNN 2002) July 22 to July 26, 2002 (Toulouse)
7) Patterned Magnetic Permalloy and Nickel Films: Fabrication by E-Beam and X-Ray Lithographic Techniques A. Gerardino, E. Di Fabrizio, S. Cabrini, G. Giannini, L. Mastrogiacomo, M Ciria, R.C. O'Handley, G. Gubbiotti, P. Candeloro, G. Carlotti Jpn. J. Appl.Phys. Vol. 41 (2002) pp 5149-5152
8) Spin-wave frequency discretization in submicron rectangular prisms P. Candeloro, L. Businaro, E. Di Fabrizio, G. Gubbiotti, A. Gerardino, R. Zivieri, M. Conti, G. Carlotti. Accettato per pubblicazione su JAP Gennaio 2003
9) a-Si:H BASED TWO-DIMENSIONAL PHOTONIC CRYSTALS, E.Bennici, F.Giorgis, C.F.Pirri, R.Rizzoli, P.Schina, L.Businaro, E.Di Fabrizio; Accettato per pubblicazione su Physica E Gennaio 2003
10) Optical properties and photonic bands of GaAs photonic crystal waveguides with tilted square lattice, M.Galli,M.Agio, L.C.Andreani, L.Atzeni, D.Bajoni, G.Guizzetti, L.Businaro,E.DiFabrizio, F.Romanato, A.Passaseo Eur.Phys.J.B 27 ,79 –87 (2002)
11) Second-harmonic generation in reflection and diffraction by a GaAs photonic-crystal waveguide A.M. Malvezzi, F. Cattaneo, G. Vecchi, G. Guizzetti, L. C. Andreani, F. Romanato, L.Businaro, E. Di Fabrizio, A. Passaseo, M. De Vittorio J. Opt. Soc. Am. B/ Vol. 19, No. 9/ September 2002
12) Fabrication by means of x-ray lithography of two-dimensional GaAs/AlGaAs photonic crystals with an unconventional unit cell F. Romanato, L. Businaro, E. Di Fabrizio, A. Passaseo, M. De Vittorio, R Cingolani, M Patrini ,M Galli , D Bajoni, L.C. Andreani, F. Giacometti, M. Gentili, D. Peyrade, Y. Chen Nanotechnology **13** (2002) 644–652
13) Design and prototyping of a micropropulsion system for microsatellites attitude control and orbit correction L. Vaccari, G. Manzoni, Fabio Feri, F. Santoni, F. Graziani, E. Di Fabrizio
Accettato per la pubblicazione su JVST Dicembre 2002
14) X-ray lithography of 2D GaAs/AlGaAs photonic crystals with unconventional unit cell.L. Businaro, F. Romanato, P. Candeloro, C. Andreani , M. Galli , M. Patrini, A. Passaseo, M. De Vittorio and E. Di Fabrizio. Accettato per la pubblicazione su JVST Dicembre 2002
15) “Differential interference contrast for x-ray microscopy: fabrication and characterization of twin zone plate optics” Enzo Di Fabrizio, Burkhard Kaulich, Thomas Wilhein, Jean Susini,
Surface Review and Letters, Vol. 9, No. 1 (2002) 243-248
16) Design and fabrication of diffractive optical elements for photonic applications by means of nanolithography, M. Prasciolu, S. Cabrini, L. Businaro, D. Cojoc, C. Liberale, R. Kumar, E. Di Fabrizio, V. Degiorgio G.Gigli, D.Pisignano, R.Cingolani

Accettato per pubblicazione su *Microelectronic Engineering* Marzo 2003

17) Novel diffractive optics for X-ray beam shaping E. Di Fabrizio , S. Cabrini, D. Cojoc, F. Romanato , M. Altissimo, B. Kaulich , R. Kumar, T Wilhein, J. Susini, M.De Vittorio, E.Vitale, G.Gigli R.Cingolani Accettato per pubblicazione su *Microelectronic Engineering* Marzo 2003

18) “3D photonic crystal fabrication by X-ray lithography” F. Romanato, L. Businaro, M. Tormen, L. Vaccari, S. Cabrini, P. Candeloro, R. Kumar, E. Di Fabrizio, Accettato per pubblicazione su *Microelectronic Engineering* Marzo 2003

19) “Nanofabrication of high index contrast two-dimensional photonic crystal
Waveguides” M.T. Todaro, T. Stomeo, V. Vitale, M. De Vittorio, A. Passaseo R. Cingolani, E. Di Fabrizio Accettato per pubblicazione su *Microelectronic Engineering* Marzo 2003

20) “Fabrication of Diffractive Optical Elements on-fiber for Photonic Applications by Nanolitography” M. Prasciolu, P. Candeloro, R. Kumar, D. Cojoc, S.Cabrini, E. Di Fabrizio, C. Liberale, V. Degiorgio Accettato per pubblicazione su Jap.J.App.Phys Marzo 2003

21) “X-Ray Lithography for Magnetic Patterns and their Characterization”
P. Candeloro, M. Conti, R. Kumar, E. Di Fabrizio, G. Gubbiotti, A. Gerardino, R. Zivieri, O. Donzelli G. Carlotti Accettato per pubblicazione su Jap.J.App.Phys Marzo 2003

22) “Diffracting aperture based differential phase contrast for scanning X-ray microscopy” B.Kaulich F. Polack,U Neuhaeusler, J. Susini, E. Di Fabrizio,T. Wilhein Accettato per la pubblicazione su Optics Express Dicembre 2002

23) “Design and fabrication of new optics for X-ray microscopy and material science”E. Di Fabrizio, D. Cojoc, S. Cabrini, B. Kaulich , T. Wilheim , J. Susini Accettato per la pubblicazione su Journal de Physique IV Aprile 2003

24) “Novel Diffractive Optics for X-Ray Beam Shaping” E. Di Fabrizio, D. Cojoc, S. Cabrini, ,B. Kaulich, T. Wilhein, J. Susini Accettato per la pubblicazione come *proceedings* SPIE conference on Microfabricated X-Ray Optics January 2003

25) “Nanotechnology for optoelectronic applications” E. Di Fabrizio, D. Cojoc, S. Cabrini, M. Prasciolu
verra’ presentato alla conf. SPIE ATOM 2002 22-26 Novembre 2002 Bucarest

26) Resonant second-harmonic generation in a GaAs photonic crystal waveguide
A.M.Malvezzi,G.Vecchi ,M.Patrini,G.Guizzetti,L.C.Andreani, F.Romanato,L.Businaro,E.
Di Fabrizio,A.Passaseo,M.DeVittorio Sottomesso a Physical review letters Ottobre 2002

27) Shaping x-rays by diffractive coded nano-optics, E. Di Fabrizio, D. Cojoc , B. Kaulich, S. Cabrini, L. Businaro, J. Susini, T. Wilhein, P. Facci.

28) Linear optical properties and photonic mode dispersion in GaAs/AlGaAs photonic crystal slabs, Physica E, 17, 418, (2003)
M. Patrini, M. Galli, M. Agio, L.C. Andreani, D. Bajoni, G. Guizzetti, L. Businaro, E. Di Fabrizio, F. Romanato, A. Passaseo.

28)“X-Ray Lithography for Magnetic Patterns and their Characterization” P. Candeloro, M. Conti, R. Kumar, E. Di Fabrizio, G. Gubbiotti, A. Gerardino, R. Zivieri, O. Donzelli G. Carlotti; Accettato per pubblicazione su
Jpn.J.Appl.Phys.Vol.42, Part 1,No.6B, June 2003

29) “Spin-wave frequency discretization in submicron rectangular prisms” P. Candeloro, L. Businaro, E. Di Fabrizio, G. Gubbiotti, A. Gerardino, R. Zivieri, M. Conti, G. Carlotti. Accettato per pubblicazione su *J. Appl. Phys. Vol. 93 (10) 7595, 15 May 2003*

30) “Fresnel Zone Plates for Imaging and Focusing of Thermal and Cold Neutrons”

D. Sacchetti, M. Altissimo, C. Petrillo, E. Di Fabrizio, S. Colleoni, and F. Ott, Neutron News, Volume 14 • Number 2 • 2003

32) “Three-dimensional micro&nano-structuring by combination of nanoimprint and x-ray lithography”
Massimo Tormen, Matteo Altissimo, Filippo Romanato, Luca Businaro, Stefano Cabrini, Patrizio Candeloro,
Enzo M. Di Fabrizio Submitted to *App. Phys. Lett*. June 2003

Advanced Photolectric Experiment – APE -Beamline

The APE beamline provides a state-of-the-art surface science laboratory as a support facility for advanced photoelectric effect experiments using polarized Synchrotron Radiation in the ultraviolet and soft X-ray range (Fig.1)

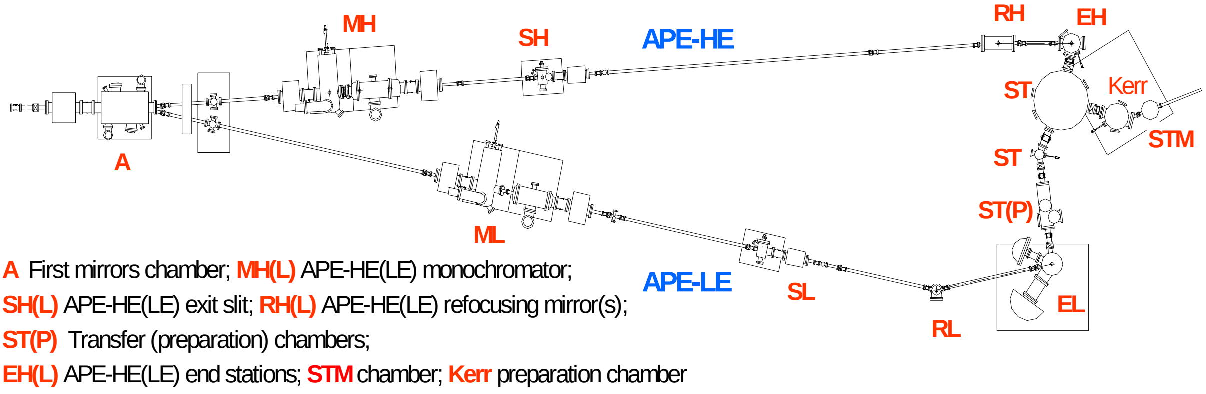

A First mirrors chamber; **MH(L)** APE-HE(LE) monochromator;
SH(L) APE-HE(LE) exit slit; **RH(L)** APE-HE(LE) refocusing mirror(s);
ST(P) Transfer (preparation) chambers;
EH(L) APE-HE(LE) end stations; **STM** chamber; **Kerr** preparation chamber

Details of APE can be found on the web page WWW.TASC.INFM.IT.

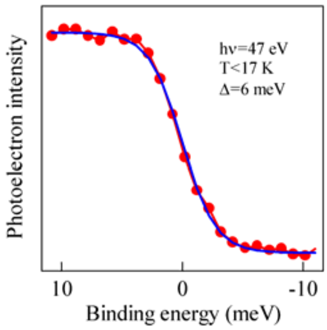

Commissioning experiments:
The APE-LE end station is dedicated to High Eenrgy and Angle Resolution Photoemission for Fermi Surface Mapping and Tomography. The experimental resolution (*i.e.* light + analyzer + sample temperature) was determined from the width of the measured Fermi edge of a polycrystalline Ag sample (see figure above).
We consistently measure <6 meV (Fig. 3) for 25-47 eV photons.
The angular resoloution can be adjusted by slicing the 2D detector to a few tenths of degree. The figure show a full measurement of the Fermi surface of Ag(100) as obtained with h =25 eV (raw data, about 7 hours of acquisition time).

The APE-HE station can exploit X-rays with variable polarization to study the magnetic properties of materials. A test experiment was performed on an iron thin film epitaxially grown on GaAs(001)-(6x4). A $Fe_{0.5}Co_{0.5}$ probing layer was deposited between two 6 ML's-thick Fe wedges to test the magnetic properties of the film as a function of distance from the interface with the semiconductor (see Fig. 7). This was done using X-Ray magnetic circular dichroism (XMCD) on the $L_{2,3}$ threshold of Co. In Fig.7 b we show two spectra taken with the X-Ray beam shining on the probing layer at different distances from the interface. The reducing of the dichroic intensity is a sign that the magnetization film is reduced when approaching the interface.

1. 1ML C_{60} on Ag(100) with impurities

We investigated the consequences of adding impurities to the two-dimensional c(6x4)-C_{60}/Ag(100) surface with respect to the low temperature changes of the Fermi surface that were described for the pure system (A. Goldoni et al., PRB 58, 2228 (1998), C. Cepek et al. PRL 86, 3100 (2001)). Doping the system with $5x10^{11}$ atoms/cm^2 of magnetic impurities (Fe, Co, Gd) eliminates altogether the pseudogap-opening phenomenon, down to 25K. Similar concentrations of nonmagnetic impurities (Au, K) do not suppress the transition. Very recent results suggest however that the behavior of the pure system was not sufficiently understood and at the moment limits any further conclusion. Further experiments on the C60/Ag(100) stepped surface have been performed, by means of STM and ARPES. A single domain arrangement for the C60 monolayer has been found with a miscut of 6.5 degrees of the Ag(100)surface.

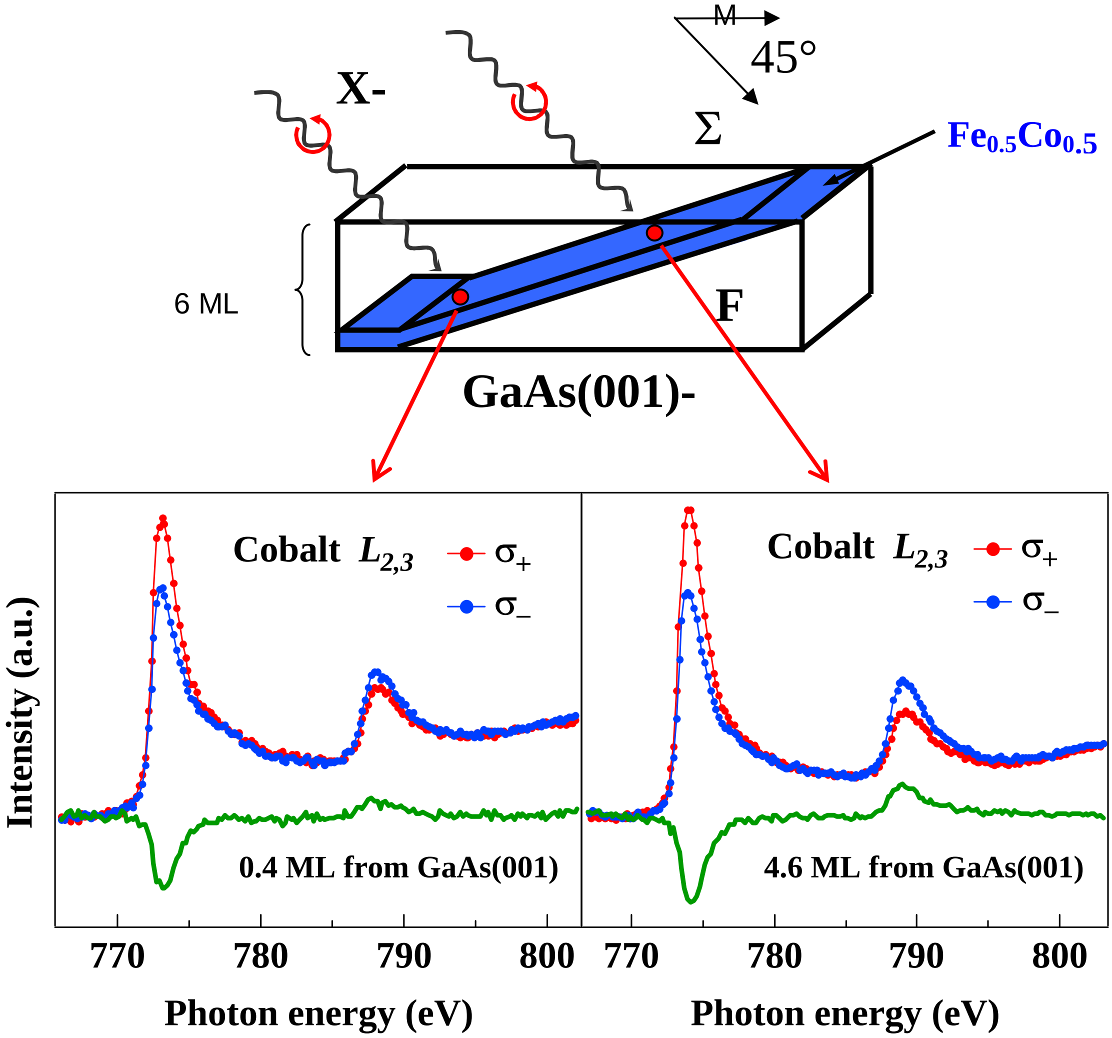

Upper part: a Fe$_{0.5}$Co$_{0.5}$ probing layer is sandwiched between two wedges of *bcc* Fe deposited on GaAs(001)-6x4; lower part: XMCD spectra taken at different probing distances from the metal/semiconductor interface.

2. C/Fe(100) STM and ARPES

The local structure of segregated nonmagnetic species on Fe(100) has been studied by combining Scanning Tunneling Microscopy (STM), LEED, Auger and ARPES spectroscopy. Both the roughness and the miscut angle of the Fe(100) single crystal induce particular surface super-structures, as confirmed by the comparison between STM images and model calculations. Distinct and ordered surface arrangements have been observed for Carbon, Phosphor and Sulphur segregation as a function of the preparation conditions (annealing and sputtering). Atomically resolved STM images reveal the presence of carbon and sulphur self-assembled stripes with a regular pattern on nanometer lateral scale, where conditions for a metastable phase with long range order are readily achievable.

Publication list (year 2002)

- M. Bertolo, S. La Rosa, A. Goldoni, G. Cautero, A.A. Zakharov, I. Lindau, I. Vobornik, R. Yoshizaki,*"Photoemission spectromicroscopy study of a Bi2Sr2CaCu2O8+x single crystal"*, Phys. Rev**. B66**, 060506(R) (2002).
- I. Vobornik, L. Giovanelli, G. Panaccione, J. Fujii, C. Cepek, M. Sancrotti, G. Rossi, *"Influence of Impurities on the Density of States at the Fermi Level in the c(6x4)-C60/Ag(100) two-dimensional superstructure"*, E-MRS 2002 Conference proceedings (Nuclear Instruments and Methods)

-J. Fujii, M.Galaktionov, L.Giovanelli, G. Panaccione, F. Bondino, I. Vobornik, G. Rossi, "*Short and Long Range Ordered Surface Structures of Segregated Species on Fe(100)*", E-MRS 2002 Conference proceedings (Thin Solid Films).

G. Rossi, F. Sirotti, and G Panaccione, *'' Magnetization dynamics of surfaces and few monolayers films''*, E-MRS 2002 Conference proceedings (Thin Solid Films) NIM A.

F. Bruno, G. Panaccione, A. Verdini, P. Torelli, F. Sirotti, M. Sacchi, R. Gotter, L. Floreano, A. Morgante, G. Rossi *''Surface and bulk contribution in ferromagnetic transition metals via photoelectron diffraction in magnetic dichroism''*, Phys. Rev. **B66**, 024417 (2002).

J. M. Mariot, L. Journel, R. Delaunay, C.F. Hague,, M. Sacchi, F. Sirotti, G. Panaccione, A. Mirone, S. Turchini and T. Prosperi, Surface Review and Lett. **9**, 977 (2002).

Participation to conferences

G. Panaccione, 4-8 May 2002, Tunis INSAT,. 'Introduction to Synchrotron Radiation', two invited talks in the framework of the bilateral Italo-Tunisian collaboration.

G. Panaccione, 4-5 June 2002, Lab. Chimie-Phisique, Univ. P.M. Curie, Paris, France, Workshop '*Diffusion Inelastique des Rayons X et Photoemission a Haute Energie'*, invited talk : 'Status of the VOLPE Project'

G.Rossi, HERCULES 2002 (Higher European Research Course for Users of Large Experimental Systems) 2002 (12th session) Lecture on Surface Science

G. Rossi,E-MRS Conference in Strasbourg June 18-21, 2002 Invited Talk on Surface Magnetization Dynamics

LEED and STM image of the C/Fe(100) surface. Zig-Zag chains of carbon produce the extra spot on the LEED.

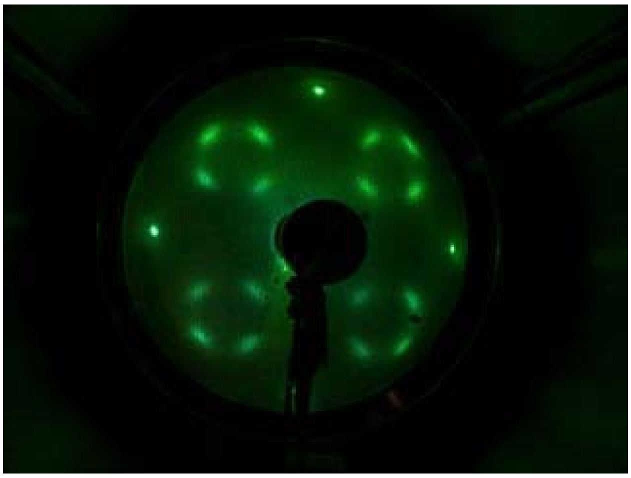

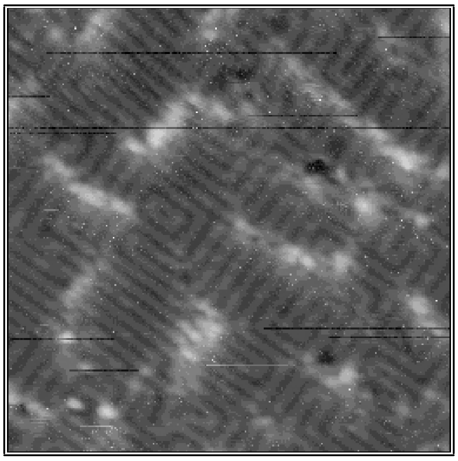

BACH : a Beamline for Advanced diCHroism

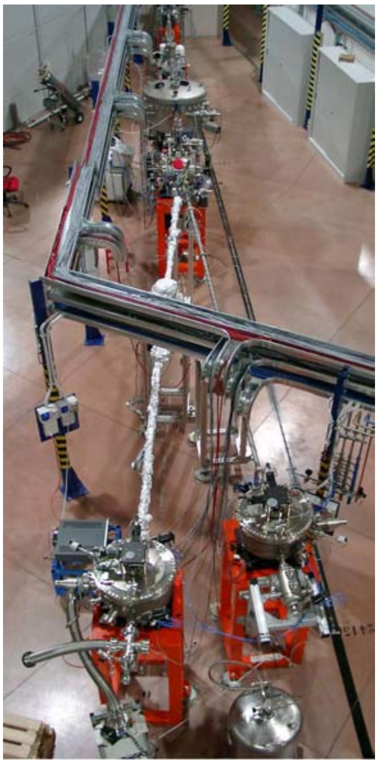

Aerial View
of the
BACH
beamline

The Beamline for Advanced diCHroism is officially opened to external users since January 2003, while from the beginning of year 2002 it has been used for the final characterization and test measurements. The facility is based on two APPLE-II undulators and a Padmore VASGM (Variable Angle Spherical Grating Monochromator) covering an energy range from 35 to 1600 eV with complete control over the polarization. The photon flux on the sample has been measured for various energies and it is always above 10^{10} photons/s on the entire energy range at the best resolution achievable.

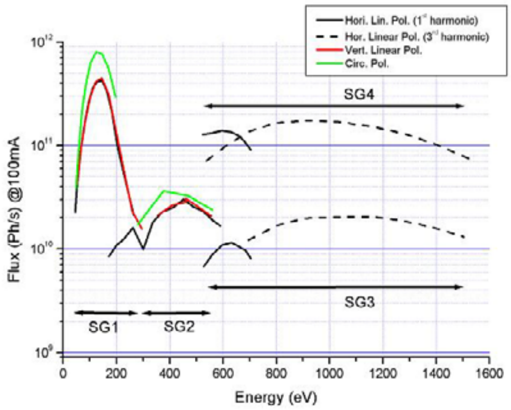

Measured Flux in
the experimental
chamber

The beamline is divided into two different branch lines differing for the spot size on the sample (200×15 μm^2 for the branch A and ~ 350×40 μm^2 for the branch B). A third branch line will host an endstation for spectromicroscopy with zone plate optics whose expected spatial resolution is 0.05 µm. The sample stage will permit to cool the sample to 30K. The chamber will be equipped for photoemission, absorption and transmission measurements. We expect to install this chamber in 2004 while the optical elements will be installed and commissioned in the second half of 2003.

On the branchline A a very compact fluorescence spectrometer, specifically designed in collaboration with ELETTRA is installed. It covers the 20-1200 eV energy range and it is characterized by a resolving power ranging from 6000 to 2000. Beside the fluorescence spectrometer the installed chamber also mounts an hemispherical analyzer with an energy resolution of 20 meV and a manipulator that allows cooling to liquid nitrogen temperature and 5 degrees of freedom. The preparation chamber hosts all the characterization tools which are needed for surface physics experiments.

Among the many active collaborations, a very important role is played by the collaboration with the groups of Philippe Sainctavit and J. Paul Kappler (ICPMS Strasbourg) and Prof. G. Krill (LURE - Universitè Paris-Sud) for XMCD/XMLD measurements. In the framework of this partnership BACH benefits by the installation of an endstation for very low temperature and high magnetic fields measurements ($T < 2K$, $H_{max} = \pm 7T$) for 12 weeks/ year. Due to the great success of this cooperation the cryostat will be installed on BACH beamline during 2004. Another particularly important collaboration in terms of technical development of the beamline involves the group of Prof. Z.X. Shen (Stanford University). The evolution of this project includes the installation of an endstation hosting a Scienta 2002 SES analyzer and a mini-Mott detector allowing simultaneous photoemission and spin resolved spectroscopy experiments, with full control of the polarization and at low temperature. The chamber will be installed in the second half of 2003.

Coordinator:	Prof Fulvio Parmigiani
Staff:	Federica Bondino
	Regina Rochow-Carbone
	Michele Zacchigna
	Marco Zangrando

ComIXS on BACH : a Compact Inelastic X-ray Spectrometer on BACH

A new Compact Inelastic X-ray Spectrometer is operative at the experimental chamber of BACH beamline. This instrument performs the spectral analysis of the fluorescence-emitted photons coming from the sample illuminated by the synchrotron radiation. In particular, it operates in the 20-1200 eV energy range with a resolving power greater than 1000 for the entire energy range. In order to do this it employs two in-vacuum interchangeable variable line spacing spherical gratings as dispersive elements: the low energy (LE) grating covers the 20-200 eV range, while the high energy (HE) grating covers the 120-1200 eV range. A back-illuminated 2D CCD (pixel size=20 m) camera is used as the photon detector and, due to its dimensions (2.6×2.6 cm^2), it can collect different energies in a single shot.

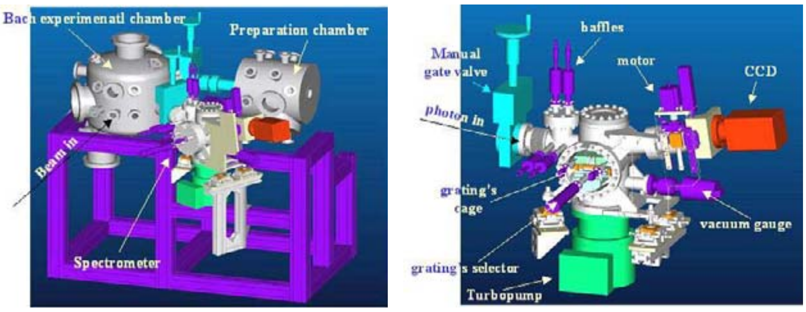

Left: BACH experimental chamber with ComIXS. Right: ComIXS

ComIXS is still in the commissioning phase but, nevertheless, some beamtimes were already carried out on it. In particular, resonant inelastic x-ray scattering (RIXS) experiments were performed on different systems such as iron oxides and sulphides (Fe_2O_3, Fe_3O_4, FeS_2) and lanthanum sodium-doped manganites ($La_{1-x}Na_xMnO_3$). Other materials like Si, Cu, Mo, HOPG were used to characterize the performances in terms of energy resolution at different energies. The latter materials showed that the instrument reaches almost entirely the predicted values and that it is becoming to be limited by the CCD pixel size while trying to get higher energy resolutions. Experiments on the former materials, on the other side, proved the high efficiency of the instrument which is characterized by short acquisition times (e.g. 5' to get a well-counted and well-resolved spectrum of the O K edge for manganites).

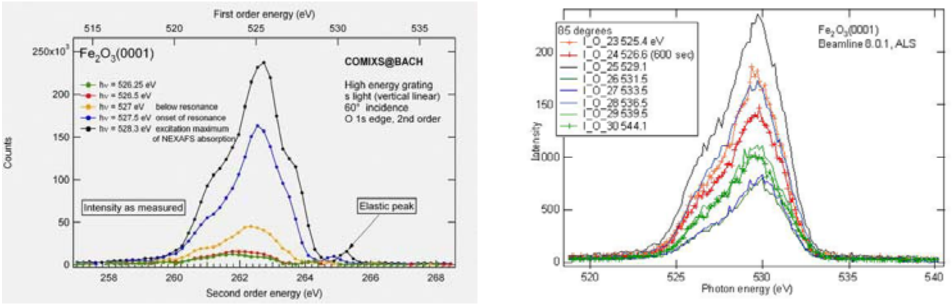

Comparison between RIXS measurements on Fe_2O_3 performed at ALS (left) and BACH (right).

Clearly, this instrument takes advantage of BACH capabilities and consequently it is possible to perform polarization dependent fluorescence measurements. These peculiarities will be even improved after the installation of a new cryostat in BACH experimental chamber which will permit the cooling of the sample down to about 10 K.

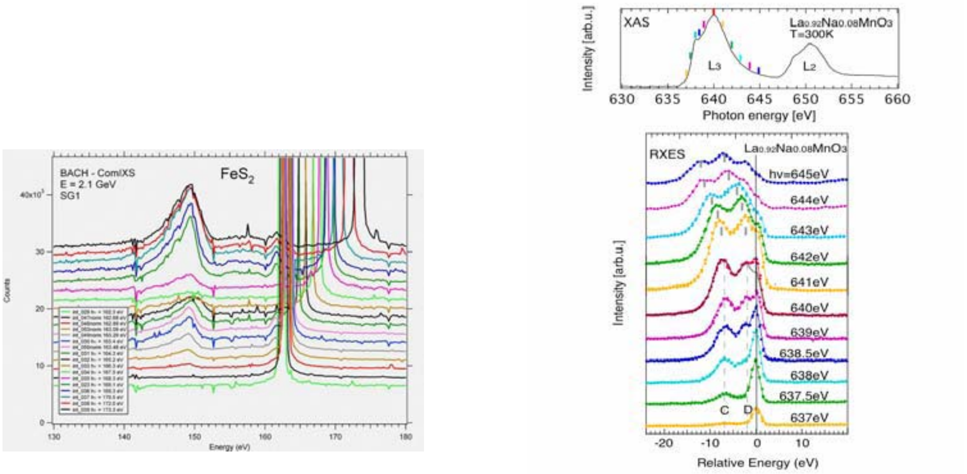

Left: RIXS on the S 2P edge of FeS2. Right: TOP: XAS spectra of Mn $L_{2,3}$ edge of $La_{0.92}Na_{0.08}MnO_3$; BOTTOM: RIXS on Mn $L_{2,3}$ edge of $La_{0.92}Na_{0.08}MnO_3$.

Magnetic anisotropy of NiO epitaxial thin films on Fe(001)

A. Brambilla[a;_], M. Portalupi[a], M. Finazzi[a], G. Ghiringhelli[a], L. Duò[a], F. Parmigiani[b],
M. Zacchigna[c], M. Zangrando[c] and F. Ciccacci[a]

a *INFM - Dip. di Fisica del Politecnico di Milano, P.za L. Da Vinci 32, 20133 Milano, Italy.*
b *INFM - Dip. di Matematica e Fisica, UCSC, Via dei Musei 41, 25121 Brescia, Italy.*
c *INFM - TASC, Basovizza S.S. 14, Km 163.5, 34012 Trieste, Italy.*

Interfaces between a ferromagnetic (F) and an antiferromagnetic (AF) material are very attractive systems for fundamental reasons, related to the exchange bias effect, as well as for the possible technological applications in giant magnetoresistance tunnelling devices. Despite the large variety of studies about F/AF interfaces available in the literature, scarce information exist concerning the spectacular case of the AF/F reverse interface.

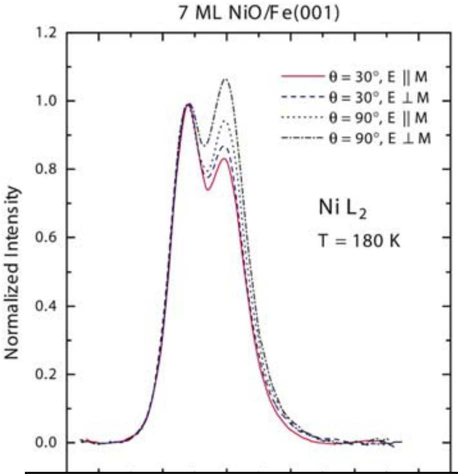

Normalized Ni *L*2 absorption spectra obtained at 180 K on a 7 ML-thick NiO sample grown on Fe(001).

We performed an X-Ray Magnetic Linear Dichroism (XMLD) study at the Ni *L*2 absorption edge of thin NiO films grown on a Fe(001) substrate. We decided to start from a Fe(001)-*p*(1× 1)O surface, which is prepared by annealing a clean Fe(001) surface while exposed to O2. This surface is stable and well characterized [1]. Hereafter, we will refer to the Fe(001)-*p*(1× 1)O surface simply as Fe(001). High quality epitaxial thin NiO films are finally prepared by Ni electron beam evaporation in a O_2 atmosphere [2], on a Fe(001) substrate remanently magnetized along the in plane [010] direction.
The XMLD data were collected at the beamline BACH [3] at the ELETTRA synchrotron radiation facility in Trieste, Italy. The absorption spectra were obtained measuring the drain current from the sample in four different geometries. The angle between the surface normal and the polarization of the incoming light can have the values $\theta =$ 90° (normal incidence) $\theta =$ 30° (grazing), while the Fe substrate magnetization **M** is kept parallel (**M** // **E**) or perpendicular (**M** ⊥ **E**) to the photon electric field **E**. The Figure shows the Ni *L*2 spectra collected in the our geometries for a 7ML-thick NiO/Fe(001) film. These spectra are normalized to unity at the low photon energy peak, after subtraction of a background. The spectra reported clearly show a strong dependence with the angle θ as well as with the relative orientation of **M** and **E**.
To exclude the possibility that the measured anisotropy may be caused by the uniaxial crystal field at the surface, we remark that the mentioned field gives a constant contribution to the absorption spectra collected when the azimuth angle of he NiO films is rotated by 90°, since the NiO(001) surface normal is a fourfold symmetry axis for the crystal field. Thus, the differences observed between the spectra measured at normal incidence rotating the azimuth can be fully attributed to the presence of a long-range antiferromagnetic order with uniaxial anisotropy in the plane of the NiO film. The data collected at grazing incidence could instead be influenced by the uniaxial crystal field.
Anyway, results on thin films of NiO grown on Ag(001) [4] show that the crystal field is responsible of little variations of the NiO *L*2 ratio, defined as the ratio between the high- and the low-photon energy peak at the Ni *L*2 absorption edge, with respect to the polar angle [4]. Due to the small (less than 0.7%) difference between the in-plane lattice parameters of thin NiO layers epitaxially grown on Ag (001) or Fe(001) substrates, we expect that the effects of the crystal field on the absorption spectra should be about the same for NiO/Fe and NiO/Ag films of equal thickness.We conclude that a large part of the variation of the *L*2 ratio in 7 ML NiO/Fe(001), going from $\theta =$ 90° *to* $\theta =$ 30° with **M** fixed, can be confidently assigned to magnetic effects.
A general expression relates the value of the NiO *L*2 ratio to the angle between the Ni local magnetic moment and the linear light polarization [5]. The analysis of the collected data reveals that, on the average, the component of the magnetic moments localized on the nickel atoms is larger along the in-plane direction perpendicular to the substrate magnetization rather than parallel to it. On the other hand, the average projection of the Ni local magnetic moments in the film plane is larger than that on the surface normal. In conclusion, our 7 ML thick NiO/Fe(001) film has a strong in-plane uniaxial anisotropy with an easy axis perpendicular to **M**. This is radically different from what has been observed so far in F/AF interfaces, where the coupling is collinear. These unexpected findings indicate that the mag netic structure of a F/AF interface is heavily influenced by the growth sequence and conditions.

References

[1] R. Bertacco *et al.* Phys. Rev. B **59**, 4207 (1999).
[2] L. Du_o *et al.* Surf. Sci. **518**, 234 (2002).
[3] M. Zangrando *et al.* Rev. Sci. Instrum. **72**, 1313 (2001)
[4] S. Altieri *et al.* to be published.
[5] D. Alders *et al.* Phys. Rev. B **57**, 11623 (1998).

ComIXS spectrometer unravels the bulk electronic structure of manganites

M. Platè[1], F. Bondino[2], M. Zacchigna[2], M. Zangrando[2], I. Alessandri[3], A. Comin[5], D. Cocco[4], M. Matteucci[4], K.C. Prince[4] and F. Parmigiani[2,5,]*

[1] Dipartimento di Fisica, Università di Pavia, Via Bassi 6, I-27100 Pavia, Italy
[2] INFM-TASC, Beamline BACH, Basovizza-Trieste, Italy
[3] Lab. di Strutturistica Chimica, Università degli Studi di Brescia, 25123 Brescia, Italy
[4] Sincrotrone Trieste, Area Science Park, Basovizza-Trieste, Italy
[5] Dipartimento di Matematica e Fisica, Università Cattolica del Sacro Cuore, Brescia, Italy

High-storage-density magnetic devices require materials with a large magneto-resistance (MR) near room temperature. The recent discover of “doped” manganites – $Ln_{1-x}A_xMnO_3$ - (Ln = Lanthanoids; A = alkali or alkaline earth metals) well respond to this technological demand. For these reasons an intense effort has been spent to synthesize new “doped” manganites and to understand the origin of the unique properties shown by these intriguing materials [1].

In these mixed oxides the colossal magneto-resistance phenomena is accompanied by a wide range of exotic behavior such as magnetic ordering, metal-insulator transition, charge and orbital ordering. In addition, depending on temperature, pressure and “doping”, they exhibit a very rich phase diagram, including insulating antiferro-magnetic, paramagnetic and metallic ferromagnetic phases [1].

The beautiful complexity of these phenomena arises from the interplay among several competing structural and electronic mechanisms, not fully understood, such as double exchange and cooperative Jahn-Teller distortions. In particular, ambiguities and missed information about the interplay between occupied and unoccupied states as well as controversies concerning the strength of the electronic correlations and the size of the band energy gap need to be addressed.

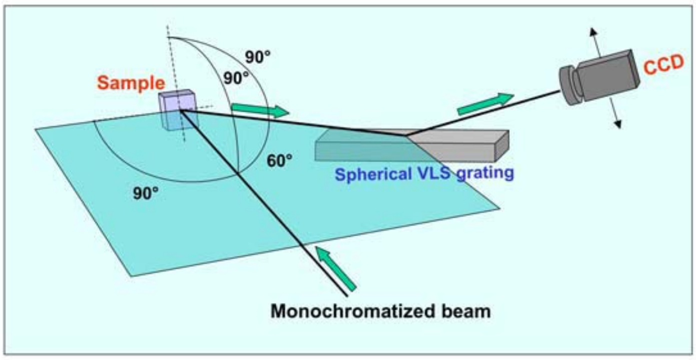

Experimental set-up and scattering geometry for RXE measurements at the BACH beamline.

A powerful technique to investigate the elementary excitations in solids with element specificity is the Resonant X-ray Emission (RXE) spectroscopy. In RXE an incident x-ray photon excites a core electron to the absorption threshold and the x-ray emission, resulting from the decay of the excited state, is energetically analyzed. In recent years this spectroscopy has progressed remarkably becoming an extremely effective tool to study low-energy neutral electronic transitions, charge transfer (CT) excitations, inter-band transitions and energy band dispersion [2].

Aim of this experiment is to study the X-ray emission in $La_{1-x}Na_xMnO_3$ (x = 0, 0.08 and 0.15) compounds. The samples were grown by radio-frequency-magnetron sputtering [3]. In these manganites J-T effect, that favors the double exchange and hence the ferromagnetic pairing of the spins the peculiarity, is the less pronounced with respect to systems “doped” with divalent alkaline-earth ions (Ca and Sr).

The scattering geometry and the experimental set up are shown in Fig. 1. The spectra were collected with vertical polarization, *i.e.* the electric vector of the incident radiation perpendicular to the scattering plane (highlighted in Fig. 1). In this configuration the peak at zero energy loss, i.e. the elastic scattering, is well visible in almost all the spectra, allowing an accurate calibration of the energy scale.

Fig. 2 (a) shows the RXE spectra obtained for the sample with x=0.08 of Na “doping” at 300 K. The RXE raw data are plotted against the transferred energy. The excitation-energies are indicated with ticks in the x-ray absorption (XA) spectrum shown in the upper panel of Fig. 2. Resonant and non-resonant features can be easily identified. The non-resonant features appear at constant emission energy (hence dispersing peaks in the figure). These structures arise from ionization and subsequent normal X-ray fluorescence emission. The onset of Mn $3p_{3/2}$ ionization is located between 640 eV and 641 eV. Resonating loss features appear at constant energy, below the elastic peak. Two well-resolved emissions are observed between 637 eV to 640 eV. Structure A, at about 6.8 eV (A) and structure B, at about 2.1 eV. For the sake of comparison, some spectra were recorded with horizontal polarization, *i.e.* with the electric vector of the incident light in the scattering plane. In Fig. 2 (a), one of these spectra is displayed as a dotted line at hν = 640 eV. As expected from dipole transition selection rules [4], the elastic peak is strongly suppressed. This helps to avoid possible ambiguities on the origin of the energy scale.

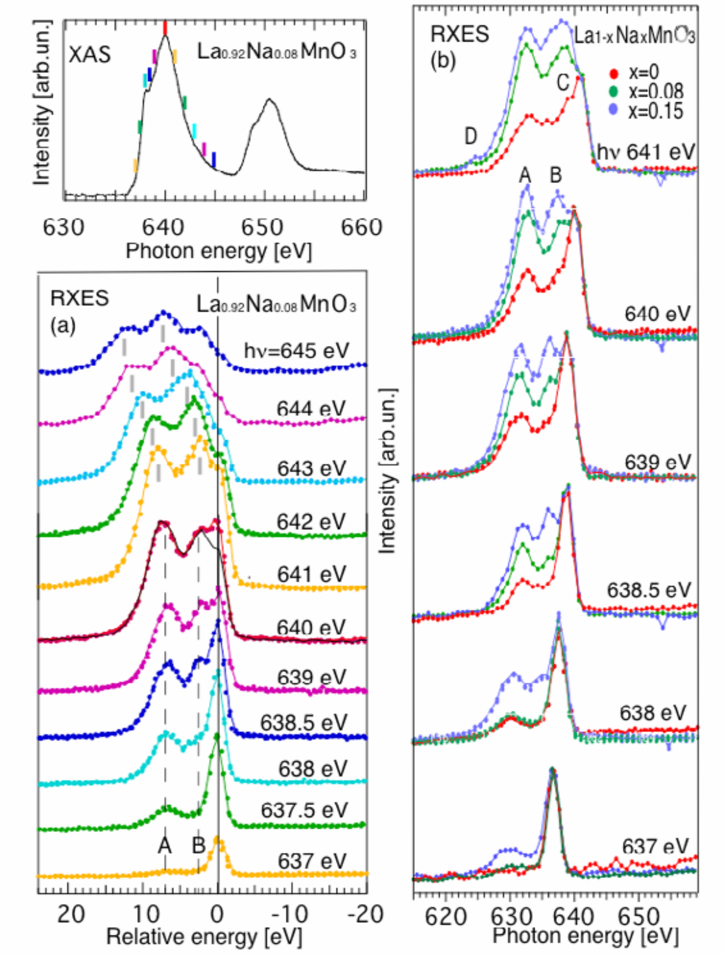

Top: Mn $L_{3,2}$-edge XA spectrum of $La_{0.92}Na_{0.08}MnO_3$ at 300 K. Bottom: (a) RXE spectra measured with vertical polarization from the same $La_{0.92}Na_{0.08}MnO_3$ sample at different excitation energies across the Mn L_3 threshold at 300 K. One of the spectra recorded with horizontal polarization is shown (black dotted line, at 640 eV excitation energy). The RXE raw data are plotted against the transferred energy (curves are offset for clarity) and the excitation energies are indicated with ticks in the XA spectrum. (b) Variation of the Mn 3d->2p RXE spectra of $La_{1-x}Na_xMnO_3$ with the "doping" concentration (x=0, 0.08 and 0.15)

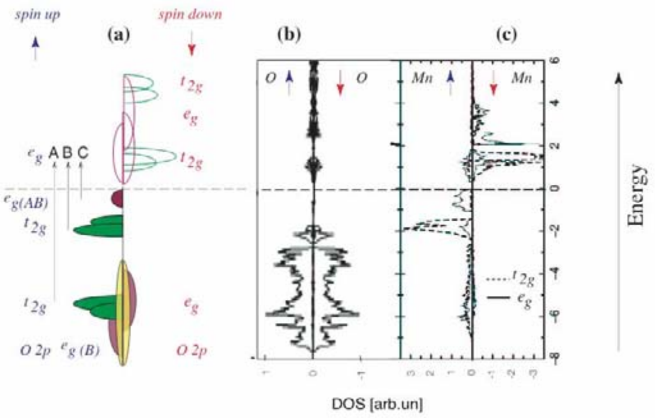

Mn 3d and O partial DOS for A-antiferromagnetic $LaMnO_3$ with orthorhombic $GdFeO_3$ structure obtained by full-potential linearized augmented plane-wave LSDA calculations. Adapted from ref. [5]

Fig. 2 (b) shows the "doping"-induced changes in the electronic structure of $La_{1-x}Na_xMnO_3$. The spectra are displayed in the emission energy scale and the data are normalized to the elastic peak.

The results of recent *ab-initio* partial DOS calculations for distorted orthorhombic $LaMnO_3$ derived from spin polarized density functional theory and the schematic diagram of the observed transitions are shown in Fig. 3 [5].

According to these calculations, the dominant contribution to the density of states (DOS) closer to the E_F is given by Mn $e_g\uparrow$-like bands, split by a strong electron-phonon coupling of the Jahn-Teller type. Mn t_{2g} electrons are well localized at –2 eV. Emission B [Fig. 2 (a)] can be associated to *dd* transitions from the occupied t_{2g} electrons to the e_g-like empty states.

Remarkably in RXE spectroscopy the optically dipole forbidden *dd* transitions have a cross-section strongly enhanced.

Peak B is significantly more intense in the "doped" samples. This effect can be explained considering the weaker hybridization of the t_{2g} and O 2p electrons due to a more pronounced structural distortion induced by the "doping" ions. However, the strong enhancement of peak B in the "doped" samples can be rationalized with the higher density of empty $e_g\uparrow$ states in the lower part of the CB related to the presence of the Mn^{4+} ions. This interpretation is consistent with the band observed in optical conductivity measurements at 2.3 eV and associated with the presence of Mn^{4+} and/or O^- self-trapped holes in possible non-stoichiometric $LaMnO_3$ samples [6].

Both the Mn- t_{2g}- and $e_g\uparrow$ bonding bands, hybridized with O 2p states, give a broad contribution in the occupied DOS around 5-6 eV. Peak A in Fig. 2 (a) can be assigned to an electronic excitation from this band to the empty $e_g\uparrow$ band.

A weak inelastic scattering loss (C) at about 1.6 eV is observed in $LaMnO_3$ at hν = 641 eV. This feature can be tentatively assign to the energy-gap transition between the highest occupied e_g bands to the unoccupied e_g majority bands. According to this interpretation it is possible to estimate a band gap of about 1.6 eV. Since in the present spectra this excitation lies below the strong elastic peak a higher spectral resolution could help to better estimate the band gap energy.

Finally, a weak loss structure appears at around 17-17.5 eV [peak D in Fig. 2 (b)], however the origin of this feature require more deep investigations.

It is also interesting to compare the RXE spectra with optical conductivity measurements for alkali-"doped" and "undoped" $LaMnO_3$. Optical conductivity essentially probes the same elementary excitations observed in RXE but without elemental selectivity and different selection rules [7]. The optical absorption spectra display several broad bands at ~1.9-2.3, 4.6, 7, 9, 17 and 25 eV. The features at about 4.6 eV, and 25.0 eV are not detected in RXE spectra, for any "doping". This observation leads to the conclusion that Mn ions are not directly involved in these transitions.

In conclusion, RXE spectra on "undoped" $LaMnO_3$ are in fair agreement with the theoretical predictions based on partial DOS calculations for distorted orthorhombic $LaMnO_3$ derived from spin polarized density functional theory. This agreement is used as a frame to interpret the RXE data for the "doped" materials. In particular it is possible to identify some resonant inelastic loss.

Furthermore, RXE experiments made possible to observe the weak losses corresponding to a gap excitation between e_g bands split by the strong Jahn-Teller electron-phonon coupling. Remarkable is also the dependence on "doping" of the transition involving the t_{2g}-like states in the valence band, which can be observed and explained.

[1] J.M. D. Coey et al., Adv. In Phys., **48**, 167 (1999). E. Dagotto, "Nanoscale Phase Separation and Colossal Magnetoresistance", Springer-Verlag (2002).
[2] See the special issue of the J. Elect. Spectrosc. Rel. Phenom., **110-111** (2000)
[3] L. Malvasi, I. Alessandri, M.C. Mozzati, P. Ghigna, G. Chiodelli, C.B. Azzoni, G. Flor, Phys. Chem. B, in publication.
[4] M. Nakazawa, H. Ogasawara, A. Kotani, Surf. Rev. and Lett., **9**, 1149 (2002).
[5] P. Ravindran et al., Phys. Rev. B, **65**, 64445 (2002).
[6] N.N Kovaleva et al., condmat/0108207
[7] T. Arima et al. Phys. Rev. B, **48**, 17006 (1993); Y. Okimoto et al. Phys. Rev. B, **55**, 4206 (1997); J.F. Lawer et al., Appl. Phys. Lett. **65**, 3017 (1994); J.H. Jung et al., Phys. Rev. B, **55**, 15489 (1997)
[8] D. Cocco, M. Matteucci, K. Prince, M. Zangrando, Proceedings SPIE, Vol. 4506 (2001)
[9] M. Zangrando, M. Finazzi, G. Paolucci, G. Comelli, B. Diviacco, R.P.Walker, D. Cocco, F. Parmigiani, Review of Scientific Instruments **72**, 2 (2001) 1313-1319; M. Finazzi, R. Rochow, M. Zangrando, D. Cocco, M. Zacchigna, and F. Parmigiani,

GasPhase Beamline

Coordinator L. Avaldi (CNR) Staff:

The Gas Phase Photoemission beamline is a joint venture between the Istituto Nazionale di Fisica della Materia (INFM), the Consiglio Nazionale delle Ricerche (CNR) and Elettra, and is operated as a Gruppo di Ricerca (GdR) at the synchrotron radiation facility ELETTRA, Trieste. It is the only beamline at ELETTRA which is specifically devoted to research on gaseous systems. The beamline has been operational since the end of 1997 and was officially opened to public users in the second semester of 1998. The line is fed by an undulator (U12.5 at exit U6.2), which delivers light in the range from 16 eV to above 1000 eV. The monochromator is a Variable Angle Spherical Grating Monochromator, with fixed positions of the slits. The optical design includes a toroidal prefocussing and two refocussing mirrors (spherical and plane elliptical). The monochromator was commissioned and not only met its specifications ($\Delta E/E$ = 10000 over all the planned working range (20 ÷ 800 eV) but even exceeded them considerably. A resolving power of 60.000 has been measured at 48 eV, it remains higher than 10.000 at 540 eV and a value of 8000 is obtained at 860 eV.

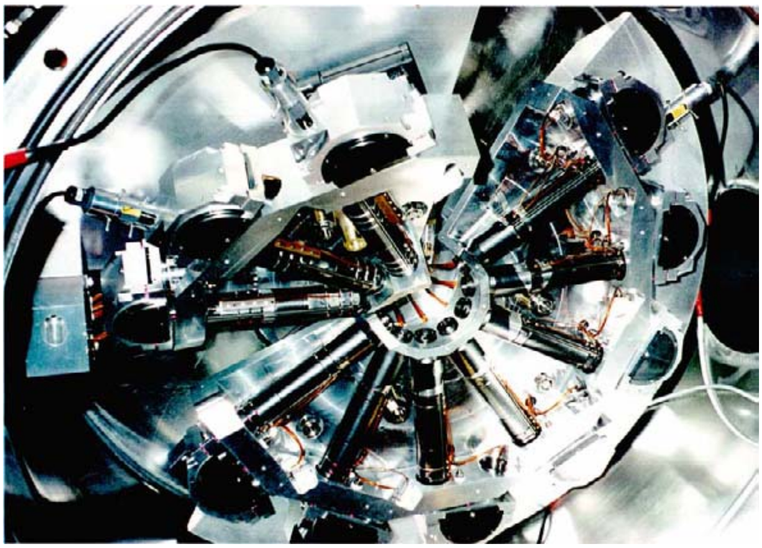

The two arrays of electrostatic analyzers of the multicoincidence endstation

The use of two refocussing mirrors provides a roughly circular spot at the sample (diameter dimension ≈350μ for a 20 micron exit slit, decreasing to less than 150μ as the photon energy increases above 200 eV). The beamline is connected to the experimental station through a differential pumping section (5 orders of magnitude difference in pressure), to decouple the UHV section of the mirrors chambers from the HV in the experimental region. At variance with other beamlines built at ELETTRA, the experimental station is not fixed at Gas Phase. Each user can bring his own apparatus to perform experiments, provided it is compatible with the beamline requirements.

For further information on the beamline : http://www.elettra.trieste.it/experiments/beamli

In 2002 the research group has continued its activity in the areas of i) photoionization dynamics and electron correlation studied by e-e coincidence experiments, ii) production and characterization of radicals and reactive species and iii) core excitation spectroscopy. The main results are :

- **Observation of coherence in the photoionization of non-degenerate states :** The multicoincidence end-station of the beamline has been successfully used to study the coherence in the photoionization of non-degenerate states in Kr. In this experiment the photoionization of the spin-orbit Kr^+ $3d^{-1}_{3/2,5/2}$ doublet

$$\begin{aligned} h\nu + Kr &\rightarrow Kr^+ 3d^{-1}(^2D_{3/2}) + e^1_{ph}(l=1,3) \\ &\rightarrow Kr^{2+} 4s4p^5(^1P^o) + e^1_{Au}(l=1,3; E^1_{Au}=39.08eV) \end{aligned} \qquad (1\text{-}1)$$

$$\begin{aligned} h\nu + Kr &\rightarrow Kr^+ 3d^{-1}(^2D_{5/2}) + e^2_{ph}(l=1,3) \\ &\rightarrow Kr^{2+} 4s4p^5(^1P^o) + e^2_{Au}(l=1,3; E^2_{Au}=37.84eV) \end{aligned} \qquad (1\text{-}2)$$

has been studied by detecting in coincidence the photoelectron and the $M_{4,5}N_1N_{23}$ Auger electrons produced in the decay of the intermediate state to the Kr^{2+} $(4s^1 4p^5)$ $^1P^o$ final state.By tuning the photon energy at 132.88 eV, the $3d_{3/2}^{-1}$ photoline is made to overlap the $M_5N_1N_{23}$ Auger peak at 37.84 eV kinetic energy, and conversely the $3d_{5/2}^{-1}$ photoline is now overimposed to the $M_4N_1N_{23}$ Auger peak. In this condition the two processes (1-1) and (1-2) become indistinguishable and the coherence between the two non-degenerate intermediate states should occur. The measured coincidence angular distribution clearly showed the interference patterns due to coherence. The analysis of the results have provided for the first time a complete information of the basic quantities (matrix elements and relative phases) needed to describe the two photoionization processes. This is a basic quantum-mechanical experiment which can be considered the analogue for the photoelectrons of the Young's two slit experiment in optics.

- **Observation of ultrafast dissociation in methanol**: The goal of the experiment was to study the resonant Auger Raman spectrum of methanol at the O 1s edge in its normal and deuterated forms. The question asked was whether the OH bond or the CO bond will break before the molecule ionizes:

$$CH_3OH + h\nu \rightarrow CH_3O^*H \rightarrow CH_3 + O^*H \rightarrow CH_3O^* + H$$

Kinetically, OH bond scission is favoured as H is light, but thermodynamically CO bond breaking is favoured as the energy of the system is lower. The Resonant Auger Raman spectra of the deuterated and normal forms measured near the O 1s->3s resonance were compared. Two sharp peaks were observed just below the valence band in the normal form. On deuteration one of these is strongly suppressed. This has be taken to be the signature of ultrafast dissociation, as in the case of water: the deuterium atom is much heavier than hydrogen and so moves more slowly. The peak is then assigned to the Resonant Auger Raman decay of a methanol molecule without the hydrogen atom of the alcohol entity, that is the decay of CH_3O^*, the O 1s core excited methoxy species.

Publications

40. "*Mass spectrometric study of double photoionization of HBr molecules*", M. Alagia, M. Boustimi, B.G. Brunetti, P. Candori, S. Falcinelli, R. Richter, S. Stranges and F. Vecchiocattivi, J. Chem. Phys. **117**, 1098-1102 (2002)

39. "*Photoionization of ethylene clusters by synchrotron radiation in the energy range 17-50 eV*", P. Franceschi, P. Tosi, D. Ascenzi, D. Bassi, M. Coreno and M. de Simone Int. J. Mass Spect. 220, 281-288 (2002)

38. "*Interference effects between 2p photoionization and resonant Auger decay channels at $2s^{-1}$ np (n = 4,5) inner-shell resonances in Ar*", R. Sankari, A. Kivimäki, M. Huttula, T. Matila, H. Aksela, S. Aksela, M. Coreno, G. Turri, R. Camilloni, M. de Simone and K. C. Prince, Phys. Rev. A **65**, 042702 (2002).

37. "*The O 1s->σ^* Resonance in O_2: Exchange Splitting Revisited*", M.N. Piancastelli, A. Kivimäki, V. Carravetta, I. Cacelli, R. Cimiraglia, C. Angeli, H. Wang, M. Coreno, M. de Simone, G.Turri and K.C. Prince, Phys. Rev. Lett. **88**, 243002-1 (2002)

36. "*High resolution threshold photoelectron measurements fo the Ne+2p4nl satellite states*", P. Bolognesi, L. Avaldi, D. Cooper, M. Coreno, R. Camilloni, G. King, J. Phys. B35, 2927 (2002).

35. *"Gas Phase photoemission study of 2-mercaptobenzothiazole* ", G. Contini, V. Di Castro, S. Stranges, R. Richter, M. Alagia, J. Phys. Chem. A **106**, pp. 2833-2837, (2002).

34. "*High-resolution inner-shell photoabsorption of the OH and OD free radicals*" S. Stranges, R. Richter, and M. Alagia, J. Chem. Phys. **116** (2002) 3676.

33. "*Inner shell excitation spectroscopy of the tetrahedral molecules CX_4,*
(X = H, F, Cl)", M. de Simone, M. Coreno, M. Alagia, R. Richter and K.C. Prince, J. Phys. B: At. Mol. Opt. Phys. 35 (2002) 61.

32. "*X-ray absorption spectra of some small polyatomic molecules*" , K. Prince, R. Richter, M. de Simone and M. Coreno; Surf. Rev. and Lett. **9**, 159 (2002)

31. "*Double photoionization of He at 80 eV excess energy in the equal-energy sharing condition*", G. Turri, L. Avaldi, P. Bolognesi, R. Camilloni, M. Coreno, J. Berakdar, A.S. Kheifets and G. Stefani, Phys. Rev. A**65**, 034702, (2002).

BEAR/X-MOSS Beamline

See on WWW.TASC.INFM.IT or on WWW.ELETTRA.TRIESTE.IT

THE TASC TECHCNICAL SUPPORT GROUP

Coordinator: Roberto Gotter
Staff: Benedetti Davide, Bertoch Paolo, Bigaran Stefano, Carpentiero Alessandro, De Luisa Aleksander, De Marco Massimiliano, Furlanetto Davide, Gruden Ales, Martin Andrea, Pertot Alessandro, Salvador Federico, Suran Fabio, Tonezzer Matteo, Varas Stefano

Since the beginning of 2002, the TASC technical support has been powered in terms of personnel and unified in a unique group, supporting the TASC laboratories as well as the INFM synchrotron light project (LDS) at Elettra. The group is under the coordination of a development scientist who spend a small percent of his time in the research activity in order to keep a tight link between the technical development and the experimental research and to be more sensitive to the physics of the instrumental requirements.

The group consists of 14 technicians (4 employed as permanent staff), 11 of which are employed in the true transverse group, supporting all the research groups, the 3 remaining being assigned to specifics laboratories (TEM, CVD/clean room and lithography) both of them mainly specialized in sample preparation.

The full transverse technical service for the 6 synchrotron beamlines and the 10 TASC laboratories, with a conspicuous activity as facility for external users, is thus achieved by 11 technicians, divided in:

2 project design (4)[1]
4 mechanical workshop (6)
3 electronic laboratory (5)
1 plants (2)
1 information technology (2)

The management of the technical support is mainly achieved by means of a web page, in which each user (experimentalists) can quickly send a request (ticket) for a technical intervention, that typically needs more than one hour of work, specifying the necessary competence and the priority. An emergency priority is available for intervention without which the research activity could be seriously affected, in particular for the scheduled experiments involved in the facility activities. For the large amount of the quick interventions requiring less than one hour (like sample holder accessories and small tools for carrying out experiments), a bureaucracy-free/help desk/real time service is guaranteed.

The politic of the interventions is also based on combining young technicians with expert researchers and vice versa in order to favor the professional growth of both of them.

Finally, the mechanical workshop has been recently moved in a new wider and more comfortable location (Fig.1).

Fig.1 The new allocation of the mechanical workshop.

Activity 2001-2002

In the 2001-2002 period the main technical support activity has been focused in the completing of the four new INFM beamlines, in the up-grade of the two old ones (Aloisa and Gasphase) and in the start-up/regime consolidation of the younger TASC laboratories.

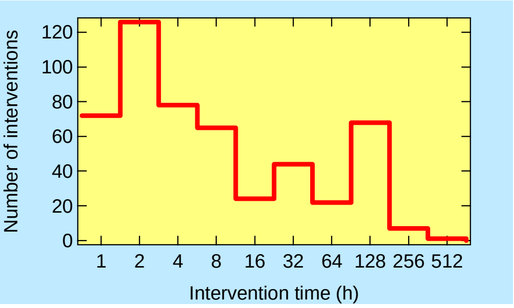

Fig.2 Histogram of the intervention time per ticket.

---

[1] In parenthesis are given, as an example, the employed people at the Department of Physics of the University of Trento (less than thirty students per year), supporting 8 experimental groups (14 additional specific technicians for the several laboratories have to be added).

Since the end of January 2002 about 750 ticket has been requested, 140 of which with emergency priority. The distribution of the intervention times per ticket is showed in the histogram (Fig.2).

Most of them have been carried out in a couple of hours but a sizable amount of technical support interventions have required one (o several) hundreds of hours. The latter mainly concern the full development (project design, mechanical/electronic realization, test and implementation) of complex custom made instrumentation.

In the following the most significant examples of instrumentation developments are given.

Aloisa manipulator.

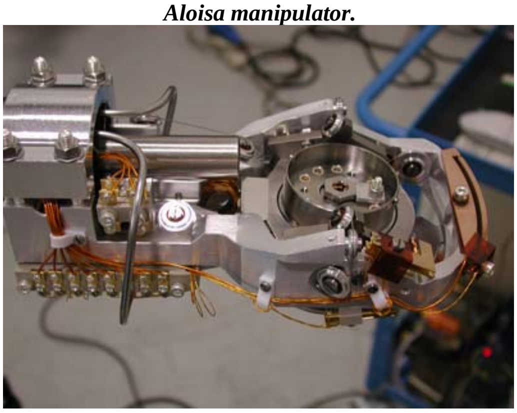

The Cinel factory in Padova has been followed in developing the new manipulator for the Aloisa beamline by taking the advantage of the expertise in using the old (VG) one. By means of a differential pumped based system and a novel mechanical solution (the centers of rotation of the incidence angle has been positioned in correspondence with the axis of the straps that transmits the movement to the azimuth angle), the three angular degree of freedom have maintained the angular resolution for surface diffraction measurements, the tilt (glancing incidence) angle range has been enhanced from 10^{O} to 40^{O}, thus permitting a wider working condition in photoemission/absorption measurements, and the surface-horizon-free condition for in plane diffraction has been further improved. Finally the reliability of the heating/cooling system and of the harmonic-drive gear system for the 1:200 transmission ratio have been improved. (Under mechanical testing and electronic development)

Aloisa66 Analyzer

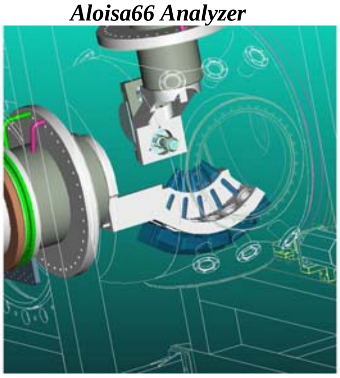

A new 66 mm hemispherical electron analyzer with multi channel energy detection is going to substitute the couple of 33 mm analyzer of the bimodal frame. In collaboration with the Rome III INFM Unit (Under testing)

APE & LT-STM cryostat

Particular of the end part of the cryostat hosting two sample custom made for the APE beamline and the low temperature STM lab. (Operative)

APE deposition stages

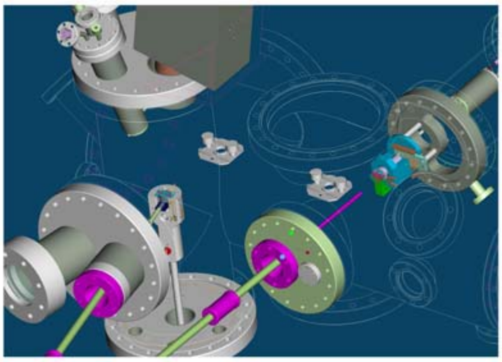

The APE preparation chamber has been equipped with two deposition stages, one for high temperature and double sample holder capability and one for musk deposition.

APE Mott detector deflecotor

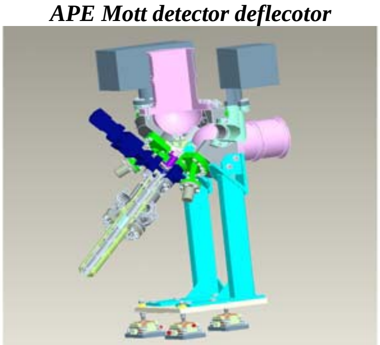

GaPh MPC

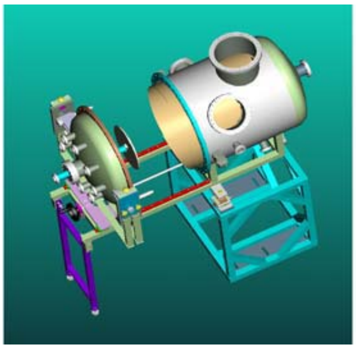

The new multipurpose chamber for the Gasphase beamline (Under construction)

TEDA

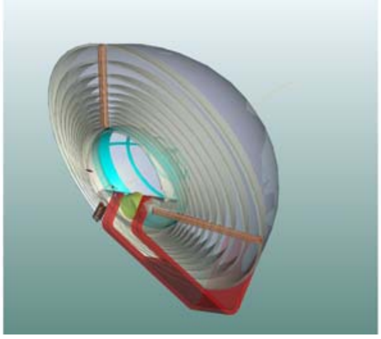

Time of Flight Electron Display Analyzer. Prototyping of a new electron analyzer that combine a wide angular acceptance (but keeping a resolution sufficient for photoelectron diffraction measurements) of the display mirror analyzer with the good energy resolution needed for singling out typical spectroscopic features of photoemission/Auger line shapes by means of a position sensitive/time of flight detection. Project INFM-PURS (Projects for the Utilization of the Synchrotron Radiation), dedicated to the instrumental development for FEL sources, in collaboration with the Rome III University INFM-Unit. (The mechanical realization is under study)

Bear experimental chamber

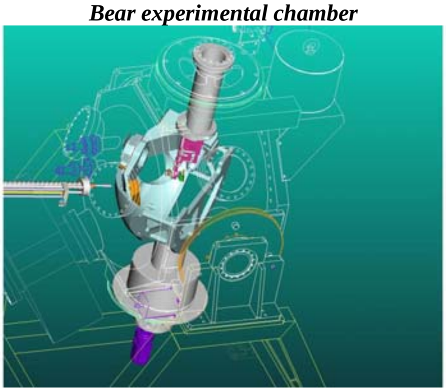

After the design of the Aloisa and the GasPhase experimental chambers, another milestone of the fruitful collaboration between the TASC technical support and the Cinel factory in Padova, is the Bear experimental chamber. Here the goniometry for the electron analyzer (bottom-center), the compact manipulator (top-center) and the screwdriver for sample precession adjustment are evidenced.

The very compact manipulator has been developed in collaboration with the APE Research factory. The x,y,z adjustments and one of the two rotational degree of freedom are accomplished by piezoelectric inchworm motors. The possibility to perform precession correction by means of a third rotation is achieved by means of the screwdriver.(Operative)

VOLPE analyzer

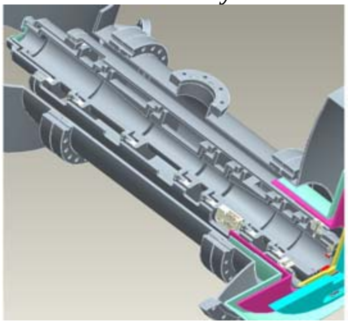

Mechanical design of the high energy electron analyzer of the European VOLPE (Volume Potoemission) project (Under study)

TEM sample holder

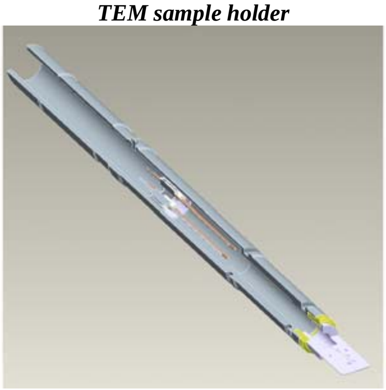

A new sample holder, UHV compatible for further developments, and with electrical connections terminating with screened conductive paths in the scattering region will permit SPM/MEMS in situ measurements.(Under study)

INFM personnel formation.

Formation of the TASC personnel has been taken into account with respect to the past.

In 2001 a C++ course has been organized for young researchers and degree-PhD students for introducing the object oriented programming where the concept of structures and classes can be easily exported to other programming languages as java, delphi and idl. The mechanism of memory allocation in the management of static and dynamical array has been also treated in order to achieve a more efficient utilization of them in any programming language.

In 2002, with our support, the Elettra technical staff has organized a LabVIEW course for instrument interfacing and data acquisition. Six TASC people and two from the INFM-OGG in Grenoble have attended the course with the main aim to improve the capability of the beamline's people involved in the software development and to standardize their products for a better sharing of control software of common hardware.

Participation of technical personnel to the National School on Vacuum Technology organized by the University of Trento INFM Unit and to some exhibitions have been promoted in order to keep a high quality and motivated working level of the technical staff.

Public technical professional formation and scientific divulgation.

The technical staff is strongly motivated in performing public high tech professional formation to young under graduated students, with the awareness that this is also one of the most effective means for scientific divulgation.

In 2001 this activity has been mainly focused in organizing stages for students of technical institutes for a total amount of about 2000 hours by man.

Since the second half of 2002 a more incisive formation plan has been developed, that has brought to a novel formation project, that have got a huge resonance on the media (four article on local newspapers, three 5min local TV presentations and one 40min radio interview). With the funding of the regional government, a collaboration between the TASC technical group, the APE Research (a private enterprise) and the IRSIP (Slovenian Regional Institute for Professional Instruction), a double two years formation intervention is operative since the end of 2002 for the students of the last two years of the Josef Stefan Technical Institute. The first is named *technician of control systems in the field of nanotechnology* (electronics) and the second *technician for the equipment in the field of nanotechnology* (mechanics). More then 40 hours of lectures on modern physics background, scanning probe microscopes, fundamental on top-down and bottom-up nanotechnology, vacuum technology (Roberto Gotter TASC), 3D CAD designing (Alksander De Luisa TASC), technology of nano-positioning, tip preparation and assembly for SPM (Paolo Sigalotti Ape Research), are followed by a five week stage for several students in our laboratories and workshops, where they don't experience prepared didactic experiments but really participate to the construction of new instrumentation. A similar activity is repeated the second year focusing on lithography and CVD techniques.

The more than 1800 hours by man made for the 2002/2003 academic year should be more than 3600 if the project will be approved also for the next two years.

The aim of this formation activity is double. On one side to produce a more effective scientific awareness, also for people that in the future will not be again in direct contact with the scientific community, and to attract more young students toward scientific and high tech studies. On the other side to prepare highly qualified young technicians in the local area, already experienced and efficiently introduced in our activities, in virtue to the new politic concerning job contracts, the so called project contracts. The word itself clarify the contest with scientific research.